Investigating viral subversion of intercellular communication

Patrick James Calhoun II

Dissertation submitted to the faculty of the Virginia Polytechnic Institute and State University in partial fulfillment of the requirements for the degree of

Doctor of Philosophy
In
Biological Sciences

James W. Smyth, Chair
Michael Fox
Robert Gourdie
Sarah McDonald
David Ornelles
Florian Schubot

May 11th, 2020
Roanoke, VA

Keywords: Adenovirus, Gap junction, Connexin43, β-catenin, viral myocarditis

Investigating viral subversion of intercellular communication

Patrick James Calhoun

ABSTRACT

Adenoviruses are non-enveloped, dsDNA tumor viruses responsible for a breadth of pathogenesis including acute respiratory disease and viral myocarditis. Gap junctions, which are formed by connexin proteins, directly couple the cytoplasms of apposed cells enabling immunological, metabolic, and electrical intercellular communication. The gap junction protein connexin43 (Cx43; gene name – *GJA1*) is the most widely expressed human connexin protein and is the predominant connexin in the working myocardium. Given the immunological role for Cx43 gap junctions, we hypothesized that gap junctions would be targeted during adenoviral infection. We find reduced Cx43 protein due to suppression of *GJA1* transcription dependent upon β-catenin during adenoviral infection, with viral protein E4orf1 sufficient to induce β-catenin phosphorylation. Loss of gap junction function occurs prior to reduced Cx43 protein levels with Ad5 infection rapidly inducing Cx43 phosphorylation at residues previously demonstrated to alter gap junction conductance. Direct Cx43 interaction with ZO-1 plays a critical role in gap junction regulation. We find loss of Cx43/ZO-1 complexing during Ad5 infection by co-immunoprecipitation, with complementary studies in human induced pluripotent stem cell derived-cardiomyocytes revealing Cx43 gap junction remodeling concomitant with reduced ZO-1 complexing. These findings demonstrate specific targeting of gap junction function by Ad5

leading to disruptions in intercellular communication which would contribute to dangerous pathological states including arrhythmias in infected hearts.

Intercellular junction proteins belonging to classically defined unique junctions exhibit extensive cross-talk and interdependency for expression and localization. We find reduced connexin43 (Cx43) phosphorylation at a known internalization motif, leading us to hypothesize that gap junctions are maintained during adenoviral infection in order to stabilize intercellular junctions and adenoviral receptors therein. Utilizing immunofluorescence confocal microscopy, we demonstrate that Cx43 reductions are primarily cytosolic with Cx43 preservation at the plasma membrane. Click-IT chemistry, a non-radioactive pulse-chase technique, reveals that Cx43 ½ life is extended during adenoviral infection. In order to test if remaining Cx43 exists in *de facto* gap junctions (i.e. not undocked or cytosolic connexons) we utilized 1 % Triton X-100 solubility fractionation and find Cx43 is indeed primarily junctional during adenoviral infection. Having demonstrated increases in junctional Cx43, we next asked how tightly coupled cells were during adenoviral infection and by ECIS measurements of electrical resistance we demonstrate a transient increase in mechanical coupling during infection. Our future aims are to uncover changes in Coxsackievirus and adenovirus receptor (CAR) protein localization to determine if adenoviral-induced changes to subcellular architecture predisposes neighboring cells to infection and enhances viral spread. These findings will add to the existing model of adenoviral

infection and more broadly, contribute to the therapeutic design of adenoviral vectors for cancer and gene therapy.

Investigating viral subversion of intercellular communication

Patrick J Calhoun

GENERAL AUDIENCE ABSTRACT

The human heart will beat more than 3 billion times during the average lifetime. This is accomplished by billions of individual heart muscle cells, called cardiomyocytes, contracting in synchrony. Cardiomyocytes require direct cell to cell communication in order to receive the proper cues and work in concert. Outside of the heart, including the lining of the lungs which acts as a first line of defense against invading pathogens, direct cell to cell communication is important for mounting proper immune responses. A primary means by which cells communicate directly with neighboring cells is through gap junctions made up of proteins called connexins. Connexin proteins form channels in the cell surface that bind to similar channels on neighboring cells to couple the cell interiors directly. The most widely expressed human connexin, and the most abundant connexin in the heart, is connexin43 (Cx43; gene name – *GJA1*). Adenoviruses are pathogens commonly associated with respiratory illnesses in addition to more serious diseases including viral myocarditis, or infection of the heart. Given that Cx43 gap junctions enable direct communication between cells important in initiating immune responses, we hypothesized that adenovirus would target Cx43 and gap junctions during infection. While adenovirus is a leading cause of viral myocarditis, our study is one of the first investigating how this virus would cause heart attacks in patients.

We find reduced Cx43 protein in cells infected with human adenovirus, and reveal that the expression of the *GJA1* gene is suppressed. We next focused on potential pathways in the cell that are changed during adenoviral infection and find the mechanism that reduces *GJA1* gene expression together with a specific viral protein that activates this pathway. These findings represent a new avenue for antiviral therapy where development of drugs targeting this pathway or inhibiting function of this viral protein would restore Cx43 gap junctions and potentially limit viral replication in patients. We next determined that direct cell to cell communication through gap junctions is reduced before the virus induced loss of the gap junction protein Cx43 during infection. Therefore adenovirus infection involves a double-hit on gap junction communication. This led us to investigate human heart cell infection as gap junction losses are observed in nearly all forms of cardiac disease. We find similar Cx43 suppression and gap junction alterations in cardiomyocytes revealing arrhythmogenic potential during acute adenoviral infection in human hearts. Therapeutic interventions informed by these data could prevent gap junction closure and protect patients with a wide array of heart diseases from heart attacks.

Interestingly, despite reduced Cx43 levels and reduced gap junction function (cell to cell communication), we detected decreases in the cellular pathway associated with gap junction degradation. Utilizing high resolution microscopy we find loss of Cx43 is primarily inside the cells while Cx43 in gap junction structures is maintained, although channels are closed. Given Cx43 gap junction

maintenance found during adenoviral infection, we sought to determine changes in the strength of cell-cell junctions as this provides clues to enrichment of cell-cell junctional proteins including viral receptors. We hypothesize that through this pathway viruses can predispose uninfected neighboring cells to infection. These findings represent a new paradigm in understanding how viruses spread through the body and open up several new avenues in slowing this spread therapeutically in infected patients.

Dedication

For my brothers, Ryan Cook, Rodolpho Rodriguez, Tyler Springman, and Kenneth Elwell, who made the ultimate sacrifice in Afghanistan in 2011. The opportunities you've granted me through your selfless actions will be leveraged to advance science and to reduce human suffering.

Alpha Company - Assassins

3rd Battalion, 21st Infantry Regiment - Gimlets

1st Brigade, 25th Infantry Division - Arctic Wolves

Acknowledgments

A heartfelt thank you to my advisor, Jamie Smyth, whose mentorship both in and out of the laboratory has provided me with unique opportunities to grow. From cell biology to culinary experiments, I would not have wanted to work with anyone else.

My sincerest gratitude to my committee, Mike Fox, Rob Gourdie, Sarah McDonald, David Ornelles, and Florian Schubot. Your constant support and enthusiasm in my work is contagious and motivating. Thank you for your expertise over these past several years.

Inordinate appreciation for my family: my daughter, Ava, who keeps me focused and driven; my parents, Wanda and Pat, who lead by example; and my sister, Ashley, who challenges me constantly.

Thank you to my lab members, Mike Zeitz, Rachel Padget, and Carissa James, who supported me every step of the way. I likely would have abandoned science for coal mining long ago without you. Live life on hard mode.

Table of Contents

List of Figures

List of Abbreviations

Cx43 – connexin43

GJIC – gap junction intercellular communication

PDZ – postsynaptic density 95/disc large/zonula occludens-1

Ad5 – Human adenovirus serotype 5

AdlacZ – Adenoviral vector (ΔE1/E3) constitutively expressing lacZ

PKA – protein kinase A

AKT – protein kinase B

PKC – protein kinase C

cGAMP – cyclic guanosine monophosphate-adenosine monophosphate

cGAS – cGAMP synthetase

IFN – Interferon

ISG – Interferon stimulated genes

ISRE – Interferon stimulated response element

Chapter 1 – Introduction

A. Adenoviridae and Adenoviral Pathogenesis

Adenoviridae are a vertebrate specific family of viruses which include Mastadenovirus (mammals), Aviadenovirus (birds), Atadenovirus (high A-T, reptiles, birds, mammals, and marsupials), and Siadenovirus (birds and reptiles).[1] All human adenoviruses exist under the family Adenoviridae, genus Mastadenovirus, and species are denoted with a letter (A-G) determined by serology, hemagglutination, and genome homology.[1]

Adenoviruses were first independently isolated by two distinct groups in 1953; Hilleman and Werner who were attempting to isolate influenza during an acute respiratory disease outbreak, and Rowe et al at who discovered a then-unknown agent killing adenoid tissue in cell culture.[2,3] The tumorigenic potential of adenovirus was first observed in 1962 by Trintin et al and confirmed in 27 different serotypes by 1968, leading to their naming as a DNA tumor virus.[4,5] Human adenovirus type 5 DNA was experimentally shown to transform rat embryo or baby rat kidney cells in 1973.[6] DNA of other tumor viruses such as simian virus 40 (SV40) has also been utilized for both transformation properties and understanding cell cycle regulation.[7-12]

Adenoviruses are non-enveloped icosahedral viruses which measure approximately 100 nm in diameter. On the exterior, they are composed of major and minor capsid proteins (Figure 1.1, 1.2). Major capsid proteins include Hexon proteins which coat most of the surface, along with 12 fiber proteins which protrude from the surface as a shaft with a knob domain at the distal end. At the base of the fiber protein is a fiber tail which is anchored to the other major capsid protein, the penton base. These 3 viral coat proteins play roles in virus-host receptor-mediated tropism. The minor capsid proteins play an important role in stabilizing the major capsid proteins, enabling them to exist in different chemical environments based on arrangement and orientation.[13,14] This is of special importance during cell invasion when the virus must become partially uncoated to escape the endosome. The 7 known core proteins work to condense the viral dsDNA, anchor the core to the capsid proteins, and also encompass terminal proteins attached to the 5' ends which act as primers for DNA replication.[15,16]

Human adenovirus genomes contain 10 transcription units under temporal control. There are five early units which are transcribed initially, four intermediate units, and one late transcriptional unit known as the major late unit. The early transcription units work cooperatively to uncouple cell cycle regulation and push the cell into S-phase, prevent the cell from undergoing apoptosis, subvert antiviral cellular responses, and synthesize proteins required for viral DNA replication. The intermediate units begin transcription upon viral DNA synthesis and facilitate preferential translation of viral mRNAs in addition to inducing

expression of late genes.[17-19] The late transcriptional units are under control of a single promoter known as the major late promoter (MLP) which gives rise to 5 families of mRNAs that are translated into proteins which cooperatively condense viral DNA and package virions.[20-23]

Adenoviruses cause a spectrum of disorders and diseases. While most appreciated for their ability to transform and transduce cells, along with their potential as an anti-cancer therapeutic, the pathologies caused by these viruses are under appreciated. Regarding cancer therapy, mutant E1B-55kDa deleted adenovirus (ONYX-015) was approved for clinical trials but ultimately failed at efficacy of a single dose.[24-26] Adenoviruses have been reported to cause endemic respiratory infection, epidemic keratoconjunctivitis, acute hemorrhagic cystitis, diarrhea and celiac disease, meningoencephalitis, and myocarditis.[27-32] The variance in pathogenesis is correlative to both virus ability to bind host receptors and tissue specific differences in cellular processes including transcriptional and translational regulation and cell cycle control.

B. Human Adenovirus Serotype 5

Human adenovirus serotype 5 (Ad5) belongs to species C of Mastadenoviridae. Like the other adenoviruses, the Ad5 genome consists of linear dsDNA under temporal regulation. The E1 gene products block apoptosis and uncouple cell cycle control. The E2 genes encode the required proteins for viral DNA

replication. The E3 gene proteins target several anti-viral mechanisms. The E4 genes contribute to a similar outcome of E1 and E3, but through distinct E4orf proteins. The intermediate and late transcriptional units work to package the virus and provide structural integrity for infectious virions after cellular lysis. Ad5 is commonly associated with endemic respiratory infection, especially in young children, and occasionally leads to sudden cardiac death due to viral myocarditis.[33-39]

The primary host-cell receptor for Ad5 is the coxsackie and adenovirus receptor (CAR).[40-42] While CAR is the primary receptor, it has been shown that CAR isn't required for invasion via endocytosis followed by viral infection.[43] Cellular CAR expression in polarized cells is primarily basolateral. It should be noted that in addition to binding CAR, adenoviral penton proteins have been shown to target integrin proteins leading to an increase in endocytosis but not an increase in binding.[44] Clathrin-mediated endocytosis is followed by virion trafficking to the microtubule organization center where the viral dsDNA genome is shuttled into the nucleus. As previously stated, the E1 transcription unit works to uncouple the cell cycle and push the cell into S-phase, as well as block apoptotic pathways, resulting in a prime viral replication center. The E1 transcription unit is divided into two units, E1A and E1B, which are each divided into two more units, E1A (large), e1a (small), E1B-55k, and E1B-19k. Specifically, adenoviral e1a relocalizes retinoblastoma (RB) proteins such as RB1 in addition to p300/CBP resulting in a stimulation of cell cycling.[45] Furthermore, E1A binds E2F promoters

displacing RB proteins, causing a reconfiguration of chromatin structure required to overcome quiescent mechanisms in addition to leading to transcriptional activity of genes downstream of E2F.[46,47] Adenoviral E1B proteins inhibit p53-dependent apoptosis by different mechanisms. Specifically, E1B-19k mimics anti-apoptotic MCL-1 preventing the release of pro-apoptotic cytochrome C.[48,49] E1B-55k both binds p53 directly, stabilizing and downregulating p53 activity, in addition to forming a complex with E4-orf6 and host cellular proteins leading to p53 ubiquitination and proteosomal degradation.[50,51] Additionally, E1B-55k prevents viral replication suppression by type I interferon by blocking expression of interferon inducible genes which regulate cell cycle control.[52,53]

The E4 transcription unit is divided into open reading frames named the E4-orfs. There are six E4orf proteins, E4orf1, 2, 3, 4, 6, and 6/7. The fifth open reading frame is understood not to be translated. E4orf1 and E4orf4 both mimic mitogen and growth factor signaling, resulting in host-cellular behavior of a growth factor rich environment, even in the absence of these molecules. E4orf1 activates mTOR through the PI3K/AKT pathway by interacting with host-cell plasma membrane proteins PDZ domains.[54,55] A specific mechanism of E4orf1 has been shown in that a E4orf1-trimer directly bind Discs Large 1 protein (Dlg1) resulting in PI3K activation.[56] E4orf4 activates mTOR independently of AKT by binding the Bα subunits of host cell protein phosphatase 2A (PP2A).[57-59]

Evolutionary pressure drives the genetic makeup of viruses, including adenovirus, to target and subvert host-cell mechanisms that would otherwise limit viral replication and/or spread. Importantly for multicellular organisms, intercellular communication allows for the exchange of molecules which initiate antiviral responses (further discussed below) and is therefore likely targeted by numerous viruses through unique viral-mediated mechanisms.

C. Gap Junctions and Gap Junction Intercellular Communication

Gap junction intercellular communication (GJIC) is the primary means by which cells in physical contact with one another communicate directly by the exchange of small molecules (approximately 1 kDa. or less). This is accomplished through an array of cellular structures known as gap junctions (Figure 1.3). A network of these cell-to-cell communication pathways result in a tightly regulated and sophisticated means for intercellular communication required in multicellular organisms. GJIC effects the intercellular exchange of ions, metabolites, and second messenger molecules which allow for cooperative cellular function.[60] Furthermore, in excitable cells like cardiac muscle tissue and neurons, GJIC facilitates the transmission of electrical impulses.[61]

Gap junctions in chordates are composed of two protein complexes known as connexons, which are each composed of six connexin proteins (Figure 3B,3C). Connexin proteins in humans are denoted Cx followed by a number indicating

their approximate molecular weight (i.e. connexin43, or Cx43 is ~43kDa.). Connexons on apposed cells dock with one another forming an intercellular channel excluding the extracellular space. These docked connexons aggregate and form gap junction plaques at the cell-to-cell interface. Connexons have the ability to oligomerize as homo- or heteromeric channels incorporating various connexon isoforms which have specific transportation properties including conductance.[62]

The knowledge of gap junctions was expanded upon structurally with the aid of transmission electron microscopy in 1957,1960, and 1962 by several groups.[63-65] They were described functionally in 1966, 1968, 1969, and 1970 by Lowenstein, Goodenough, and several others who experimentally showed the movement of large molecules from cell interior to interior without extracellular leaking.[66-70] With the technological advance of sequencing came the sequence of connexin32 (Cx32) in 1986.[71,72] Cx32 was subsequently the first gap junction protein cloned in 1986 by Paul.[73] Cx43 was first cloned by Goodenough et al one year later in 1987.[74]

D. Cx43, gene GJA1

Connexin43 (Cx43) is the most ubiquitously expressed and most studied of the connexin family of proteins. Cx43 protein synthesis is well described in the heart

and skin, performing vital roles in wound healing and ventricular cardiomyocyte synchronous contraction.[75-77]

Cx43 in the heart. The human heart-beat, an event that occurs billions of times during the human lifetime, is made possible by synchronous contraction of cardiomyocytes which requires the appropriate distribution of Cx43 gap junctions at intercalated discs.[78] In humans, three main connexin isoforms occur in the heart; Cx40, Cx43, and Cx45. The distribution of connexin isoforms in the heart effects specific conduction velocities and is restricted to distinct anatomical structures.[79-81] Of the primary connexin proteins expressed in the heart, Cx43 is enriched in ventricular cardiomyocytes where it is concentrated into gap junction plaques localized to the intercalated discs.[82] Organizational and distribution irregularities of gap junctions in the myocardium have been shown to have pathological consequences.[83,84]

Regulation of Cx43 is complex, with many key steps in the life cycle of this relatively short-lived membrane protein. Regarding transcriptional regulation, whole transcriptomic analysis has been coupled with computational approaches to reveal likely candidates for regulating *GJA1* expression (e.g. OCT4, Mef2a, Gata4, and Srf).[85,86] Experimentation has also identified distinct transcription factors which can regulate Cx43 expression temporally and in a tissue-specific manner (e.g. Irx3, Nkx2.5, Snail1, and Tbx2).[87-90] Cx43 gap junctions undergo constant dynamic regulation via forward (anterograde) and reverse (retrograde)

trafficking, with these regulatory steps impacting cardiac function and health. It has been shown that the half-life of Cx43 is 1.5 – 2 hours in primary cultures of neonatal myocytes while in rat whole heart tissue a half-life of 1.3 hours has been observed.[91] Work has been done in the investigation of anterograde trafficking which suggests post-ER assembly, likely within the trans-Golgi network prior to actual trafficking; additionally, it has been shown that transient phosphorylation in the ER/Golgi is not subject to rapid degradation and allows for a pool of Cx43 available for gap junction channel assembly.[92,93] Furthermore, at the plasma membrane, data suggests an effect of gap junction life cycle due to protein-protein interactions including those with other membrane proteins and scaffolding proteins such as Zonula Occludens-1, which is shown to regulate gap junction size.[94] Indeed, Cx43 is known to interact with PDZ-domain containing proteins providing further evidence of the importance of Cx43 in intracellular signaling while at the plasma membrane. Retrograde trafficking is largely subject to regulation by post-translational modification events at the plasma membrane, including specific phosphorylation events. These have been experimentally shown to affect pathological remodeling of gap junctions.[95-101] Taken together, these sophisticated mechanisms of Cx43 trafficking can be interpreted as having a profound effect on cardiac conductivity due to the sum of their differences being proportional to the amount of GJIC and conductance.

Cx43 in cancer biology. Cx43 and gap junction biology has been a focus for study in the quest to cure cancer. GJIC and Cx43 emerged as a candidate

therapeutic target when it was noted that tumor cells lacked electrical conductivity and that there was a loss of gap junctions between cells in cancer.[102,103] Although an ongoing subject of cancer therapeutics, the link between Cx43, GJIC, and cancer is complex. It has been shown that Cx43 has tumor-suppressive functions in both GJIC-dependent and GJIC-independent roles, which combined has created some degree of discussion within the field of connexin biology. In one example, two different Cx43 mutants demonstrated growth-inhibition; however, one of the two mutants (A253V) failed to suppress GJIC capacity while the other mutant (L160M) inhibited GJIC capacity, demonstrating that the growth suppressive pathway may be unrelated to GJIC.[104] These findings are in line with the more popular hypothesis that the Cx43 protein is sufficient for tumor suppression. However, another study showed that small molecules including polyamines which regulate cell growth and upregulate Cx43 GJIC, may allow for cell-cycle synchronization, leading to a reduction in factors causing a single cell to proliferate.[105] Furthermore, another study showed intercellular exchange of cAMP being capable of causing a delay at the G1/S phase leading to a decrease in cellular division.[106] Collectively, these data show that there is not a clear answer as to the mechanism by which connexin proteins are capable of cell-cycle regulation (GJIC-dependent or GJIC-independent) and it should be considered that there may be, and likely are, contributions from both.

Cx43 in immunomodulatory function. Cx43 gap junctions immunologically couple cells and, additionally, Cx43 hemichannels are capable of initiating immune

responses through release of small molecules and recruitment of leukocytes. The antiviral immune stimulating secondary signaling molecular 2'3'-cyclic guanosine monophosphate-adenosine monophosphate (cGAMP) is produced by cGAMP synthetase (cGAS) upon cGAS binding of cytosolic DNA and is transferable through gap junctions to neighboring cells.[107,108] cGAMP activates interferon stimulated genes (ISG) through the STING/TBK-1/IRF-3 pathway resulting in production of cellular factors which attempt to inhibit viral replication or clear the virus through innate and adaptive immune mechanisms.[109] cGAMP transfer via gap junctions allows for both amplification of interferon responses by increasing the number of cells activating ISGs as well as a mechanism by which host cells can evade viral targeting of immune modulatory function as uninfected cells are transitioned to an antiviral state in addition to the infected cell. Given what is known of viral antagonization of innate and adaptive immune responses and the role of gap junctions in propagating immune signals, it likely targeted by several viruses in effort to reduce inhibitory effects of ISGs of neighboring cells. Cx43 hemichannels have been demonstrated to be permeable channels for ATP release.[110] ATP has a well-established role in regulating the immune system, primarily by recruiting macrophages to a site of apoptosis or necrosis as a "find me" purinergic paracrine signaling molecule.[111] Taken together, this provides another example by which Cx43 can modulate the immune system, but independent of gap junctions. Viral-induced post translational modifications of Cx43 (mentioned above and a focus of Chapter 3) is therefore a mechanism by

which viruses likely exploit in order to inhibit immune cell recruitment and increase the chance of completing the viral replication cycle.

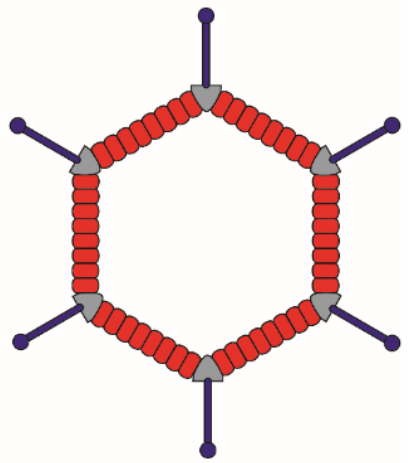

Figure 1.1) Schematic of major capsid proteins of adenovirus. Hexon is shown in red, Penton in gray, and Fiber in blue. Hexon proteins are the most abundant capsid proteins contributing primarily to virion structure. Fiber and Penton proteins attach to primary and secondary receptors respectively to facilitate infection. Adenoviral capsid structure is icosahedral with three distinct rotational symmetry axes.

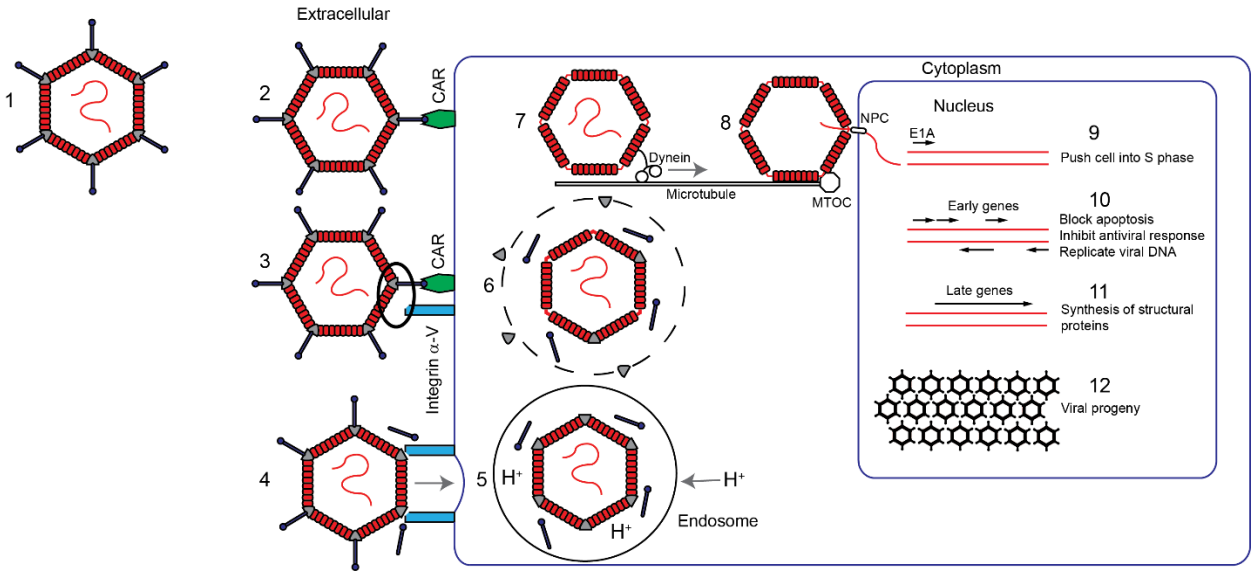

Figure 1.2) Schematic overview of adenovirus infection and replication cycle. Adenovirus binds to the host-cell primary receptor with distal portion of adenoviral fiber protein (CAR is a primary receptor for Ad5) bringing the adenoviral penton protein in close proximity to secondary receptors (Integrin α-V is a secondary receptor for Ad5). Binding of the Integrin α-V secondary receptor causes intracellular signaling events resulting in endocytosis. The endosome undergoes acidification resulting in a rearrangement of adenoviral hexon and penton proteins and release of minor capsid proteins including pVI which lyses the endosome. The partially uncoated adenovirus is trafficked on microtubules to the MTOC and the virus dsDNA is transported through a nuclear pore complex into the nucleus. The genes are expressed in a temporal manner known as early and late. E1A gene expression is robust after the viral genome enters the nucleus, resulting in coercion of the host-cell into S phase and transactivation of other early genes. After viral DNA is replicated by E2 proteins, the late proteins, under control of the Major Late Promoter (MLP), are upregulated in order to package infectious virions for subsequent infection.

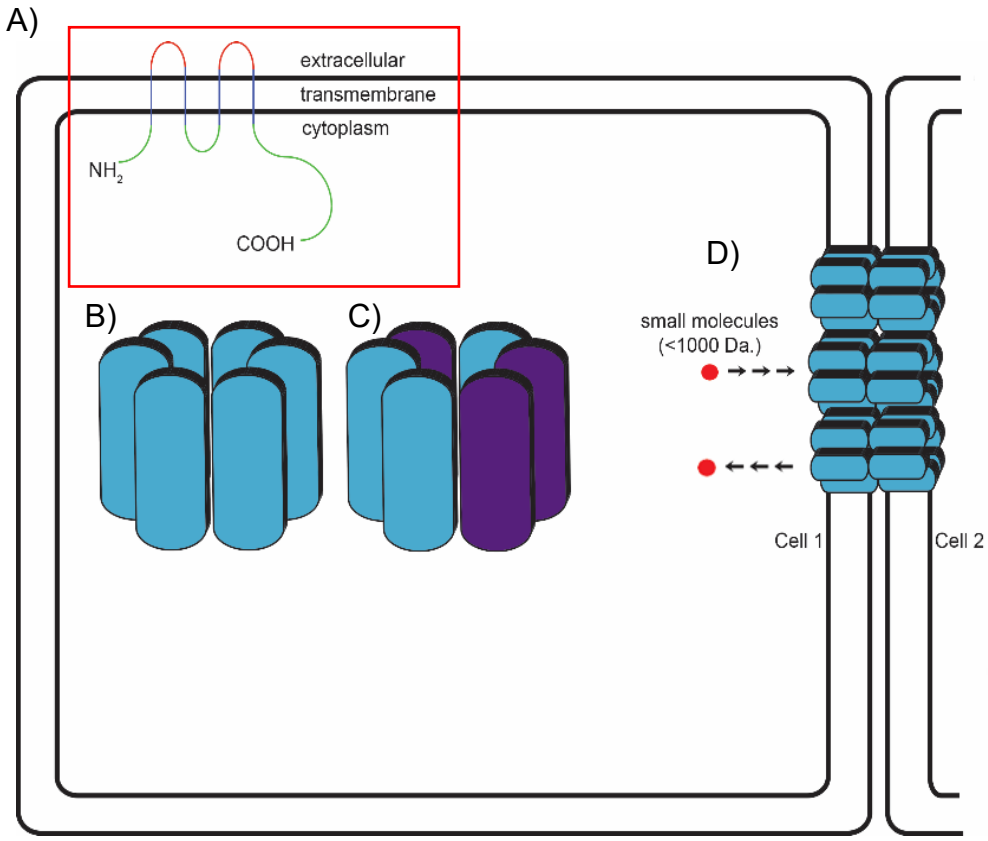

Figure 1.3) Connexins, connexons, and gap junctions.
A) Schematic of connexin structure. The four transmembrane domains are in blue, the two extracellular loops are in red, and the one cytoplasmic loop along with the N- and C-termini are in green. B) Homo- and C) hetero-oligomeric structure of a connexon (hemichannel). D) Connexons on apposed cells dock with one another in a densely packed array to form gap junctions and facilitate GJIC.

References

1 Knipe, D. M. & Howley, P. *Fields Virology*. (Wolters Kluwer, 2013).

2 Rowe, W. P., Huebner, R. J., Gilmore, L. K., Parrott, R. H. & Ward, T. G. Isolation of a cytopathogenic agent from human adenoids undergoing spontaneous degeneration in tissue culture. *Proceedings of the Society for Experimental Biology and Medicine. Society for Experimental Biology and Medicine (New York, N.Y.)* **84**, 570-573, doi:10.3181/00379727-84-20714 (1953).

3 Hilleman, M. R. & Werner, J. H. Recovery of new agent from patients with acute respiratory illness. *Proceedings of the Society for Experimental Biology and Medicine. Society for Experimental Biology and Medicine (New York, N.Y.)* **85**, 183-188, doi:10.3181/00379727-85-20825 (1954).

4 Trentin, J. J., Van Hoosier, G. L., Jr. & Samper, L. The oncogenicity of human adenoviruses in hamsters. *Proceedings of the Society for Experimental Biology and Medicine. Society for Experimental Biology and Medicine (New York, N.Y.)* **127**, 683-689 (1968).

5 Trentin, J. J., Yabe, Y. & Taylor, G. The quest for human cancer viruses. *Science* **137**, 835-841 (1962).

6 Graham, F. L., Smiley, J., Russell, W. C. & Nairn, R. Characteristics of a human cell line transformed by DNA from human adenovirus type 5. *The Journal of general virology* **36**, 59-74, doi:10.1099/0022-1317-36-1-59 (1977).

7 Tegtmeyer, P. Function of simian virus 40 gene A in transforming infection. *J Virol* **15**, 613-618 (1975).

8 Steinberg, M. L. & Defendi, V. Altered pattern of growth and differentiation in human keratinocytes infected by simian virus 40. *Proc Natl Acad Sci U S A* **76**, 801-805 (1979).

9 Gluzman, Y. SV40-transformed simian cells support the replication of early SV40 mutants. *Cell* **23**, 175-182 (1981).

10 Taylor-Papadimitriou, J., Purkis, P., Lane, E. B., McKay, I. A. & Chang, S. E. Effects of SV40 transformation on the cytoskeleton and behavioural properties of human keratinocytes. *Cell differentiation* **11**, 169-180 (1982).

11 Serrano, M., Hannon, G. J. & Beach, D. A new regulatory motif in cell-cycle control causing specific inhibition of cyclin D/CDK4. *Nature* **366**, 704-707, doi:10.1038/366704a0 (1993).

12 Kastan, M. B. *et al.* A mammalian cell cycle checkpoint pathway utilizing p53 and GADD45 is defective in ataxia-telangiectasia. *Cell* **71**, 587-597 (1992).

13 Liu, H., Wu, L. & Zhou, Z. H. Model of the trimeric fiber and its interactions with the pentameric penton base of human adenovirus by cryo-electron microscopy. *J Mol Biol* **406**, 764-774, doi:10.1016/j.jmb.2010.11.043 (2011).

14 Reddy, V. S., Natchiar, S. K., Stewart, P. L. & Nemerow, G. R. Crystal structure of human adenovirus at 3.5 A resolution. *Science* **329**, 1071-1075, doi:10.1126/science.1187292 (2010).

15 Perez-Vargas, J. *et al.* Isolation and characterization of the DNA and protein binding activities of adenovirus core protein V. *J Virol* **88**, 9287-9296, doi:10.1128/JVI.00935-14 (2014).
16 Tamanoi, F. & Stillman, B. W. Function of adenovirus terminal protein in the initiation of DNA replication. *Proc Natl Acad Sci U S A* **79**, 2221-2225 (1982).
17 Manley, J. L., Fire, A., Cano, A., Sharp, P. A. & Gefter, M. L. DNA-dependent transcription of adenovirus genes in a soluble whole-cell extract. *Proc Natl Acad Sci U S A* **77**, 3855-3859 (1980).
18 Dolph, P. J., Racaniello, V., Villamarin, A., Palladino, F. & Schneider, R. J. The adenovirus tripartite leader may eliminate the requirement for cap-binding protein complex during translation initiation. *J Virol* **62**, 2059-2066 (1988).
19 Buratowski, S., Hahn, S., Guarente, L. & Sharp, P. A. Five intermediate complexes in transcription initiation by RNA polymerase II. *Cell* **56**, 549-561 (1989).
20 Black, B. C. & Center, M. S. DNA-binding properties of the major core protein of adenovirus 2. *Nucleic Acids Res* **6**, 2239-2354 (1979).
21 Shaw, A. R. & Ziff, E. B. Transcripts from the adenovirus-2 major late promoter yield a single early family of 3' coterminal mRNAs and five late families. *Cell* **22**, 905-916 (1980).
22 Ziff, E. B. & Evans, R. M. Coincidence of the promoter and capped 5' terminus of RNA from the adenovirus 2 major late transcription unit. *Cell* **15**, 1463-1475 (1978).
23 Berget, S. M., Moore, C. & Sharp, P. A. Spliced segments at the 5' terminus of adenovirus 2 late mRNA. *Proc Natl Acad Sci U S A* **74**, 3171-3175 (1977).
24 Kirn, D. Clinical research results with dl1520 (Onyx-015), a replication-selective adenovirus for the treatment of cancer: what have we learned? *Gene Ther* **8**, 89-98, doi:10.1038/sj.gt.3301377 (2001).
25 Nemunaitis, J. *et al.* Selective replication and oncolysis in p53 mutant tumors with ONYX-015, an E1B-55kD gene-deleted adenovirus, in patients with advanced head and neck cancer: a phase II trial. *Cancer Res* **60**, 6359-6366 (2000).
26 Khuri, F. R. *et al.* a controlled trial of intratumoral ONYX-015, a selectively-replicating adenovirus, in combination with cisplatin and 5-fluorouracil in patients with recurrent head and neck cancer. *Nat Med* **6**, 879-885, doi:10.1038/78638 (2000).
27 Dawson, C. R., Hanna, L., Wood, T. R. & Despain, R. Adenovirus type 8 keratoconjunctivitis in the United States. 3. Epidemiologic, clinical, and microbiologic features. *American journal of ophthalmology* **69**, 473-480 (1970).
28 Alsaad, K. O. *et al.* Late-onset acute haemorrhagic necrotizing granulomatous adenovirus tubulointerstitial nephritis in a renal allograft. *Nephrol Dial Transplant* **22**, 1257-1260, doi:10.1093/ndt/gfl843 (2007).

29 Kagnoff, M. F. *et al.* Evidence for the role of a human intestinal adenovirus in the pathogenesis of coeliac disease. *Gut* **28**, 995-1001 (1987).
30 Johansson, M. E., Uhnoo, I., Kidd, A. H., Madeley, C. R. & Wadell, G. Direct identification of enteric adenovirus, a candidate new serotype, associated with infantile gastroenteritis. *J Clin Microbiol* **12**, 95-100 (1980).
31 Davis, D., Henslee, P. J. & Markesbery, W. R. Fatal adenovirus meningoencephalitis in a bone marrow transplant patient. *Annals of neurology* **23**, 385-389, doi:10.1002/ana.410230412 (1988).
32 Bowles, N. E., Ni, J., Marcus, F. & Towbin, J. A. The detection of cardiotropic viruses in the myocardium of patients with arrhythmogenic right ventricular dysplasia/cardiomyopathy. *Journal of the American College of Cardiology* **39**, 892-895, doi:10.1016/s0735-1097(02)01688-1 (2002).
33 Matsuse, T. *et al.* Latent adenoviral infection in the pathogenesis of chronic airways obstruction. *The American review of respiratory disease* **146**, 177-184, doi:10.1164/ajrccm/146.1.177 (1992).
34 Ma, G. *et al.* Species C is Predominant in Chinese Children with Acute Respiratory Adenovirus Infection. *Pediatr Infect Dis J* **34**, 1042, doi:10.1097/INF.0000000000000791 (2015).
35 Tabain, I. *et al.* Adenovirus respiratory infections in hospitalized children: clinical findings in relation to species and serotypes. *Pediatr Infect Dis J* **31**, 680-684, doi:10.1097/INF.0b013e318256605e (2012).
36 Brandt, C. D. *et al.* Infections in 18,000 infants and children in a controlled study of respiratory tract disease I. Adenovirus pathogenicity in relation to serologic type and illness syndrome. *American Journal of Epidemiology* **90**, 484-500 (1969).
37 Bowles, N. E. *et al.* Detection of viruses in myocardial tissues by polymerase chain reaction: evidence of adenovirus as a common cause of myocarditis in children and adults. *Journal of the American College of Cardiology* **42**, 466-472, doi:https://doi.org/10.1016/S0735-1097(03)00648-X (2003).
38 Fujioka, S. *et al.* Evaluation of viral infection in the myocardium of patients with idiopathic dilated cardiomyopathy. *Journal of the American College of Cardiology* **36**, 1920-1926, doi:10.1016/s0735-1097(00)00955-4 (2000).
39 Treacy, A. *et al.* First report of sudden death due to myocarditis caused by adenovirus serotype 3. *J Clin Microbiol* **48**, 642-645, doi:10.1128/JCM.00815-09 (2010).
40 Bergelson, J. M. *et al.* Isolation of a Common Receptor for Coxsackie B Viruses and Adenoviruses 2 and 5. *Science* **275**, 1320-1323, doi:10.1126/science.275.5304.1320 (1997).
41 Dmitriev, I. *et al.* An adenovirus vector with genetically modified fibers demonstrates expanded tropism via utilization of a coxsackievirus and adenovirus receptor-independent cell entry mechanism. *J Virol* **72**, 9706-9713 (1998).

42 Roelvink, P. W. *et al.* The coxsackievirus-adenovirus receptor protein can function as a cellular attachment protein for adenovirus serotypes from subgroups A, C, D, E, and F. *J Virol* **72**, 7909-7915 (1998).
43 Meier, O. & Greber, U. F. Adenovirus endocytosis. *J Gene Med* **6 Suppl 1**, S152-163, doi:10.1002/jgm.553 (2004).
44 Wickham, T. J., Mathias, P., Cheresh, D. A. & Nemerow, G. R. Integrins αvβ3 and αvβ5 promote adenovirus internalization but not virus attachment. *Cell* **73**, 309-319, doi:https://doi.org/10.1016/0092-8674(93)90231-E (1993).
45 Ferrari, R. *et al.* Epigenetic reprogramming by adenovirus e1a. *Science* **321**, 1086-1088, doi:10.1126/science.1155546 (2008).
46 Ghosh, M. K. & Harter, M. L. A Viral Mechanism for Remodeling Chromatin Structure in G0 Cells. *Molecular Cell* **12**, 255-260, doi:10.1016/s1097-2765(03)00225-9 (2003).
47 Sha, J., Ghosh, M. K., Zhang, K. & Harter, M. L. E1A interacts with two opposing transcriptional pathways to induce quiescent cells into S phase. *J Virol* **84**, 4050-4059, doi:10.1128/JVI.02131-09 (2010).
48 Cuconati, A., Mukherjee, C., Perez, D. & White, E. DNA damage response and MCL-1 destruction initiate apoptosis in adenovirus-infected cells. *Genes Dev* **17**, 2922-2932, doi:10.1101/gad.1156903 (2003).
49 Cuconati, A. & White, E. Viral homologs of BCL-2: role of apoptosis in the regulation of virus infection. *Genes Dev* **16**, 2465-2478, doi:10.1101/gad.1012702 (2002).
50 Sarnow, P., Ho, Y. S., Williams, J. & Levine, A. J. Adenovirus E1b-58kd tumor antigen and SV40 large tumor antigen are physically associated with the same 54 kd cellular protein in transformed cells. *Cell* **28**, 387-394, doi:https://doi.org/10.1016/0092-8674(82)90356-7 (1982).
51 Harada, J. N., Shevchenko, A., Shevchenko, A., Pallas, D. C. & Berk, A. J. Analysis of the Adenovirus E1B-55K-Anchored Proteome Reveals Its Link to Ubiquitination Machinery. *Journal of Virology* **76**, 9194-9206, doi:10.1128/jvi.76.18.9194-9206.2002 (2002).
52 Chahal, J. S., Qi, J. & Flint, S. J. The human adenovirus type 5 E1B 55 kDa protein obstructs inhibition of viral replication by type I interferon in normal human cells. *PLoS Pathog* **8**, e1002853, doi:10.1371/journal.ppat.1002853 (2012).
53 Turner, R. L., Groitl, P., Dobner, T. & Ornelles, D. A. Adenovirus replaces mitotic checkpoint controls. *J Virol* **89**, 5083-5096, doi:10.1128/JVI.00213-15 (2015).
54 Chung, S. H., Frese, K. K., Weiss, R. S., Prasad, B. V. & Javier, R. T. A new crucial protein interaction element that targets the adenovirus E4-ORF1 oncoprotein to membrane vesicles. *J Virol* **81**, 4787-4797, doi:10.1128/JVI.02855-06 (2007).
55 Frese, K. K. *et al.* Selective PDZ protein-dependent stimulation of phosphatidylinositol 3-kinase by the adenovirus E4-ORF1 oncoprotein. *Oncogene* **22**, 710-721, doi:10.1038/sj.onc.1206151 (2003).

56 Kong, K., Kumar, M., Taruishi, M. & Javier, R. T. The Human Adenovirus E4-ORF1 Protein Subverts Discs Large 1 to Mediate Membrane Recruitment and Dysregulation of Phosphatidylinositol 3-Kinase. *PLOS Pathogens* **10**, e1004102, doi:10.1371/journal.ppat.1004102 (2014).
57 Marcellus, R. C. *et al.* Induction of p53-independent apoptosis by the adenovirus E4orf4 protein requires binding to the Balpha subunit of protein phosphatase 2A. *J Virol* **74**, 7869-7877 (2000).
58 Zhang, Z. *et al.* Genetic analysis of B55alpha/Cdc55 protein phosphatase 2A subunits: association with the adenovirus E4orf4 protein. *J Virol* **85**, 286-295, doi:10.1128/JVI.01381-10 (2011).
59 Peterson, R. T., Desai, B. N., Hardwick, J. S. & Schreiber, S. L. Protein phosphatase 2A interacts with the 70-kDa S6 kinase and is activated by inhibition of FKBP12–rapamycinassociated protein. *Proceedings of the National Academy of Sciences of the United States of America* **96**, 4438-4442 (1999).
60 Harris, A. L. Connexin channel permeability to cytoplasmic molecules. *Prog Biophys Mol Biol* **94**, 120-143, doi:10.1016/j.pbiomolbio.2007.03.011 (2007).
61 Neyton, J. & Trautmann, A. Single-channel currents of an intercellular junction. *Nature* **317**, 331-335 (1985).
62 He, D. S., Jiang, J. X., Taffet, S. M. & Burt, J. M. Formation of heteromeric gap junction channels by connexins 40 and 43 in vascular smooth muscle cells. *Proc Natl Acad Sci U S A* **96**, 6495-6500 (1999).
63 Robertson, J. D. New observations on the ultrastructure of the membranes of frog peripheral nerve fibers. *The Journal of biophysical and biochemical cytology* **3**, 1043-1048 (1957).
64 Karrer, H. E. Cell interconnections in normal human cervical epithelium. *The Journal of biophysical and biochemical cytology* **7**, 181-184 (1960).
65 Dewey, M. M. & Barr, L. Intercellular Connection between Smooth Muscle Cells: the Nexus. *Science* **137**, 670-672, doi:10.1126/science.137.3531.670-a (1962).
66 Kanno, Y. & Loewenstein, W. R. Cell-to-cell passage of large molecules. *Nature* **212**, 629-630 (1966).
67 Bennett, M. V. L. & Trinkaus, J. P. Electrical coupling between embryonic cells by way of extracellular space and specialized junctions. *The Journal of Cell Biology* **44**, 592-610 (1970).
68 Goodenough, D. A. & Revel, J. P. A fine structural analysis of intercellular junctions in the mouse liver. *J Cell Biol* **45**, 272-290 (1970).
69 Ito, S. & Loewenstein, W. R. Ionic communication between early embryonic cells. *Developmental biology* **19**, 228-243 (1969).
70 Brightman, M. W. & Reese, T. S. Junctions between intimately apposed cell membranes in the vertebrate brain. *The Journal of Cell Biology* **40**, 648-677 (1969).
71 Kumar, N. M. & Gilula, N. B. Cloning and characterization of human and rat liver cDNAs coding for a gap junction protein. *J Cell Biol* **103**, 767-776 (1986).

72 Cruciani, V. & Mikalsen, S. O. The vertebrate connexin family. *Cell Mol Life Sci* **63**, 1125-1140, doi:10.1007/s00018-005-5571-8 (2006).
73 Paul, D. L. Molecular cloning of cDNA for rat liver gap junction protein. *J Cell Biol* **103**, 123-134 (1986).
74 Beyer, E. C., Paul, D. L. & Goodenough, D. A. Connexin43: A protein from rat heart homologous to a gap junction protein from liver. *The Journal of Cell Biology* **105**, 2621-2629 (1987).
75 Guo, H., Acevedo, P., Parsa, F. D. & Bertram, J. S. Gap-Junctional Protein Connexin 43 Is Expressed in Dermis and Epidermis of Human Skin: Differential Modulation by Retinoids. *Journal of Investigative Dermatology* **99**, 460-467, doi:10.1111/1523-1747.ep12616154 (1992).
76 van Veen, A. A., van Rijen, H. V. & Opthof, T. Cardiac gap junction channels: modulation of expression and channel properties. *Cardiovasc Res* **51**, 217-229 (2001).
77 Rhett, J. M., Jourdan, J. & Gourdie, R. G. Connexin 43 connexon to gap junction transition is regulated by zonula occludens-1. *Molecular biology of the cell* **22**, 1516-1528, doi:10.1091/mbc.e10-06-0548 (2011).
78 Gros, D. B. & Jongsma, H. J. Connexins in mammalian heart function. *BioEssays : news and reviews in molecular, cellular and developmental biology* **18**, 719-730, doi:10.1002/bies.950180907 (1996).
79 Davis, L. M., Rodefeld, M. E., Green, K., Beyer, E. C. & Saffitz, J. E. Gap junction protein phenotypes of the human heart and conduction system. *Journal of cardiovascular electrophysiology* **6**, 813-822 (1995).
80 Gros, D. *et al.* Restricted distribution of connexin40, a gap junctional protein, in mammalian heart. *Circ Res* **74**, 839-851 (1994).
81 Coppen, S. R. *et al.* Connexin45, a major connexin of the rabbit sinoatrial node, is co-expressed with connexin43 in a restricted zone at the nodal-crista terminalis border. *The journal of histochemistry and cytochemistry : official journal of the Histochemistry Society* **47**, 907-918, doi:10.1177/002215549904700708 (1999).
82 Matsuda, T. *et al.* N-cadherin signals through Rac1 determine the localization of connexin 43 in cardiac myocytes. *J Mol Cell Cardiol* **40**, 495-502, doi:10.1016/j.yjmcc.2005.12.010 (2006).
83 Smyth, J. W. *et al.* Limited forward trafficking of connexin 43 reduces cell-cell coupling in stressed human and mouse myocardium. *J Clin Invest* **120**, 266-279, doi:10.1172/JCI39740 (2010).
84 Smith, J. H., Green, C. R., Peters, N. S., Rothery, S. & Severs, N. J. Altered patterns of gap junction distribution in ischemic heart disease. An immunohistochemical study of human myocardium using laser scanning confocal microscopy. *The American journal of pathology* **139**, 801-821 (1991).
85 Schlesinger, J. *et al.* The cardiac transcription network modulated by Gata4, Mef2a, Nkx2.5, Srf, histone modifications, and microRNAs. *PLoS Genet* **7**, e1001313, doi:10.1371/journal.pgen.1001313 (2011).

86 Boyer, L. A. *et al.* Core transcriptional regulatory circuitry in human embryonic stem cells. *Cell* **122**, 947-956, doi:10.1016/j.cell.2005.08.020 (2005).
87 Zhang, S. S. *et al.* Iroquois homeobox gene 3 establishes fast conduction in the cardiac His-Purkinje network. *Proc Natl Acad Sci U S A* **108**, 13576-13581, doi:10.1073/pnas.1106911108 (2011).
88 Kasahara, H. Nkx2.5 homeoprotein regulates expression of gap junction protein connexin 43 and sarcomere organization in postnatal cardiomyocytes. *Journal of Molecular and Cellular Cardiology* **35**, 243-256, doi:10.1016/s0022-2828(03)00002-6 (2003).
89 de Boer, T. P. *et al.* Connexin43 repression following epithelium-to-mesenchyme transition in embryonal carcinoma cells requires Snail1 transcription factor. *Differentiation* **75**, 208-218, doi:10.1111/j.1432-0436.2006.00133.x (2007).
90 Chen, J. R. *et al.* Tbx2 represses expression of Connexin43 in osteoblastic-like cells. *Calcif Tissue Int* **74**, 561-573, doi:10.1007/s00223-003-0106-5 (2004).
91 Beardslee, M. A., Laing, J. G., Beyer, E. C. & Saffitz, J. E. Rapid turnover of connexin43 in the adult rat heart. *Circ Res* **83**, 629-635, doi:10.1161/01.res.83.6.629 (1998).
92 Laird, D. W., Castillo, M. & Kasprzak, L. Gap junction turnover, intracellular trafficking, and phosphorylation of connexin43 in brefeldin A-treated rat mammary tumor cells. *J Cell Biol* **131**, 1193-1203, doi:10.1083/jcb.131.5.1193 (1995).
93 Musil, L. S. & Goodenough, D. A. Multisubunit assembly of an integral plasma membrane channel protein, gap junction connexin43, occurs after exit from the ER. *Cell* **74**, 1065-1077, doi:https://doi.org/10.1016/0092-8674(93)90728-9 (1993).
94 Hunter, A. W., Barker, R. J., Zhu, C. & Gourdie, R. G. Zonula occludens-1 alters connexin43 gap junction size and organization by influencing channel accretion. *Molecular biology of the cell* **16**, 5686-5698, doi:10.1091/mbc.e05-08-0737 (2005).
95 Remo, B. F. *et al.* Phosphatase-resistant gap junctions inhibit pathological remodeling and prevent arrhythmias. *Circ Res* **108**, 1459-1466, doi:10.1161/CIRCRESAHA.111.244046 (2011).
96 Smyth, J. W. & Shaw, R. M. The gap junction life cycle. *Heart Rhythm* **9**, 151-153, doi:10.1016/j.hrthm.2011.07.028 (2012).
97 Smyth, J. W. *et al.* A 14-3-3 mode-1 binding motif initiates gap junction internalization during acute cardiac ischemia. *Traffic* **15**, 684-699, doi:10.1111/tra.12169 (2014).
98 Dunn, C. A. & Lampe, P. D. Injury-triggered Akt phosphorylation of Cx43: a ZO-1-driven molecular switch that regulates gap junction size. *J Cell Sci* **127**, 455-464, doi:10.1242/jcs.142497 (2014).
99 Lampe, P. D., Cooper, C. D., King, T. J. & Burt, J. M. Analysis of Connexin43 phosphorylated at S325, S328 and S330 in normoxic and ischemic heart. *J Cell Sci* **119**, 3435-3442, doi:10.1242/jcs.03089 (2006).

100 Nimlamool, W., Andrews, R. M. & Falk, M. M. Connexin43 phosphorylation by PKC and MAPK signals VEGF-mediated gap junction internalization. *Molecular biology of the cell* **26**, 2755-2768, doi:10.1091/mbc.E14-06-1105 (2015).
101 Norris, R. P., Baena, V. & Terasaki, M. Localization of phosphorylated connexin 43 using serial section immunogold electron microscopy. *J Cell Sci* **130**, 1333-1340, doi:10.1242/jcs.198408 (2017).
102 McNutt, N. S. & Weinstein, R. S. Carcinoma of the cervix: deficiency of nexus intercellular junctions. *Science* **165**, 597-599 (1969).
103 Loewenstein, W. R. & Kanno, Y. Intercellular communication and the control of tissue growth: lack of communication between cancer cells. *Nature* **209**, 1248-1249 (1966).
104 Omori, Y. & Yamasaki, H. Mutated connexin43 proteins inhibit rat glioma cell growth suppression mediated by wild-type connexin43 in a dominant-negative manner. *International journal of cancer* **78**, 446-453 (1998).
105 Shore, L., McLean, P., Gilmour, S. K., Hodgins, M. B. & Finbow, M. E. Polyamines regulate gap junction communication in connexin 43-expressing cells. *The Biochemical journal* **357**, 489-495 (2001).
106 Chandrasekhar, A. *et al.* Intercellular redistribution of cAMP underlies selective suppression of cancer cell growth by connexin26. *PLoS One* **8**, e82335, doi:10.1371/journal.pone.0082335 (2013).
107 Ablasser, A. *et al.* Cell intrinsic immunity spreads to bystander cells via the intercellular transfer of cGAMP. *Nature* **503**, 530-534, doi:10.1038/nature12640 (2013).
108 Sun, L., Wu, J., Du, F., Chen, X. & Chen, Z. J. Cyclic GMP-AMP synthase is a cytosolic DNA sensor that activates the type I interferon pathway. *Science (New York, N.Y.)* **339**, 786-791, doi:10.1126/science.1232458 (2013).
109 Yoneyama, M. *et al.* Direct triggering of the type I interferon system by virus infection: activation of a transcription factor complex containing IRF-3 and CBP/p300. *The EMBO journal* **17**, 1087-1095, doi:10.1093/emboj/17.4.1087 (1998).
110 Kang, J. *et al.* Connexin 43 hemichannels are permeable to ATP. *The Journal of neuroscience : the official journal of the Society for Neuroscience* **28**, 4702-4711, doi:10.1523/JNEUROSCI.5048-07.2008 (2008).
111 Cekic, C. & Linden, J. Purinergic regulation of the immune system. *Nature reviews. Immunology* **16**, 177-192, doi:10.1038/nri.2016.4 (2016).

Chapter 2

Literature review

TITLE

Viral manipulation of intercellular junction components

Patrick J. Calhoun[1,2], James W. Smyth[1,2,3,*]

[1] Fralin Biomedical Research Institute, Roanoke, VA 24016, USA

[2] Department of Biological Sciences, Virginia Tech, Blacksburg, VA 24060, USA

[3] Virginia Tech Carilion School of Medicine, Roanoke, VA 24016, USA

* correspondence:

James W. Smyth

The Fralin Biomedical Research Institute at VTC

2 Riverside Circle

Roanoke, VA 24016

smythj@vtc.vt.edu

Introduction

Viruses are obligate intracellular parasites, which must overcome cellular barriers in order to replicate their viral genome and produce infectious viral progeny. The infection process can be generally summarized as invasion by which viruses utilize host-cell proteins as a mechanism for attachment and entry followed by a virus-specific varying level of cellular reprogramming, viral replication, and ultimately egress for subsequent infection. Viruses must spread through and across the epithelium in addition to spread within tissue where cells are coupled together in three-dimensional space. This presents a unique set of challenges whereby the proteins that couple these cells act as a first line of defense against viral infection and spread. Virally-induced changes in cellular signaling, altered transcriptional and translational control, and immunological responses to infection are well studied aspects of virology as a field. More recently, it is of interest to understand cell architectural changes and how that contributes to pathogenesis and viral spread. This review will focus on the current state of knowledge on viral subversion of intercellular junctional components and what that means for viral replication and infection.

Intercellular junctions mechanically and metabolically couple cells in tissue. This network of intercellular junctions is necessary for the development of tissue and organs and consists of tight junctions (TJ), adherens junctions (AJ), desmosomes, and gap junctions (GJ). These intercellular junctions and their corresponding junctional components exhibit structurally and functionally distinct

properties necessary for the integrity of tissue. Briefly, TJs anchor cells together and establish a semipermeable barrier, which selectively excludes the extracellular space. Given TJs ability to establish a barrier, it is not a surprise that of the intercellular junctions, they are the most apical in polarized epithelium. Therefore, it is also less surprising that, of the intercellular junctions, TJ components are currently the most understood in their involvement in infection by various viruses and may truly be the most widely utilized route of infection. Mechanical stress is dispersed via AJs and desmosomes. Primary differences in AJ- and desmosomal-proteins include their adhesion properties and dependency on calcium ions. Additionally, AJs and desmosomes utilize different cytoskeletal components actin and intermediate filaments, respectively. GJs facilitate the exchange of ions, and small molecules of less than approximately 1,000 Daltons allowing for immunological, metabolic, and electrical coupling. Furthermore, independent of their well-established ability to connect the cytoplasms of apposed cells, GJs provide mechanical coupling and their ability to facilitate direct cell-to-cell communication is altered by mechanical stress *in vitro*. While distinct, all of these intercellular junctions act in concert to create functional tissue and organs necessary to many multicellular organisms.

Tight junctions (TJ)

TJs along with closely associated AJs are often referred to collectively as the apical junction complex (APC), and separate the apical domain from the basolateral domain of epithelial and endothelial cells, as well as form intracellular

signaling domains. Indeed, there is extensive interplay and interdependency of TJ and AJ proteins. TJs form a continuous semipermeable layer that is both size and charge selective (reviewed in [1-3]) and are composed primarily of claudins, occludin, tricellulin, and MarvelD3. Occludin, a four-pass transmembrane protein with an extensive C terminus, was the first junctional component identified of TJs and experiments suggest it to be more important in barrier function and junctional integrity than the formation of *de novo* TJ.[4,5] Claudin proteins are essential for TJ formation and establishing barrier and paracellular selective channel function.[6] Claudin paracellular selective channel function has been demonstrated to be dynamic and permissive of reversible gating kinetics.[7] Several other transmembrane junctional proteins localize to TJs and of relevance to this review are junctional adhesion molecules (JAM) and the Coxsackievirus and adenovirus receptor (CAR). JAM and CAR are type I transmembrane proteins containing 2 extracellular immunoglobulin domains and facilitate homophilic or heterophilic protein-protein binding with receptors on neighboring cells and additionally in the case of CAR, binding extracellular matrix proteins.[8-10] The importance of CAR is highlighted as it is necessary for embryonic cardiac development.[11] JAM proteins are thought to indirectly interact with the extracellular matrix protein vitronectin through *cis* heterotypic binding of integrins.[12] Furthermore, these interactions include transient interactions between endothelial cells and leukocytes, implicating these junctional proteins as receptors to mediate immune responses and inflammation.[13,14] Occludin, claudin, JAM, and CAR proteins additionally serve as molecular platforms for intracellular signaling through their C termini

(reviewed in [15-18]). Abnormalities in TJs and TJ proteins are associated with a multitude of diseases including diabetic retinopathy and cancer metastasis.[19] Additionally, TJs are manipulated during infectious diseases by bacterial toxins and invading viruses.[20-22]

Viral subversion of tight junction components

It is interesting to speculate on the evolutionary pressure that has driven many viruses to utilizing TJ proteins, that laterally localize in a region excluding extracellular space, as receptors and yet, for several viruses, this is the case. Hepatitis C virus (HCV) is a hepatotropic enveloped RNA virus of *Flaviviridae* resulting in chronic liver inflammation and ultimately fibrosis and cirrhosis (reviewed in [23]). Occludin and claudin-1 have been demonstrated to be a required entry factor and coreceptor, respectively, for HCV entry and infection.[24,25] More recently it has been found that claudin-1/CD81 complexes are critical for initiating clathrin and dynamin dependent endocytosis for viral particle delivery.[26] Occludin has additionally been shown to be directly bound by HCV sequentially last, following claudin-1/CD81, before endocytosis, taken together experimental data demonstrates that TJ components are a final binding step prior to entry.[27] Interestingly, HCV upregulates occludin expression, potentially increasing homophilic occludin interactions with neighboring cells and predisposing them for infection.[28]

Rotavirus and Reovirus belong to the family *Reoviridae* and consists of a segmented dsRNA genome encapsulated in a nonenveloped protein shell, and primarily cause gastroenteritis and respiratory illnesses in mammals including humans (reviewed in [29,30]). JAM has been shown to be a receptor for Reovirus serotypes 1 and 3, and ectopic expression of JAM in cells not permissive to reoviral infection converts cells to a reovirus-infectable phenotype. Additionally, in JAM-independent reovirus infection, it has been demonstrated that the interaction between reoviral protein σ1 and JAM is necessary for the lytic stage of the reovirus replication cycle by activating NF-κB, providing evidence for entry-independent intracellular signaling events initiating from TJ proteins.[31] *In vivo* data demonstrates that JAM-A is necessary for systemic whole organism reovirus infection in mice by promoting reovirus infection to endothelial cells, but is dispensable for replication in organs directly infected including the intestines and the brain.[32] Strain-dependent rotavirus also utilize JAM-A as a coreceptor determined by structure of the rotavirus spike protein VP4.[33]

Coxsackieviruses of the *Picornaviridae* family are ssRNA non-enveloped viruses associated with life-threatening pathogenesis including viral myocarditis and meningoencephalitis (reviewed in [34]). Coxsackie B viruses bind CAR as a primary receptor, and ectopic expression of CAR in uninfectable hamster cells caused them to be permissive to Coxsackievirus infection.[22] Occludin, in concert with the GTPases Rab34 and Rab35, is also required for viral particle endocytosis, but is not directly bound by Coxsackievirus.[35] Additionally many

Coxsackie B viruses bind decay-accelerating factor (DAF) to initiate endocytosis through signaling cascades at the kinases Abl and Fyn, resulting in rearrangements in the actin cytoskeleton directing viral movement into the tight junction.[36]

Human adenovirus of the *Adenoviridae* family are non-enveloped dsDNA tumor viruses responsible for a breadth of disease including respiratory illnesses, gastroenteritis, meningoencephalitis, and viral myocarditis (reviewed in [29,37]). Interestingly, species C adenovirus serotypes 2 and 5 were discovered to utilize CAR as a primary receptor concurrently with Coxsackie B virus.[22] CAR exists as several alternatively spliced isoforms including two isoforms with distinct basolateral or apical localization referred to as CAR^{Ex7} and CAR^{Ex8} ,respectively.[38] CAR^{Ex8} apical localization is shown to be utilized by neutrophils for transepithelial migration and that species C adenoviruses have evolved to coopt this innate immune mechanism.[39] CAR cytoplasmic and transmembrane domains are dispensable for adenoviral mediated gene transfer demonstrating the extracellular domains are sufficient for adenoviral attachment.[40] Furthermore, of the two extracellular immunoglobulin domains, lack of glycosylation of the distal domain is shown to decrease adenovirus binding.[41] Despite being the primary receptor for species C adenoviruses, CAR-independent mechanisms of adenoviral infection are also understood to occur, although CAR-negative cells do infect at a much lower rate. This is at least partially explained through an

interaction between adenoviral penton and integrin $\alpha_V\beta3$ and/or $\alpha_V\beta5$, inducing endocytosis of the virus.[42-44]

The structural and functional necessity of TJ proteins along with their proximal location to the apical regions of epithelial cells predisposes them as likely targets as viral receptors, coreceptors, and entry factors as they are statistically more likely to be encountered in an unwounded monolayer of cells. Given that more viruses utilize TJ components over any other intercellular junctional component, this logical model of opportunistic evolution appears to be true.

Adherens junctions (AJ)

In addition to the selective extracellular exclusion via cell-cell contacts achieved by TJs, cells must also be able to stretch, compress, and migrate without dissociating and this is achieved, at least in part, by AJs. AJs consists of cadherin, nectin, and nectin-like (Necl) transmembrane adhesion molecules, catenin and afadin cytoplasmic scaffolding proteins, and cytoskeletal actin (reviewed in [45]). Cadherin proteins are responsible for homophilic and heterophilic calcium-dependent adhesion and their differential distribution across tissue type is thought to sort subpopulations of cells into distinct tissue/organs during development, independent of adhesive forces.[46,47] Nectin proteins contribute calcium-independent adhesive forces and work either cooperatively or independently of cadherins to form cell-cell junctions, and are localized to AJs through actin rearrangement by cadherins.[48] Nectin-like (Necl) proteins are

similar in domain structure and function to nectin proteins however fail to bind the scaffolding protein afadin.[49,50] An additional cellular adhesion molecule relevant to viral infection is carcinoembryonic antigen family of cell adhesion molecule 1-Long (CEACAM1-L), which localizes both apically and in AJs and mediates cell-cell adhesion.[51,52] CEACAM1 has been shown *in vivo* to be important for endothelial barrier function and endothelial homeostasis in adult mice.[53] AJs, partially due to intermixing with TJ proteins at intercellular junctions, are attractive targets for viral binding and likely results in broad cell-type tropism for viral attachment.

Viral subversion of adherens junctional components

Herpesviridae viruses herpes simplex virus 1 and 2 (HSV-1, HSV-2) are neurovirulent dsDNA enveloped viruses of approximately 190 nm diameter capable of lifelong latency in the host, and when activated can appear as mucosal ulcers and additionally rarely cause death by central nervous system infection (reviewed in [29]). Originally identified as poliovirus receptor proteins 1 and 2 (Prr1, Prr2) and then designated as herpesvirus entry proteins B and C (HveB, HveC), it was discovered that the cellular adhesion molecules nectin-1 and nectin-2 both confer vulnerability to HSV to resistant Chinese hamster ovarian cells.[54-56] Additional members of *Herpesviridae*, pseudorabies virus (PRV) and bovine herpesvirus 1 (BVH-1) utilize nectin-1 as a receptor and given the extensive role of nectin-1 in in cell-cell adhesion is thought to contribute to broad species tropism for alphaherpesviruses.[54] Measles virus of the family

Paramyxoviridae is a negative strand RNA virus associated with fever, cough, conjunctivitis, rash, and temporary immune suppression (reviewed in [57]), and has been demonstrated to utilize nectin-4 as a primary receptor.[58,59]

In addition to nectin proteins, other AJ components have been identified as viral receptors including Necl proteins and CEACAM1-L. Necl-5 (also known as CD155) was originally discovered as a cellular receptor for poliovirus.[60] Furthermore, Necl-5 interacts with both integrin $\alpha_v\beta_3$ and dynein motor proteins and this interaction has been hypothesized to enable neurotropic viruses to utilize neuronal retrograde transport and facilitate directional movement to neuronal cell bodies.[61,62] Mouse hepatitis virus (MHV) is a murine coronavirus constituted of a ssRNA genome and associated with nonlethal enteric infections (reviewed in [63]). MHV was discovered to bind CEACAM1 in mice and CEACAM1 disruption leads to reduced infectivity.[64-66] HCV (introduced in viral subversion of TJ components) depends on the AJ protein E-cadherin as an entry factor as demonstrated by blocking HCV infection with anti-E-cadherin antibodies, but E-cadherin likely acts more in regulating the localization of tight junction components rather than being a receptor[67,68]. Interestingly, several viruses including HCV, hepatitis B virus, and Epstein-Barr virus negatively regulate the expression of E-cadherin which may promote viral spread to uninfected cells if utilized as an entry factor.[69-72]

Desmosomes

Desmosomes are cell-cell contact architecture critical for anchoring together cells that regularly undergo mechanical stress such as myocardium, bladder and skin. Desmosomes are primarily composed of extracellular adhesive desmoglein and desmocollin, and intracellular scaffolding proteins plakoglobin, plakophilin, and desmoplakin, which tie the extracellular junction to intermediate filaments such as keratin (reviewed in [73]). Desmoglein and desmocollin are referred to collectively as desmosomal cadherins and similar to cadherins of AJ mediate calcium-dependent cell-cell adhesion participate in heterophilic interactions.[74-76] Desmosomal cadherins interact with the scaffolding protein plakoglobin through desmosomal cadherin C termini and a plakoglobin hydrophobic domain.[77] The plakophilin proteins (plakophilin 1, 2, and 3) are important for recruitment and stabilization of other desmosomal proteins and loss of plakophilin results in loss of desmosomal adhesion.[78,79] Desmoplakin links the cytoskeletal intermediate filaments to desmosomal cadherins through interactions with plakoglobin and plakophilin.[80] Targeting of desmosomal proteins rather than components of the AJC results in varied tissue tropism for different viruses.

Desmosomes as targets for viral infection

Adenovirus species B serotypes 3, 7, 11, and 14 (adenoviruses are introduced above) bind desmoglein 2 directly through adenoviral fiber protein knob domain. Oligomerization of adenoviral serotype 3 fiber proteins facilitate separation of epithelial cell junctions, increasing availability of masked viral receptors and

infectability of cells.[81,82] Although not identified as a receptor or entry factor, EBV targets the desmosomal protein plakoglobin transcriptionally through the viral transforming EBV latent membrane protein 1,resulting in a cellular switch from E-cadherin to N-cadherin expression and inducing epithelial-to-mesenchymal transition (EMT).[83] Furthermore, plakoglobin is reported to regulate desmocollin expression. Therefore, loss of plakoglobin during EBV infection likely induces loss of desmocollin as well.[84] As of now desmocollin is not reported to be a viral receptor but given the cross talk between desmocollin and desmoglein, it is exciting to suggest an indirect mechanism by which desmocollin expression and localization may influence infectability of cells. Influenza A viral replication has been demonstrated to be negatively regulated by plakophilin 2 in the nucleus (i.e. nuclear / non-scaffolding plakophilin 2) through binding influenza A viral protein PB1.[85] While significant contributions have demonstrated desmosomal proteins as viral receptors, it is still a developing field of virology and desmosome biology. Findings from this research may result in broad therapeutic interventions, including cancer, as several viruses that are known to manipulate desmosomal structures are capable of transforming cells as well as induce EMT, analogous to cellular processes in tumor formation and metastasis respectively.

Gap Junctions (GJ)

GJs are formed through the synthesis, oligomerization, and trafficking of connexin proteins by apposed cells, each cell contributing a hexomeric hemichannel (connexon) that docks *in trans* with another connexon resulting in a

channel permeable to ions, molecules less than approximately 1,000 Daltons, small peptides, and linear miRNAs (reviewed in [86]). Specifically, gap junction intercellular communication (GJIC) is a mechanism for the direct exchange of antiviral immune priming molecules including cyclic GMP-AMP (cGAMP), a small molecular synthesized by cGAMP synthase (cGAS) upon detection of cytosolic DNA.[87] In addition to establishing a shared pool of small molecules and metabolites, the importance of GJIC is further highlighted in excitable cells including cardiomyocytes and neurons, where their dysregulation and redistribution is present in a broad spectrum of pathologies. Given their role in intrinsic propagation of antiviral immune responses, it is possible viruses have evolved a mechanism targeting GJ structures or GJIC, yet little is known about viral subversion of GJs. To date, no connexin proteins are identified as viral receptors or entry factors. The highly coordinated cross-talk at the plasma membrane and at cell-cell interfaces between junctional components supports the model however that GJs may be directly or indirectly involved in viral spread.

Gap junctions as targets during viral infection

Our current understanding of viruses that target gap junctions is limited. Human papilloma viruses contain circularized dsDNA genomes and are most commonly associated with skin-to-skin contact predominantly transmitted through sexual contact resulting in anogenital warts, neoplasms, and cancer depending on serotype (reviewed in [88]). HPV16 is a “high-risk” serotype widely prevalent in HPV-associated cervical cancers. The HPV16 oncoprotein E6 is shown to affect

the location of Cx43 in cervical cancers where Cx43 is primarily localized in the cytoplasm as a Cx43/Disks large 1 (Dlg1) complex, which can be rescued to the cell-cell border through siRNA-mediated knockdown of HPV16 E6.[89] Additionally, MHV (introduced in the *AJs section*) has been demonstrated to negatively regulate Cx43 protein and mRNA and cause Cx43 ER/Golgi retention and reduce GJIC.[90] Given the strong rationale for targeting GJIC to limit antiviral immune signaling, it is possible that many more viruses manipulate GJs and connexin proteins.

Directed transmission of viruses at cell-cell interfaces

The classical infection paradigm model of a virus infecting a cell accompanied by subsequent release of many infection virions which then travel by diffusion to infect the local population is increasingly understood to be incomplete and an additional model of cell-to-cell direct transmission is evident to contribute to viral spread. Host-cell membrane and junctional molecules are increasingly reported to facilitate viral infection and allow for direct transmission of virus from one cell to another with or without viral particles interacting with the extracellular milieu.

Both enveloped and non-enveloped viruses have adopted several strategies for direct cell-to-cell dissemination. A heavily investigated mechanism of enveloped viruses capable of directed cellular spread is by cell-cell fusion and the formation of syncytia. HSV-1 has been shown to induce syncytia formation *in vivo* resulting in infected-donor cells transferring viruses to uninfected-acceptor cells, however,

mutants had to be generated to recapitulate syncytia formation *in vitro.*[91,92] Measles virus induces syncytium in signaling lymphocyte activation molecule (SLAM/CD150)-dependent and -independent mechanisms as well as utilization of cellular receptor CD46 with most work focusing on interactions involving measles virus H protein[93-95]. Respiratory syncytial virus (RSV), and human parainfluenza virus-3 establish syncytium formation through RhoA manipulation both *in vitro* and *in vivo*[96]. Directed cell-cell transmission by non-enveloped viruses is less described but emerging evidence supports a model by which syncytia formation can aid in directed viral spread for non-enveloped viruses. Syncytia formation induced by specific reoviruses has been shown to enhance viral replication and pathogenesis *in vivo* through utilization of fusion-associated small transmembrane proteins, mirroring cell-cell transmission of many enveloped viruses[97]. Furthermore, it has been shown that antibody neutralized reovirus can be delivered as replication-competent to tumor cells by monocytes *in vitro* while cell-free antibody neutralized reovirus fails to infect tumor cells[98]. Syncytium formation is likely the most studied form of direct cell-to-cell transfer of viral particles.

Neural and immunological synapses are regions of interaction between proximal but generally unfused cells where protein complexes aggregate in order to exchange information and alter the neighboring cell (reviewed in [99,100]). Viral synapses mimic neural and immunological synapses (or hijack the cellular synapse in place) and are an increasingly appreciated way for directed viral spread. As with neurological and immunological synapses, virological synapses

occur between neighboring cells, directing viral egress and in the case of several viruses, more efficiently than by cell-free viral spread. Virological synapses, like other cellular reprogramming, are formed by viruses through their hijacking of subcellular machinery and cytoskeletal rearrangement. Viral synapse formation is induced by several viruses to direct infection to leukocytes and neuronal cells, including HSV-1, rabies virus, human immunodeficiency virus, and measles virus.[101-104]

References

1 Zihni, C., Mills, C., Matter, K. & Balda, M. S. Tight junctions: from simple barriers to multifunctional molecular gates. *Nature Reviews Molecular Cell Biology* **17**, 564-580, doi:10.1038/nrm.2016.80 (2016).

2 Anderson, J. M. & Van Itallie, C. M. Physiology and function of the tight junction. *Cold Spring Harbor perspectives in biology* **1**, a002584-a002584, doi:10.1101/cshperspect.a002584 (2009).

3 Schneeberger, E. E. & Lynch, R. D. The tight junction: a multifunctional complex. *American Journal of Physiology-Cell Physiology* **286**, C1213-C1228, doi:10.1152/ajpcell.00558.2003 (2004).

4 Saitou, M. *et al.* Occludin-deficient embryonic stem cells can differentiate into polarized epithelial cells bearing tight junctions. *J Cell Biol* **141**, 397-408, doi:10.1083/jcb.141.2.397 (1998).

5 Chen, Y., Merzdorf, C., Paul, D. L. & Goodenough, D. A. COOH terminus of occludin is required for tight junction barrier function in early Xenopus embryos. *The Journal of cell biology* **138**, 891-899, doi:10.1083/jcb.138.4.891 (1997).

6 Furuse, M. *et al.* Claudin-based tight junctions are crucial for the mammalian epidermal barrier: a lesson from claudin-1-deficient mice. *J Cell Biol* **156**, 1099-1111, doi:10.1083/jcb.200110122 (2002).

7 Weber, C. R. *et al.* Claudin-2-dependent paracellular channels are dynamically gated. *Elife* **4**, e09906, doi:10.7554/eLife.09906 (2015).

8 Patzke, C. *et al.* The Coxsackievirus–Adenovirus Receptor Reveals Complex Homophilic and Heterophilic Interactions on Neural Cells. *The Journal of Neuroscience* **30**, 2897-2910, doi:10.1523/jneurosci.5725-09.2010 (2010).

9 Cohen, C. J. *et al.* The coxsackievirus and adenovirus receptor is a transmembrane component of the tight junction. *Proceedings of the National Academy of Sciences* **98**, 15191-15196, doi:10.1073/pnas.261452898 (2001).

10 Martìn-Padura, I. *et al.* Junctional Adhesion Molecule, a Novel Member of the Immunoglobulin Superfamily That Distributes at Intercellular Junctions and Modulates Monocyte Transmigration. *The Journal of Cell Biology* **142**, 117-127, doi:10.1083/jcb.142.1.117 (1998).

11 Dorner, A. A. *et al.* Coxsackievirus-adenovirus receptor (CAR) is essential for early embryonic cardiac development. *Journal of Cell Science* **118**, 3509-3521, doi:10.1242/jcs.02476 (2005).

12 Naik, M. U. & Naik, U. P. Junctional adhesion molecule-A-induced endothelial cell migration on vitronectin is integrin alpha v beta 3 specific. *J Cell Sci* **119**, 490-499, doi:10.1242/jcs.02771 (2006).

13 Verdino, P., Witherden, D. A., Havran, W. L. & Wilson, I. A. The molecular interaction of CAR and JAML recruits the central cell signal transducer PI3K. *Science (New York, N.Y.)* **329**, 1210-1214, doi:10.1126/science.1187996 (2010).

14 Liang, T. W. *et al.* Vascular Endothelial-Junctional Adhesion Molecule (VE-JAM)/JAM 2 Interacts with T, NK, and Dendritic Cells Through JAM 3.

The Journal of Immunology **168**, 1618-1626, doi:10.4049/jimmunol.168.4.1618 (2002).
15 Nomme, J. *et al.* Structural Basis of a Key Factor Regulating the Affinity between the Zonula Occludens First PDZ Domain and Claudins. *The Journal of biological chemistry* **290**, 16595-16606, doi:10.1074/jbc.M115.646695 (2015).
16 Cummins, P. M. Occludin: one protein, many forms. *Molecular and cellular biology* **32**, 242-250, doi:10.1128/MCB.06029-11 (2012).
17 Severson, E. A. & Parkos, C. A. Structural determinants of Junctional Adhesion Molecule A (JAM-A) function and mechanisms of intracellular signaling. *Curr Opin Cell Biol* **21**, 701-707, doi:10.1016/j.ceb.2009.06.005 (2009).
18 Excoffon, K. J. D. A., Hruska-Hageman, A., Klotz, M., Traver, G. L. & Zabner, J. A role for the PDZ-binding domain of the coxsackie B virus and adenovirus receptor (CAR) in cell adhesion and growth. *Journal of Cell Science* **117**, 4401-4409, doi:10.1242/jcs.01300 (2004).
19 Sawada, N. *et al.* Tight junctions and human diseases. *Medical electron microscopy : official journal of the Clinical Electron Microscopy Society of Japan* **36**, 147-156, doi:10.1007/s00795-003-0219-y (2003).
20 Katahira, J. *et al.* Clostridium perfringens enterotoxin utilizes two structurally related membrane proteins as functional receptors in vivo. *J Biol Chem* **272**, 26652-26658, doi:10.1074/jbc.272.42.26652 (1997).
21 Wu, Z., Nybom, P. & Magnusson, K. E. Distinct effects of Vibrio cholerae haemagglutinin/protease on the structure and localization of the tight junction-associated proteins occludin and ZO-1. *Cellular microbiology* **2**, 11-17, doi:10.1046/j.1462-5822.2000.00025.x (2000).
22 Bergelson, J. M. *et al.* Isolation of a Common Receptor for Coxsackie B Viruses and Adenoviruses 2 and 5. *Science* **275**, 1320-1323, doi:10.1126/science.275.5304.1320 (1997).
23 Manns, M. P. *et al.* Hepatitis C virus infection. *Nature Reviews Disease Primers* **3**, 17006, doi:10.1038/nrdp.2017.6 (2017).
24 Ploss, A. *et al.* Human occludin is a hepatitis C virus entry factor required for infection of mouse cells. *Nature* **457**, 882-886, doi:10.1038/nature07684 (2009).
25 Evans, M. J. *et al.* Claudin-1 is a hepatitis C virus co-receptor required for a late step in entry. *Nature* **446**, 801-805, doi:10.1038/nature05654 (2007).
26 Farquhar, M. J. *et al.* Hepatitis C virus induces CD81 and claudin-1 endocytosis. *J Virol* **86**, 4305-4316, doi:10.1128/jvi.06996-11 (2012).
27 Sourisseau, M. *et al.* Temporal Analysis of Hepatitis C Virus Cell Entry with Occludin Directed Blocking Antibodies. *PLOS Pathogens* **9**, e1003244, doi:10.1371/journal.ppat.1003244 (2013).
28 Branche, E. *et al.* Hepatitis C Virus Increases Occludin Expression via the Upregulation of Adipose Differentiation-Related Protein. *PLOS ONE* **11**, e0146000, doi:10.1371/journal.pone.0146000 (2016).
29 Knipe, D. M. & Howley, P. *Fields Virology*. (Wolters Kluwer, 2013).

30 Crawford, S. E. *et al.* Rotavirus infection. *Nature Reviews Disease Primers* **3**, 17083, doi:10.1038/nrdp.2017.83 (2017).
31 Barton, E. S. *et al.* Junction Adhesion Molecule Is a Receptor for Reovirus. *Cell* **104**, 441-451, doi:https://doi.org/10.1016/S0092-8674(01)00231-8 (2001).
32 Antar, A. A. R. *et al.* Junctional Adhesion Molecule-A Is Required for Hematogenous Dissemination of Reovirus. *Cell host & microbe* **5**, 59-71, doi:https://doi.org/10.1016/j.chom.2008.12.001 (2009).
33 Torres-Flores, J. M., Silva-Ayala, D., Espinoza, M. A., López, S. & Arias, C. F. The tight junction protein JAM-A functions as coreceptor for rotavirus entry into MA104 cells. *Virology* **475**, 172-178, doi:https://doi.org/10.1016/j.virol.2014.11.016 (2015).
34 Sin, J., Mangale, V., Thienphrapa, W., Gottlieb, R. A. & Feuer, R. Recent progress in understanding coxsackievirus replication, dissemination, and pathogenesis. *Virology* **484**, 288-304, doi:10.1016/j.virol.2015.06.006 (2015).
35 Coyne, C. B., Shen, L., Turner, J. R. & Bergelson, J. M. Coxsackievirus entry across epithelial tight junctions requires occludin and the small GTPases Rab34 and Rab5. *Cell host & microbe* **2**, 181-192, doi:10.1016/j.chom.2007.07.003 (2007).
36 Coyne, C. B. & Bergelson, J. M. Virus-Induced Abl and Fyn Kinase Signals Permit Coxsackievirus Entry through Epithelial Tight Junctions. *Cell* **124**, 119-131, doi:10.1016/j.cell.2005.10.035 (2006).
37 Ghebremedhin, B. Human adenovirus: Viral pathogen with increasing importance. *Eur J Microbiol Immunol (Bp)* **4**, 26-33, doi:10.1556/EuJMI.4.2014.1.2 (2014).
38 Excoffon, K. J. *et al.* Isoform-specific regulation and localization of the coxsackie and adenovirus receptor in human airway epithelia. *PLoS One* **5**, e9909, doi:10.1371/journal.pone.0009909 (2010).
39 Kotha, P. L. N. *et al.* Adenovirus Entry From the Apical Surface of Polarized Epithelia Is Facilitated by the Host Innate Immune Response. *PLOS Pathogens* **11**, e1004696, doi:10.1371/journal.ppat.1004696 (2015).
40 Wang, X. & Bergelson, J. M. Coxsackievirus and Adenovirus Receptor Cytoplasmic and Transmembrane Domains Are Not Essential for Coxsackievirus and Adenovirus Infection. *Journal of Virology* **73**, 2559-2562 (1999).
41 Excoffon, K. J. D. A., Gansemer, N., Traver, G. & Zabner, J. Functional effects of coxsackievirus and adenovirus receptor glycosylation on homophilic adhesion and adenoviral infection. *Journal of virology* **81**, 5573-5578, doi:10.1128/JVI.02562-06 (2007).
42 Hidaka, C. *et al.* CAR-dependent and CAR-independent pathways of adenovirus vector-mediated gene transfer and expression in human fibroblasts. *The Journal of clinical investigation* **103**, 579-587, doi:10.1172/JCI5309 (1999).

43 Wickham, T. J., Mathias, P., Cheresh, D. A. & Nemerow, G. R. Integrins αvβ3 and αvβ5 promote adenovirus internalization but not virus attachment. *Cell* **73**, 309-319, doi:https://doi.org/10.1016/0092-8674(93)90231-E (1993).
44 Lyle, C. & McCormick, F. Integrin αvβ5 is a primary receptor for adenovirus in CAR-negative cells. *Virology Journal* **7**, 148, doi:10.1186/1743-422X-7-148 (2010).
45 Harris, T. J. C. & Tepass, U. Adherens junctions: from molecules to morphogenesis. *Nature Reviews Molecular Cell Biology* **11**, 502-514, doi:10.1038/nrm2927 (2010).
46 Prakasam, A. K., Maruthamuthu, V. & Leckband, D. E. Similarities between heterophilic and homophilic cadherin adhesion. *Proceedings of the National Academy of Sciences* **103**, 15434-15439, doi:10.1073/pnas.0606701103 (2006).
47 Godt, D. & Tepass, U. Drosophila oocyte localization is mediated by differential cadherin-based adhesion. *Nature* **395**, 387-391, doi:10.1038/26493 (1998).
48 Troyanovsky, R. B., Indra, I., Chen, C.-S., Hong, S. & Troyanovsky, S. M. Cadherin controls nectin recruitment into adherens junctions by remodeling the actin cytoskeleton. *Journal of Cell Science* **128**, 140-149, doi:10.1242/jcs.161588 (2015).
49 Takai, Y., Irie, K., Shimizu, K., Sakisaka, T. & Ikeda, W. Nectins and nectin-like molecules: Roles in cell adhesion, migration, and polarization. *Cancer Science* **94**, 655-667, doi:10.1111/j.1349-7006.2003.tb01499.x (2003).
50 Ikeda, W. *et al.* Tage4/Nectin-like molecule-5 heterophilically trans-interacts with cell adhesion molecule Nectin-3 and enhances cell migration. *J Biol Chem* **278**, 28167-28172, doi:10.1074/jbc.M303586200 (2003).
51 Sundberg, U., Beauchemin, N. & Öbrink, B. The cytoplasmic domain of CEACAM1-L controls its lateral localization and the organization of desmosomes in polarized epithelial cells. *Journal of Cell Science* **117**, 1091-1104, doi:10.1242/jcs.00944 (2004).
52 Sadekova, S., Lamarche-Vane, N., Li, X. & Beauchemin, N. The CEACAM1-L glycoprotein associates with the actin cytoskeleton and localizes to cell-cell contact through activation of Rho-like GTPases. *Molecular biology of the cell* **11**, 65-77, doi:10.1091/mbc.11.1.65 (2000).
53 Ghavampour, S. *et al.* Endothelial barrier function is differentially regulated by CEACAM1-mediated signaling. *The FASEB Journal* **32**, 5612-5625, doi:10.1096/fj.201800331R (2018).
54 Geraghty, R. J., Krummenacher, C., Cohen, G. H., Eisenberg, R. J. & Spear, P. G. Entry of Alphaherpesviruses Mediated by Poliovirus Receptor-Related Protein 1 and Poliovirus Receptor. *Science* **280**, 1618-1620, doi:10.1126/science.280.5369.1618 (1998).
55 Warner, M. S. *et al.* A Cell Surface Protein with Herpesvirus Entry Activity (HveB) Confers Susceptibility to Infection by Mutants of Herpes Simplex

Virus Type 1, Herpes Simplex Virus Type 2, and Pseudorabies Virus. *Virology* **246**, 179-189, doi:https://doi.org/10.1006/viro.1998.9218 (1998).
56 Lopez, M. *et al.* The Human Poliovirus Receptor Related 2 Protein Is a New Hematopoietic/Endothelial Homophilic Adhesion Molecule. *Blood* **92**, 4602-4611, doi:10.1182/blood.V92.12.4602 (1998).
57 Laksono, B. M., de Vries, R. D., McQuaid, S., Duprex, W. P. & de Swart, R. L. Measles Virus Host Invasion and Pathogenesis. *Viruses* **8**, 210, doi:10.3390/v8080210 (2016).
58 Mühlebach, M. D. *et al.* Adherens junction protein nectin-4 is the epithelial receptor for measles virus. *Nature* **480**, 530-533, doi:10.1038/nature10639 (2011).
59 Noyce, R. S. & Richardson, C. D. Nectin 4 is the epithelial cell receptor for measles virus. *Trends in Microbiology* **20**, 429-439, doi:https://doi.org/10.1016/j.tim.2012.05.006 (2012).
60 Mendelsohn, C. L., Wimmer, E. & Racaniello, V. R. Cellular receptor for poliovirus: Molecular cloning, nucleotide sequence, and expression of a new member of the immunoglobulin superfamily. *Cell* **56**, 855-865, doi:https://doi.org/10.1016/0092-8674(89)90690-9 (1989).
61 Mueller, S., Cao, X., Welker, R. & Wimmer, E. Interaction of the Poliovirus Receptor CD155 with the Dynein Light Chain Tctex-1 and Its Implication for Poliovirus Pathogenesis. *Journal of Biological Chemistry* **277**, 7897-7904, doi:10.1074/jbc.M111937200 (2002).
62 Minami, Y. *et al.* Necl-5/Poliovirus Receptor Interacts in cis with Integrin αVβ3 and Regulates Its Clustering and Focal Complex Formation. *Journal of Biological Chemistry* **282**, 18481-18496, doi:10.1074/jbc.M611330200 (2007).
63 Taguchi, F. & Hirai-Yuki, A. Mouse Hepatitis Virus Receptor as a Determinant of the Mouse Susceptibility to MHV Infection. *Frontiers in Microbiology* **3**, doi:10.3389/fmicb.2012.00068 (2012).
64 Dveksler, G. S. *et al.* Cloning of the mouse hepatitis virus (MHV) receptor: expression in human and hamster cell lines confers susceptibility to MHV. *Journal of virology* **65**, 6881-6891 (1991).
65 Hirai, A. *et al.* Role of mouse hepatitis virus (MHV) receptor murine CEACAM1 in the resistance of mice to MHV infection: studies of mice with chimeric mCEACAM1a and mCEACAM1b. *Journal of virology* **84**, 6654-6666, doi:10.1128/JVI.02680-09 (2010).
66 Blau, D. M. *et al.* Targeted disruption of the Ceacam1 (MHVR) gene leads to reduced susceptibility of mice to mouse hepatitis virus infection. *Journal of virology* **75**, 8173-8186, doi:10.1128/jvi.75.17.8173-8186.2001 (2001).
67 Colpitts, C. C., Lupberger, J. & Baumert, T. F. Multifaceted role of E-cadherin in hepatitis C virus infection and pathogenesis. *Proceedings of the National Academy of Sciences of the United States of America* **113**, 7298-7300, doi:10.1073/pnas.1607732113 (2016).
68 Li, Q. *et al.* Hepatitis C virus depends on E-cadherin as an entry factor and regulates its expression in epithelial-to-mesenchymal transition.

Proceedings of the National Academy of Sciences of the United States of America **113**, 7620-7625, doi:10.1073/pnas.1602701113 (2016).
69 Hu, H. *et al.* Epstein–Barr Virus Infection of Mammary Epithelial Cells Promotes Malignant Transformation. *EBioMedicine* **9**, 148-160, doi:https://doi.org/10.1016/j.ebiom.2016.05.025 (2016).
70 Arora, P., Kim, E.-O., Jung, J. K. & Jang, K. L. Hepatitis C virus core protein downregulates E-cadherin expression via activation of DNA methyltransferase 1 and 3b. *Cancer Letters* **261**, 244-252, doi:https://doi.org/10.1016/j.canlet.2007.11.033 (2008).
71 Ha, H.-L. *et al.* IGF-II induced by hepatitis B virus X protein regulates EMT via SUMO mediated loss of E-cadherin in mice. *Oncotarget* **7**, 56944-56957, doi:10.18632/oncotarget.10922 (2016).
72 Shin Kim, S., Yeom, S., Kwak, J., Ahn, H.-J. & Lib Jang, K. Hepatitis B virus X protein induces epithelial–mesenchymal transition by repressing E-cadherin expression via upregulation of E12/E47. *Journal of General Virology* **97**, 134-143, doi:https://doi.org/10.1099/jgv.0.000324 (2016).
73 Delva, E., Tucker, D. K. & Kowalczyk, A. P. The desmosome. *Cold Spring Harbor perspectives in biology* **1**, a002543-a002543, doi:10.1101/cshperspect.a002543 (2009).
74 Nilles, L. A. *et al.* Structural analysis and expression of human desmoglein: a cadherin-like component of the desmosome. *J Cell Sci* **99 (Pt 4)**, 809-821 (1991).
75 Chitaev, N. A. & Troyanovsky, S. M. Direct Ca2+-dependent heterophilic interaction between desmosomal cadherins, desmoglein and desmocollin, contributes to cell-cell adhesion. *The Journal of cell biology* **138**, 193-201, doi:10.1083/jcb.138.1.193 (1997).
76 Mechanic, S., Raynor, K., Hill, J. E. & Cowin, P. Desmocollins form a distinct subset of the cadherin family of cell adhesion molecules. *Proceedings of the National Academy of Sciences of the United States of America* **88**, 4476-4480, doi:10.1073/pnas.88.10.4476 (1991).
77 Chitaev, N. A., Averbakh, A. Z., Troyanovsky, R. B. & Troyanovsky, S. M. Molecular organization of the desmoglein-plakoglobin complex. *J Cell Sci* **111 (Pt 14)**, 1941-1949 (1998).
78 Rietscher, K. *et al.* Growth Retardation, Loss of Desmosomal Adhesion, and Impaired Tight Junction Function Identify a Unique Role of Plakophilin 1 In Vivo. *The Journal of investigative dermatology* **136**, 1471-1478, doi:10.1016/j.jid.2016.03.021 (2016).
79 Hatzfeld, M., Haffner, C., Schulze, K. & Vinzens, U. The Function of Plakophilin 1 in Desmosome Assembly and Actin Filament Organization. *Journal of Cell Biology* **149**, 209-222, doi:10.1083/jcb.149.1.209 (2000).
80 Kowalczyk, A. P. *et al.* The amino-terminal domain of desmoplakin binds to plakoglobin and clusters desmosomal cadherin-plakoglobin complexes. *J Cell Biol* **139**, 773-784, doi:10.1083/jcb.139.3.773 (1997).
81 Wang, H. *et al.* Multimerization of adenovirus serotype 3 fiber knob domains is required for efficient binding of virus to desmoglein 2 and

subsequent opening of epithelial junctions. *J Virol* **85**, 6390-6402, doi:10.1128/jvi.00514-11 (2011).
82 Wang, H. *et al.* Desmoglein 2 is a receptor for adenovirus serotypes 3, 7, 11 and 14. *Nature medicine* **17**, 96-104, doi:10.1038/nm.2270 (2011).
83 Shair, K. H. Y., Schnegg, C. I. & Raab-Traub, N. Epstein-Barr Virus Latent Membrane Protein-1 Effects on Junctional Plakoglobin and Induction of a Cadherin Switch. *Cancer Research* **69**, 5734-5742, doi:10.1158/0008-5472.can-09-0468 (2009).
84 Tokonzaba, E. *et al.* Plakoglobin as a Regulator of Desmocollin Gene Expression. *Journal of Investigative Dermatology* **133**, 2732-2740, doi:https://doi.org/10.1038/jid.2013.220 (2013).
85 Wang, L. *et al.* Comparative influenza protein interactomes identify the role of plakophilin 2 in virus restriction. *Nature communications* **8**, 13876-13876, doi:10.1038/ncomms13876 (2017).
86 Nielsen, M. S. *et al.* Gap junctions. *Compr Physiol* **2**, 1981-2035, doi:10.1002/cphy.c110051 (2012).
87 Ablasser, A. *et al.* Cell intrinsic immunity spreads to bystander cells via the intercellular transfer of cGAMP. *Nature* **503**, 530-534, doi:10.1038/nature12640 (2013).
88 Brianti, P., De Flammineis, E. & Mercuri, S. R. Review of HPV-related diseases and cancers. *The new microbiologica* **40**, 80-85 (2017).
89 Sun, P. *et al.* HPV16 E6 Controls the Gap Junction Protein Cx43 in Cervical Tumour Cells. *Viruses* **7**, 5243-5256, doi:10.3390/v7102871 (2015).
90 Basu, R., Banerjee, K., Bose, A. & Das Sarma, J. Mouse Hepatitis Virus Infection Remodels Connexin43-Mediated Gap Junction Intercellular Communication In Vitro and <em>In Vivo</em&gt. *Journal of Virology* **90**, 2586, doi:10.1128/JVI.02420-15 (2016).
91 Dingwell, K. S. *et al.* Herpes simplex virus glycoproteins E and I facilitate cell-to-cell spread in vivo and across junctions of cultured cells. *J Virol* **68**, 834-845 (1994).
92 Pertel, P. E. & Spear, P. G. Modified Entry and Syncytium Formation by Herpes Simplex Virus Type 1 Mutants Selected for Resistance to Heparin Inhibition. *Virology* **226**, 22-33, doi:https://doi.org/10.1006/viro.1996.0624 (1996).
93 Hu, C. *et al.* Characterization of a region involved in binding of measles virus H protein and its receptor SLAM (CD150). *Biochem Biophys Res Commun* **316**, 698-704, doi:10.1016/j.bbrc.2004.02.106 (2004).
94 Takeuchi, K., Miyajima, N., Nagata, N., Takeda, M. & Tashiro, M. Wild-type measles virus induces large syncytium formation in primary human small airway epithelial cells by a SLAM(CD150)-independent mechanism. *Virus Res* **94**, 11-16, doi:10.1016/s0168-1702(03)00117-5 (2003).
95 Dorig, R. E., Marcil, A., Chopra, A. & Richardson, C. D. The human CD46 molecule is a receptor for measles virus (Edmonston strain). *Cell* **75**, 295-305, doi:10.1016/0092-8674(93)80071-l (1993).

96 Pastey, M. K., Gower, T. L., Spearman, P. W., Crowe, J. E. & Graham, B. S. A RhoA-derived peptide inhibits syncytium formation induced by respiratory syncytial virus and parainfluenza virus type 3. *Nature Medicine* **6**, 35-40, doi:10.1038/71503 (2000).
97 Kanai, Y. *et al.* Cell–cell fusion induced by reovirus FAST proteins enhances replication and pathogenicity of non-enveloped dsRNA viruses. *PLOS Pathogens* **15**, e1007675, doi:10.1371/journal.ppat.1007675 (2019).
98 Berkeley, R. A. *et al.* Antibody-Neutralized Reovirus Is Effective in Oncolytic Virotherapy. *Cancer Immunology Research* **6**, 1161, doi:10.1158/2326-6066.CIR-18-0309 (2018).
99 Sudhof, T. C. Towards an Understanding of Synapse Formation. *Neuron* **100**, 276-293, doi:10.1016/j.neuron.2018.09.040 (2018).
100 Huppa, J. B. & Davis, M. M. T-cell-antigen recognition and the immunological synapse. *Nature Reviews Immunology* **3**, 973-983, doi:10.1038/nri1245 (2003).
101 Iwasaki, Y. & Clark, H. F. Cell to cell transmission of virus in the central nervous system. II. Experimental rabies in mouse. *Laboratory investigation; a journal of technical methods and pathology* **33**, 391-399 (1975).
102 Aubert, M., Yoon, M., Sloan, D. D., Spear, P. G. & Jerome, K. R. The Virological Synapse Facilitates Herpes Simplex Virus Entry into T Cells. *Journal of Virology* **83**, 6171, doi:10.1128/JVI.02163-08 (2009).
103 Koethe, S., Avota, E. & Schneider-Schaulies, S. Measles Virus Transmission from Dendritic Cells to T Cells: Formation of Synapse-Like Interfaces Concentrating Viral and Cellular Components. *Journal of Virology* **86**, 9773, doi:10.1128/JVI.00458-12 (2012).
104 Hübner, W. *et al.* Quantitative 3D Video Microscopy of HIV Transfer Across T Cell Virological Synapses. *Science* **323**, 1743, doi:10.1126/science.1167525 (2009).

Chapter 3

Manuscript 1

The FASEB Journal, In Press

TITLE

Adenovirus targets transcriptional and post-translational mechanisms to limit gap junction function

Patrick J. Calhoun[1,2], Allen V. Phan[3], Jordan D. Taylor[3], Carissa C. James[1,4], Rachel L. Padget[1,4], Michael J. Zeitz[1], James W. Smyth*[,1,2,3]

[1] Fralin Biomedical Research Institute, Roanoke, VA 24016, USA

[2] Department of Biological Sciences, Virginia Tech, Blacksburg, VA 24060, USA

[3] Virginia Tech Carilion School of Medicine, Roanoke, VA 24016, USA

[4] Graduate Program in Translational Biology, Medicine, and Health, Virginia Tech, Blacksburg, VA 24060, USA

* correspondence:

James W. Smyth

The Fralin Biomedical Research Institute at VTC

2 Riverside Circle

Roanoke, VA 24016

smythj@vtc.vt.edu

Phone: 540-526-2500

Fax: 540-985-3373

RUNNING TITLE: Adenovirus targets gap junction function

NONSTANDARD ABBREVIATIONS

Connexin43: Cx43

Gap junction intercellular communication: GJIC

E4 open reading frame 1: E4orf1

Human induced pluripotent stem cell derived-cardiomyocyte: HiPSC-CM

Multiplicity of infection: MOI

Infectious units: iu

ABSTRACT

Adenoviruses are responsible for a spectrum of pathogenesis including viral myocarditis. The gap junction protein connexin43 (Cx43, gene name *GJA1*) facilitates rapid propagation of action potentials necessary for each heartbeat. Gap junctions also propagate innate and adaptive antiviral immune responses, but how viruses may target these structures is not understood. Given this immunological role of Cx43, we hypothesized that gap junctions would be targeted during adenovirus type 5 (Ad5) infection. We find reduced Cx43 protein levels due to decreased *GJA1* mRNA transcripts dependent upon β-catenin transcriptional activity during Ad5 infection, with early viral protein E4orf1 sufficient to induce β-catenin phosphorylation. Loss of gap junction function occurs prior to reduced Cx43 protein levels with Ad5 infection rapidly inducing Cx43 phosphorylation events consistent with altered gap junction conductance. Direct Cx43 interaction with ZO-1 plays a critical role in gap junction regulation. We find loss of Cx43/ZO-1 complexing during Ad5 infection by co-immunoprecipitation and complementary studies in human induced pluripotent stem cell derived-cardiomyocytes reveal Cx43 gap junction remodeling by reduced ZO-1 complexing. These findings reveal specific targeting of gap junction function by Ad5 leading to loss of intercellular communication which would contribute to dangerous pathological states including arrhythmias in infected hearts.

KEYWORDS

Adenovirus, Gap junction, Connexin, β-catenin, myocarditis

INTRODUCTION

Gap junctions comprising connexin proteins couple the cytoplasms of apposing cells, effecting the direct exchange of factors such as signaling molecules and ions [1]. Connexin43 (Cx43, gene *GJA1*) is the most ubiquitously expressed connexin and is necessary for rapid propagation of action potentials in the working myocardium [2]. Alterations in Cx43 and remodeling of gap junctions during cardiac stress alters electrical coupling between myocytes and precipitates the arrhythmogenic substrate of sudden cardiac death [3-5]. Additionally, gap junction intercellular communication (GJIC) facilitates the propagation of innate and adaptive antiviral immune responses. Specifically, transfer of 2'3'-cyclic guanosine monophosphate–adenosine monophosphate (cGAMP), capable of activating the interferon response, and cell-to-cell exchange of peptides utilized for major histocompatibility complex (MHC) presentation by uninfected cells can both occur via GJIC [6-8]. MHC presentation and interferon activation are both well-established antiviral processes and thus GJIC provides a means for uninfected cells to amplify the host response and limit viral spread [9-13].

Extensive transcriptional and post-translational regulation of Cx43 allows dynamic control of gap junction gating and turnover [14-16]. Studies on specific transcriptional regulation of Cx43 during development and disease have identified numerous transcription factors responsible that include β-catenin, TBX2, PAR1, AP1, SP1, NKX2.5, STAT3, and IRX3 [17-19]. Interestingly, gap

junction formation is also regulated post-transcriptionally by internally translated isoforms of Cx43 which modulate channel assembly in the Golgi apparatus [20-22]. Post-translational modifications, primarily phosphorylation of the Cx43 C-terminus, are well described in modification of forward-trafficking, gap junction assembly, channel conductance, and internalization [23-26]. Furthermore, these phosphorylation events affect Cx43 protein-protein interactions with binding partners such as Zonula Occludens 1 (ZO-1) and 14-3-3 proteins [26-28]. Data suggest Cx43/ZO-1 association is increased during incorporation into and removal from the gap junction plaque, interpreting this interaction with increased Cx43 trafficking dynamics [29-32]. Additionally, tight junction associated molecules such as the Coxsackievirus and adenovirus receptor (CAR) impact gap junction formation in addition to ZO-1 [33].

Adenoviruses are non-enveloped dsDNA tumor viruses typically associated with mild respiratory illness that can also lead to life-threatening diseases including viral myocarditis [34,35]. Importantly, adenovirus is increasingly recognized as a cause of sudden cardiac death and has been detected in 59% of patients with virus-associated myocarditis [35,36]. Human adenovirus serotypes 5 and 2 are predominantly responsible for adenoviral mediated viral myocarditis, but the molecular mechanisms of adenovirus cardiotropism and infection-induced arrhythmogenesis are unknown [37]. Due to pathogen-host species specificity, modeling adenovirus-induced human viral myocarditis has been historically difficult and current knowledge of viral myocarditis mechanisms is primarily

derived from mouse models utilizing another major cause of myocarditis in humans, Coxsackievirus B3 [38-42]. Ineffective infection of murine cells with human adenovirus reveals species-dependent subcellular differences limiting development of such a model [43,44]. Previously reported mouse models of viral myocarditis utilizing mouse adenovirus have focused primarily on chronic damage caused by immune responses as opposed to alterations in cardiomyocyte biology during active infection [45-47]. Adenoviral proteins in Early Region 4 (E4) are reported to negatively regulate Cx43 while positively regulating Cx40 in the context of Early Region 1 (E1) and 3 (E3) deleted human adenoviral vectors in mouse heart tissue which may not reflect wild type infection [48]. Furthermore, adenoviral E4 open reading frame 1 (E4orf1) protein is known to activate AKT which, through phosphorylation, regulates both Cx43 and β-catenin [26,49]. With the advent of human induced pluripotent stem cell derived-cardiomyocytes (HiPSC-CM) it is now possible to study molecular mechanisms contributing to human adenoviral myocarditis and arrhythmogenesis. Indeed, HiPSC-CMs have been demonstrated as an effective model for screening antivirals for Coxsackieviral myocarditis [50].

Here, we investigate the effect of adenoviral infection on gap junctions and Cx43. Given that adenoviral early gene products activate host-cell protein kinase signaling pathways which are known to converge on Cx43, we hypothesized that Cx43 expression and GJIC would be compromised during infection [51-53]. Spontaneously immortalized human keratinocytes (HaCaT) infected with wild

type human adenovirus serotype 5 (Ad5) are employed to determine the impacts on gap junction protein expression and function as a non-transformed epithelial cell model. These experiments are complemented with studies in HiPSC-CMs to validate physiological relevance and provide insight on the impact of infection on cardiac muscle cells which require gap junctions to facilitate each heartbeat. We demonstrate a loss of Cx43 at the level of transcription through β-catenin transcriptional activity and that gap junction function is impaired prior to loss of Cx43 protein. We find altered Cx43 phosphorylation associated with reduced channel open probability as a mechanism for reduced GJIC [54]. Finally, reduced complexing of Cx43 with ZO-1 in cardiomyocytes demonstrates remodeling of cardiac electrical coupling structures during acute viral infection, which *in vivo* would contribute to an arrhythmogenic substrate.

Materials and Methods

Cell culture

HEK293FT (Thermo Fisher, Waltham, MA, USA), HEK293A (Thermo Fisher, Waltham, MA, USA), A549 (ATCC, Manassas, VA, USA), HT1080 (ATCC, Manassas, VA, USA), HaCaT (AddexBio, San Diego, CA, USA), and HaCaT-GJA1+ cells were maintained and passaged in DMEM, high glucose, with L-Glutamine (Genesee Scientific, San Diego, CA, USA) supplemented with 10 % fetal bovine serum (FBS), non-essential amino acids (Life Technologies, Carlsbad, CA, USA), and MycoZap Plus-CL (Lonza, Basel, Switzerland) unless

otherwise specified. HiPSC-CMs were obtained from Axol Bioscience and maintained in Cadiomyocyte Maintenance Basal Medium (Axol, Cambridge, UK) supplemented with Cardiomyocyte Supplement (Axol, Cambridge, UK) according to manufacturer's instructions. Cells were maintained in a humidified atmosphere of 5 % CO_2 at 37 °C.

Viruses and infection

Ad5 was obtained from ATCC (Manassas, VA, USA) and propagated in A549 cells. AdlacZ was generated according to manufacturer's instructions from pAd/CMV/V5-GW/lacZ (Thermo Fisher, Waltham, MA, USA). Viruses were purified by CsCl ultracentrifugation as previously described and titer determined by immunofluorescence confocal microscopy in HEK293A cells [55]. All infections were performed at a multiplicity of infection (MOI) of 10 in serum-free DMEM and supplemented with equal volume of supplemented DMEM (10 % FBS) 1-hour post infection (hpi). For inhibition of transcriptional activity of β-catenin using LF3, HaCaT cells were infected in serum-free DMEM as above followed by addition of equal volume supplemented DMEM (10 % FBS) containing DMSO or LF3 (final concentration 60 μM; Selleckchem, Houston, TX, USA) 1 hpi. To test LF3 effects on adenoviral replication kinetics, cells were infected and treated with LF3 as above followed by isolation of DNA using DNeasy (Qiagen, Hilden, Germany) according to manufacturer's instructions. qPCR was then performed for adenoviral genomes with SYBR Select Master Mix for CFX (Thermo Fisher, Waltham, MA, USA) on a QuantStudio 6 Flex system (Thermo Fisher, Waltham,

MA, USA) with primers designed to amplify adenoviral gDNA (forward primer- TTAGATTATGTGGAGCACCC; reverse primer- CACATAATATCTGGGTCCCC). To assay changes in *GJA1* mRNA independent of viral infection, HaCaT cells were treated with DMSO or LF3 (final concentration 60 μM) and subjected to RT-qPCR at 24 h post-treatment.

RT-qPCR

Cells were lysed in TRIzol (Thermo Fisher, Waltham, MA, USA) and clarified by phenol-chloroform phase separation before RNA isolation using PureLink RNA mini kit (Thermo Fisher, Waltham, MA, USA) and PureLink on-column DNase digestion (Thermo Fisher, Waltham, MA, USA) according to manufacturer's instructions. cDNA was generated with iScript Reverse Transcription Supermix for RT-qPCR (Bio-Rad, Hercules, CA, USA) according to manufacturer's instructions. Real-time PCR was performed with SYBR Select Master Mix for CFX (Thermo Fisher, Waltham, MA, USA) on a QuantStudio 6 Flex system (Thermo Fisher, Waltham, MA, USA). 18SrRNA (forward primer- GGCCCTGTAATTGGAATGAGTC; reverse primer- CCAAGATCCAACTACGAGCTT) and GAPDH (forward primer- ACATCGCTCAGACACCATG; reverse primer- TGTAGTTGAGGTCAATGAAGGG) were utilized as internal references. Gene expression data was collected for *CDKN1A* (forward primer- GCAGACCAGCATGACAGAT; reverse primer- GAGACTAAGGCAGAAGATGTAGAG)*, SFN* (forward primer-

CACTACGAGATCGCCAACAG; reverse primer-
GGTGCTGTCTTTGTAGGAGTC), *GJA1* (forward primer-
ACUUGGCGUGACUUCACUAC; reverse primer-
GUACUGACAGCCACACCUUC), *GJA5* (forward primer –
GCAGCCTCAGCTTTACAAATG; reverse primer –
GTGACAGATGTTGGCAGGAAT), *GJC1* (forward primer-
GGTAACCGAAGTTCTGGACAA; reverse primer-
CAATCAGAACAGTGAGCCAGA), *PKP2* (forward primer-
AAGCGATGAGAAGATGTGACG; reverse primer-
GGAGAGGTTATGAAGAATGCACA), *TJP1* (forward primer-
ATAGCTGATGTTGCCAGAGAA; reverse primer-
CAGAGCTACGTTGGTCAGTTC), *CTNNB1* (forward primer-
AAAATGGCAGTGCGTTTAG; reverse primer-TTTGAAGGCAGTCTGTCGTA),
TBX2 (forward primer- CCATCCCGCCTAGCACTAG; reverse primer-
CTAGGCTCCCGGCTGTTTC), and *F2R* (forward primer-
GTGCTGTTTGTGTCTGTGCT; reverse primer- AGCGACACAATTCAGACCCA).

Ad5 E4orf1 cloning and ectopic expression.

Ad5 E4orf1 was cloned into pSF-CAG-AMP (Sigma Aldrich, St. Louis, MO, USA) using In-Fusion cloning (Takara Bio, Kusatsu, Shiga, Japan) according to manufacturer's instructions. Briefly, Ad5 genomes were isolated from 10 µl of purified Ad5 using a DNeasy Blood & Tissue Kit (Qiagen, Hilden, Germany). E4orf1 was amplified using CloneAmp HiFi PCR Premix (Takara Bio, Kusatsu,

Shiga, Japan) with forward primer: CCGAGCTCTCGAATTATGGCTGCCGCTGTGGAAGC and reverse primer: AGTCAGTCAAGCTAGTTAAACATTAGAAGCCTGTCTTACAACAGGAAAAACA. Following pSF-CAG-AMP digestion with *Bam*HI and *Eco*RI (New England Biolabs, Ipswich, MA, USA) and purification In-Fusion cloning was performed and successful constructs purified following validation by sequencing. HaCaT cell were plated in 100 mm dishes and transfected with 5 µg of pSF-CAG-AMP-Empty or pSF-CAG-AMP-E4orf1 24 h prior to harvesting and analysis by western blotting and RT-qPCR. Validation of E4orf1 ectopic expression by RT-qPCR was performed as above with forward primer- GCGTAGAGACAACATTACAGCC and reverse primer- TGTATGTTGTTCTGGAGCGGG and mRNA abundance calculated using the formula $(1/(2^{CT\ of\ target})) / (1/(2^{CT\ of\ Reference\ Average}))$ with GAPDH and 18SrRNA utilized as internal references.

Western blotting

Cells were lysed in RIPA buffer (50 mM Tris pH 7.4, 150 mM NaCl, 1 mM EDTA, 1 % Triton X-100 (Sigma Aldrich, St. Louis, MO, USA), 1 % sodium deoxycholate, 2 mM NaF, 200 µM Na_3VO_4, 0.1 % sodium dodecyl sulfate, 5 mM n-ethylmaleimide) supplemented with HALT protease and phosphatase inhibitor cocktail (Thermo Fisher, Waltham, MA, USA). Protein was clarified by sonication and centrifugation and concentration determined by DC protein assay (Bio-Rad, Hercules, CA, USA). 4X Bolt LDS sample buffer supplemented with 400 mM DTT was added to samples then heated to 70 °C for 10 min and subjected to SDS-

PAGE using NuPAGE Bis-Tris 4-12 % gradient gels and MES (Thermo Fisher, Waltham, MA, USA) running buffer according to manufacturer's instructions. Proteins were transferred to PVDF (Bio-Rad, Hercules, CA, USA) membrane and fixed in methanol followed by air drying. PVDF membranes were reactivated in methanol followed by blocking in 5 % nonfat milk (Carnation, Los Angeles, CA, USA) or 5 % bovine serum albumin (Fisher Scientific, Waltham, MA, USA) in TNT buffer (0.1 % Tween 20, 150 mM NaCl, 50 mM Tris pH 8.0) for 1 h at room temperature. Primary antibody labeling was performed overnight at 4 °C using primary antibodies rabbit anti-Cx43 (1:5000; Sigma-Aldrich, St. Louis, MO, USA), mouse anti-α-tubulin (1:5000; Sigma Aldrich, St. Louis, MO, USA), mouse anti-GAPDH (1:2000; Fitzgerald Industry International, Acton, MA, USA), mouse anti-Adenovirus Hexon [8C4] (1:5000; Abcam, Cambridge, UK), mouse anti-β-catenin (1:200; Santa Cruz Biotechnology), rabbit anti-phospho-β-catenin (Ser552) (1:1000; Cell Signaling Technology, Danvers, MA, USA), mouse anti-Adenovirus E1A [M73] (1:2000; Abcam, Cambridge, UK), mouse anti-phospho-(Ser) 14-3-3 Mode 1 binding motif (1:1000; Cell Signaling Technology, Danvers, MA, USA), rabbit anti-phospho-Cx43(Ser368) (1:1000; Cell Signaling Technology, Danvers, MA, USA), mouse anti-ZO-1 (1:1000, BD Biosciences, San Jose, CA, USA), mouse anti-E-Cadherin (1:1000; BD Diagnostics, Franklin Lakes, NJ, USA), rabbit anti-CAR (1:500; Cell Signaling Technology, Danvers, MA, USA), goat anti-RPL22 (1:800; Abcam, Cambridge, UK), mouse anti-Cx40 (1:500; Thermo Fisher, Waltham, MA, USA), rabbit anti-Cx45 (1:500; Novus Biologicals, Littleton, CO, USA), and rabbit anti-phospho-Cx43(Ser262) (1:1000; Santa Cruz

Biotechnology, Dallas, TX, USA). Membranes were washed 6 times before secondary antibody labeling for 1 h at room temperature with goat secondary antibodies conjugated to Alexa Fluor 555, Alexa Fluor 647 (Thermo Fisher, Waltham, MA, USA), or HRP (Abcam, Cambridge, UK) or donkey anti-goat conjugated to Alexa Fluor 633 (1:5000; Thermo Fisher, Waltham, MA, USA). Fluorescently labeled membranes were soaked in methanol and air dried prior to imaging. Clarity Western ECL (Bio-Rad, Hercules, CA, USA) substrate was added to HRP labeled membranes according to manufacturer's instructions prior to imaging. Stripping was performed following phospho-Cx43 isoform detection prior to labeling for total Cx43 using ReBlot Plus Strong (EMD Millipore, Burlington, MA, USA) according to manufacturer's instructions. Membranes were imaged on a Chemidoc MP imaging system (Bio-Rad, Hercules, CA, USA).

Immunofluorescence confocal microscopy

Cells were fixed for 20 min with 4 % PFA in PBS at room temperature or for 5 min with -20 °C methanol on ice. Cells were permeabilized and blocked with 5 % normal goat serum (Invitrogen, Carlsbad, CA, USA) and 0.5 % Triton X-100 (Sigma Aldrich, St. Louis, MO, USA) in PBS for 1 h at room temperature. Primary antibody labeling was performed for 1 h at room temperature using rabbit anti-Cx43 (1:2000; Sigma Aldrich, St. Louis, MO, USA), mouse anti-E2A [B6-8] (1:250; generously provided by D. Ornelles, Wake Forest School of Medicine, Microbiology and Immunology), mouse anti-Adenovirus E1A [M73] (1:500; Abcam, Cambridge, UK), mouse anti-β-catenin (1:50; Santa Cruz Biotechnology,

Dallas, TX, USA), rabbit anti-Ad5 (1:5000; Abcam, Cambridge, UK), and mouse anti-ZO-1(1:500; BD Biosciences, San Jose, CA, USA). Cells were washed 6 times prior to secondary antibody labeling for 1 h at room temperature with goat secondary antibodies conjugated to Alexa Fluor 488 or Alexa Fluor 555 (Thermo Fisher, Waltham, MA, USA). During secondary antibody labeling cells were counterstained with DAPI and wheat germ agglutinin (WGA) conjugated Alexa Fluor 647. Slides were mounted using Prolong Gold Antifade (Life Technologies, Carlsbad, CA, USA).

Image analysis

To measure nuclear β-catenin enrichment, 8-bit single-Z image thresholding was performed on DAPI channels and divided by 255 to create fluorescence intensity values of 0 (non-nuclear) and 1 (nuclear). Single-Z images were utilized to reduce capture of axial fluorescence signal above and below nuclei. The threshold and binary DAPI channels were multiplied by the β-catenin channels to exclude non-nuclear signal and mean fluorescence intensity was subsequently normalized to total β-catenin mean fluorescence intensity after subtracting background. To measure Cx43/PDI colocalization, single Z-slices of Cx43 and PDI channels were subjected to Pearson's correlation and Manders' co-occurrence with thresholding using the JACoP plugin [56]. Colocalization of pixels were generated using the Colocalization plugin. Analyses performed in ImageJ software (NIH, Bethesda, MD, USA).

Triton X-100 solubility assay

Cells were harvested in 1% Triton X-100 buffer (50mM Tris, pH 7.4, 1 % Triton X-100, 2 mM EDTA, 2 mM ethylene glycols-bis(β-aminoethyl ether)-*N,N,N,N*-tetraacetic acid [EGTA], 250 mM NaCl, 1 mM NaF, 0.1 mM Na_3VO_4) supplemented with HALT Protease and Phosphatase Inhibitor (Thermo Fisher). Samples were rotated at 4 °C for 1 h. A small volume was removed to serve as the total protein fraction. Remaining lysate was centrifuged for 30 min at 15,000 x *g* at 4 °C and supernatant reserved as soluble fraction. Pellets containing insoluble proteins were resuspended in Bolt LDS sample buffer with DTT (Thermo Fisher). All samples were sonicated and centrifuged for 20 min. at 10,000 x *g* at 4°C followed by addition of 4X Bolt LDS sample buffer supplemented with 400 mM DTT where appropriate prior to western blotting.

Scrape-load dye-transfer assay

HaCaT cells were seeded and grown to confluency prior to infection with AdlacZ or Ad5 in 35 mm glass-bottom dishes and then washed 3 times with PBS prior to adding 0.05 % Lucifer Yellow (CH K^+; Life Technologies, Carlsbad, CA, USA) and 100 µg/mL dextran (MW-10,000 Da.) conjugated to Alexa Fluor 647 (Thermo Fisher, Waltham, MA, USA). Scrape-load dye-transfer assay was performed as previously described using 5 min room temperature incubation time post-scrape [57]. Cells were washed 3 times with PBS then immediately fixed for 20 min at room temperature with 37 °C 4 % paraformaldehyde prior to imaging.

Quantification of dye spread was performed as previously described using ImageJ software [57].

Engineering of lentivirus-mediated stable *GJA1* overexpressing HaCaT cells (HaCaT-GJA1+)

Lentivirus were produced from pLenti6.3-hGJA1 [20] according to manufacturer's instructions (ViraPower Lentiviral Expression System; Thermo Fisher, Waltham, MA, USA) and propagated in 293FT cells. Lenti-hGJA1 titer was determined according to manufacturer's instructions in HT1080 cells and normalized virus was used to transduce HaCaT cells. 48 h post transduction, lentivirus-transduced HaCaT cells were treated with blasticidin (10 µg/ml) supplemented media. Media changes were performed every 2 days and viable colonies extracted with cloning rings (Scienceware, Warminster, PA, USA). Clones were expanded and screened for expression by western blotting and immunofluorescence confocal microscopy.

Immunoprecipitation

Infected HaCaT-GJA1+ or HaCaT cells were harvested at indicated hours post infection on ice in RIPA. Cell lysates were normalized to 500 µg per reaction. Inputs were removed prior to immunoprecipitation and denatured in NuPAGE LDS sample buffer (Thermo Fisher, Waltham, MA, USA) at RT. Protein G Dynabeads (Thermo Fisher, Waltham, MA, USA) were added at 10 % sample volume to preclear lysates for 20 min at 4°C prior to immunoprecipitation with

rabbit anti-Cx43 antibody (2 µg, Sigma-Aldrich, St. Louis, MO, USA), or rabbit IgG isotype control (2 µg, Jackson, West Grove, PA, USA) for 1 h at 4°C. Samples were then incubated with Protein G Dynabeads for 45 minutes at 4°C. Samples were washed in RIPA buffer followed by eluting with NuPAGE LDS sample buffer and subject to western blotting.

Coimmunoprecipitation

Ad5- or AdlacZ-infected HaCaT cells were harvested 24 hpi on ice in CoIP buffer (50 mM HEPES pH 7.4, 150 mM KCl, 1 mM EDTA, 1 mM EGTA, 1 mM DTT, 1 mM NaF, 100 µM Na_3VO_4, 0.5% Triton X-100) with HALT protease and phosphatase inhibitor cocktail (Thermo Fisher, Waltham, MA, USA). Cell lysates were normalized to 1 mg per reaction. Inputs were removed prior to CoIP and denatured in NuPAGE LDS sample buffer. Protein G Dynabeads were added at 10 % sample volume to preclear lysates for 30 min at 4°C prior to immunoprecipitation with mouse anti-ZO-1 (2 µg, BD Biosciences, San Jose, CA, USA) or mouse IgG isotype control (2 µg, Jackson, West Grove, PA, USA) for 1 h at 4°C. Samples were incubated with Protein G Dynabeads for 30 minutes at 4°C. Samples were washed in CoIP buffer followed by eluting and denaturing with NuPAGE LDS sample buffer and subject to western blotting.

Super-resolution STORM localization and analysis

Cells were fixed with -20 °C methanol on ice for 5 min followed by 3 washes with PBS. Cells were blocked with 5 % normal donkey serum and 0.5 % Triton X-100

in PBS for 1 h at room temperature. Primary antibody labeling was performed for 1 h at room temperature with rabbit anti-Cx43 (1:2000; Sigma-Aldrich, St. Louis, MO, USA) and mouse anti-ZO-1 (1:500; BD Biosciences, San Jose, CA, USA). Cells were washed 6 times prior to secondary antibody labeling for 1 h at room temperature with donkey antibodies conjugated to Alexa Fluor 647 or CF568 (Biotium, Hayward, CA, USA). Cells were washed 6 times and stochastic optical reconstruction microscopy (STORM) conducted with a Vutara 350 microscope (Bruker, Billerica, MA, USA). Cells were imaged in 50 mM Tris-HCl, 10 mM NaCl, 10 % (wt/vol) glucose buffer containing 20 mM mercaptoethylamine, 1% (vol/vol) 2-mercaptoethanol, 168 active units/ml glucose oxidase, and 1404 active units/ml catalase. 5000 frames were acquired for each probe and 3D images were reconstructed in Vutara SRX software. Coordinates of localized molecules were used to calculate pair correlation functions in the Vutara SRX software.

Statistics

All quantification was performed on experiments repeated at least three times. Data are presented as mean ± SEM. Statistical analysis was conducted with GraphPad Prism 8.2.0 (GraphPad Software, Inc., La Jolla, CA, USA). Data were analyzed for significance using Student's t test, one-way ANOVA with Tukey's multiple comparisons test (when comparing basal gap junction gene expression data), two-way ANOVA, with Sidak's (when comparing Ad5-infected to control within time points across multiple time points) or Dunnet's (when comparing

infected time points to 0 hpi) multiple comparisons tests. A value of $p < 0.05$ was considered statistically significant.

RESULTS

Connexin43 protein levels are reduced during adenovirus type 5 infection. Given Cx43 gap junctions immunologically couple cells to effect propagation of antiviral immune responses, we sought to determine the impact on Cx43 by Ad5 infection [6-8]. To assess Cx43 levels and subcellular localization (cytosolic or membrane) during infection, HaCaT cells were infected with either AdlacZ or Ad5 at a MOI of 10 iu/cell followed by fixation 48 hpi and immunolabeled for Cx43 (green) and visualized by immunofluorescence confocal microscopy. Adenoviral E2A (red) labeling confirms 100% infection with nuclei labeled using DAPI (blue). We find global reductions of Cx43 in Ad5-infected cells compared to controls (Figure 3.1A). To confirm immunofluorescence data biochemically, HaCaT cells were infected at a MOI of 10 iu/cell with Ad5 or AdlacZ and protein lysates were harvested every 24 hpi for 72 h. We find Cx43 levels are reduced to 42% by 24 hpi declining to 5% at 72 hpi compared to AdlacZ-infected controls (Figure 3.1B, quantified in 3.1C). To test global versus specific reductions in host-cell protein levels, we also investigated Cx40, Cx45, RPL22, E-cadherin, and CAR where we reveal a reduction of CAR to 48% with no loss of Cx40, Cx45, E-cadherin, or RPL22 at 24 hpi (Figure 3S1). AdlacZ is a replication incompetent adenoviral vector and serves as a control for virus binding primary and secondary receptors,

integrin-mediated endocytosis, and cytosolic dsDNA host-cell responses. Increased Cx43 expression was observed over time in control cells which we attribute to stabilization of intercellular junctions upon confluency.

Specific targeting of gap junction gene transcription during adenovirus type 5 infection.

In order to determine if changes in Cx43 protein levels were a result of negative gene regulation, we performed RT-qPCR on Ad5-infected HaCaT cells at 24 and 48 hpi. We demonstrate dynamic host-cell gene expression at 24 hpi with both increased and decreased levels of specific host-cell mRNAs and, as such, we focused our studies on mechanisms of Cx43 gap junction modulation within this first 24 h period. By 48 hpi all genes tested were suppressed as expected as the viral life cycle had progressed to effect virally-induced host-cell global gene repression. Consistent with previous findings of active Ad5 infection inactivating and degrading p53, we confirm a reduction in known p53 transcriptional targets *CDKN1A* (p21) to 14% and *SFN* (14-3-3σ) to 7% (Figure 3.2A) [58-65]. *GJA5* (Cx40), *GJA1* (Cx43), and *GJC1* (Cx45) were detected by RT-qPCR in HaCaT cells, with *GJA1* having highest expression (Figure 3S2). After infection with Ad5, RT-qPCR analysis demonstrates a targeting of *GJA1* and *GJA5* in HaCaT cells reducing levels to 46% and 0.3% respectively (Figure 3.2B). Interestingly, although detectable, *GJC1* is not negatively regulated during adenoviral infection (Figure 3.2B). Despite *GJA5* mRNA reduction during adenoviral infection, protein levels are maintained at 24 hpi (Figure 3S1). To determine if Ad5 infection results

in dysregulation of other critical junctional genes relevant to the cardiac intercalated disc, *PKP2* (Plakophilin 2) and *TJP1* (ZO-1) expression were analyzed. *PKP2* mRNA levels are maintained while a reduction in *TJP1* mRNA to 20% is detected at 24 hpi (Figure 3.2C).

Early adenoviral factors induce β-catenin transcriptional activity through growth factor signaling.

In order to determine the mechanism by which *GJA1* is negatively regulated during Ad5 infection, RT-qPCR was performed on *GJA1*-known and -predicted transcription factors [19]. *CTNNB1* (β-catenin), *TBX2* (T-Box 2), *F2R* (PAR-1) were found elevated 24 hpi (demonstrating global host-cell gene shutoff has not occurred at this early time point) (Figure 3S3, Figure 3.3A). Given that β-catenin functions as both a transcription factor and a scaffolding protein shown to directly bind Cx43 [66,67], localization of β-catenin was determined by immunofluorescence confocal microscopy of AdlacZ- and Ad5-infected HaCaT cells 24 hpi (Figure 3.3B). Using single Z-position images, we find 64% increased nuclear β-catenin, as determined through binary mask generation and multiplication from DAPI signal (greyscale panels Figure 3.3B, quantified in 3.3C). To further validate increased nuclear β-catenin and associated transcriptional activity, phosphorylation of β-catenin at Ser552 (β-catenin$^{phos(S552)}$) by AKT which has previously been identified to result in translocation to the nucleus to effect transcriptional activity [68], was analyzed by western blot. We find a significant increase of 52% and 71% in β-catenin$^{phos(S552)}$ relative to total β-catenin at 24 and

48 hpi respectively (Figure 3.3D, quantified in 3.3E). Global effects on host cell RNA and protein would be occurring at later time points as viral assembly and cell lysis is underway so loss of significance at 72 hpi is expected. The adenoviral E4orf1 protein is known to activate AKT, leading us to ask if E4orf1 is sufficient to induce phosphorylation of β-catenin at Ser552 [49,53]. In order to determine sufficiency, we transiently transfected HaCaT cells to overexpress adenoviral E4orf1 and analyzed β-catenin$^{phos(S552)}$ levels at 24 h post transfection where we find an increase of 28% (Figure 3.3F, quantified in 3.3G). Overexpression of adenoviral E4orf1 was confirmed by RT-qPCR (Figure 3S4).

β-catenin transcriptional activity is necessary for adenoviral Cx43 transcriptional suppression.

We next sought to determine if β-catenin transcriptional activity was necessary for reduced *GJA1* mRNA during Ad5 infection in HaCaT cells. *GJA1* mRNA levels are rescued by 42% in Ad5-infected HaCaT cells 24 hpi treated with LF3, a specific small molecule inhibitor of β-catenin transcriptional activity [69,70], compared to DMSO treated infected cells (Figure 3.4A). In order to determine effects of LF3 alone in the absence of adenoviral infection on *GJA1* mRNA levels, we treated uninfected HaCaT cells with LF3 for 24 h and find no significant change in *GJA1* mRNA. Although not statistically significant but trending, LF3 in the absence of adenoviral infection appears to decrease *GJA1* mRNA, potentially supporting previous findings which describe β-catenin as a classical transcriptional activator of *GJA1* [71] (Figure 3.4B). Finally, we tested if

LF3 alters viral genomic DNA load and performed qPCR of adenoviral genomes 24 hpi in Ad5-infected, LF3-treated, HaCaT cells where no change in amount of adenoviral genomic DNA was detected when compared to Ad5-infected, DMSO-treated controls (Figure 3.4C). In conclusion, inhibition of β-catenin transcriptional activity with LF3 is sufficient to rescue *GJA1* mRNA levels during adenoviral infection independent of viral life cycle progression.

Cx43 protein occurs in reduced levels at the endoplasmic reticulum and is primarily junctional during adenovirus infection.

We next asked if Cx43 trafficking and localization were altered early during adenoviral infection. In order to determine if Cx43 is retained in the endoplasmic reticulum (ER) and therefore subjected to altered forward trafficking during adenoviral infection, HaCaT cells were infected with AdlacZ or Ad5 followed by fixation and labeled for Cx43 and the ER resident protein, Protein Disulfide Isomerise (PDI) for colocalization analysis (Figure 3.5A). Changes in colocalization were quantified utilizing Manders' cooccurrence and Pearson's correlation functions and demonstrate a 36% reduction in Manders' Coefficients and a 62% reduction in Pearson's Coefficients in Ad5-infected HaCaT cells compared to AdlacZ-infected control cells at 24 hpi (Figure 3.5B, 3.5C). Given that there is less Cx43 colocalized with the ER of Ad5-infected HaCaT cells, we next sought to determine changes in junctional status of Cx43 (ie. cytosolic or membrane Cx43 compared to gap junction Cx43) by Triton solubility fractionation. We find a 76% increase in the insoluble / soluble Cx43 ratio in Ad5-

infected HaCaT cells compared to AdlacZ-infected control cells at 24 hpi, signifying that remaining Cx43 is primarily within gap junction structures during adenoviral infection (Figure 3.5D, quantified in 3.5E).

Adenovirus inhibits gap junction intercellular communication prior to reduction of Cx43 total protein levels during infection.

In order to determine if there is a functional change in GJIC, AdlacZ- or Ad5-infected HaCaT cells were analyzed by scrape-loading and dye-transfer of gap junction permeable 442 Da. Lucifer yellow (LY) and gap junction impermeable 10,000 Da. Dextran-Alexa Fluor 647 (Dex-647). Dye spread is found to be significantly reduced by 66% at 24 hpi, coinciding with reductions in Cx43 protein levels (Supplemental Figure 3S5A, quantified in 3S5B, Figure 3.1C). In addition to transcriptional and translational regulation, previous studies have demonstrated post-translational modifications of Cx43 in regulation of trafficking, internalization, gap junction permeability, and channel conductance [15,23,25,27,54,72-75]. Given that channel function can be altered independently of total protein level, we performed scrape-load dye-transfer assays on Ad5-infected HaCaT cells at 12 hpi, prior to detectable reductions in total Cx43 protein levels (Supplemental Figure 3S5C, quantified in 3S5D). We find a significant reduction in dye spread in Ad5-infected cells compared to AdlacZ-infected controls by 69% at 12 hpi indicating direct targeting of Cx43 gap junction channel function during Ad5 infection (Figure 3.6A, quantified in 3.6B).

Direct targeting of Cx43 gap junctions through phosphorylation during adenovirus type 5 infection.

In addition to using wild-type HaCaT (HaCaT-WT) cells, we used lentiviral transduction to establish clonal HaCaT cells over-expressing *GJA1* (HaCaT-GJA1+) to circumvent reduced Cx43 levels during Ad5 infection and better enable the interrogation of Cx43 phosphorylation status. AdlacZ- or Ad5-infected wild-type HaCaT (HaCaT-WT) and HaCaT-GJA1+ cells were analyzed for phosphorylation events known to impact channel opening probability, complexing with other proteins, and internalization. Phosphorylation of Cx43 at Ser373 by AKT creates a mode-1 14-3-3 binding motif which leads to decreased interaction of Cx43 with ZO-1 [26-28]. Subsequent phosphorylation of Cx43 at Ser368 by PKC results in reduced channel open probability and/or altered conduction properties [54,73,76,77]. From infected HaCaT-GJA1+ cells, Cx43 was immunoprecipitated followed by western blotting for phospho-Serine-14-3-3 mode-1 binding motif which we find increased by 213% at 24 hpi (Figure 3.7A, quantified in 3.7B). This antibody has previously been demonstrated as specific for phosphorylation of Cx43 at Ser373 through site-directed mutagenesis [27]. Cx43 was immunoprecipitated from AdlacZ- and Ad5-infected HaCaT-WT cell lysates followed by western blotting for Cx43 phosphorylated at Ser368 and total Cx43 where we find increased Ser368 phosphorylation of 114% (Figure 3.7C, quantified in 3.7D). The AKT phosphorylated 14-3-3 mode-1 binding motif Ser373 of Cx43 has been reported to disrupt interaction between Cx43 and ZO-1[28]. Cx43/ZO-1 complexing was analyzed in Ad5- or AdlacZ-infected HaCaT-WT

cells by coimmunoprecipitating ZO-1 and immunoblotting for Cx43 where we find reduced Cx43 coimmunoprecipitated with ZO-1 relative to input Cx43, supporting our phosphoSerine-14-3-3 mode-1 binding motif findings in HaCaT-GJA1+ cells (Figure 3.7E, quantified in 3.7F). The MAPK phosphorylation site of Cx43 at Ser262 (pCx43^{S262}) has been identified as downstream of Ser373/Ser368 phosphorylation and is a key event in the internalization and subsequent degradation of Cx43 [25,27,72]. Interestingly, in Ad5-infected HaCaT-GJA1+ and HaCaT-WT cells we do not find increased Cx43 phosphorylation at Ser262 (Figure 3S6). Furthermore, we find increased total Cx43 in Ad5 infected HaCaT-GJA1+ cells supporting our finding that endogenous Cx43 is targeted at the transcriptional level, and not directly targeted for degradation during infection resulting in Cx43 being maintained in gap junctions.

Ad5 targets Cx43 in cardiomyocytes and induces Cx43-gap junction remodeling.

We next sought to determine if Cx43 expression and Cx43-gap junction remodeling occurred in Ad5-infected cardiomyocytes and could thereby contribute to arrhythmogenic potential in infected hearts. HiPSC-CMs were infected with AdlacZ or Ad5 at a MOI of 10 iu/cell prior to harvesting protein or fixing for microscopy analysis. Recapitulating our findings in HaCaT cells, we find 35% reduced Cx43 protein levels in Ad5-infected cardiomyocytes at 24 hpi compared to mock-infected controls (Figure 3.8A, quantified in 3.8B). HiPSC-CMs were analyzed by immunofluorescence confocal microscopy to specifically

determine Ad5 induced reductions to cytoplasmic or membrane localized Cx43 in which we find global reductions 48 hpi (Figure 3.8C). Cx43 interactions with ZO-1 is experimentally described to increase gap junction plaque size, stabilize gap junctions, generate functional gap junctions in cardiomyocytes, and is also altered in failing human hearts [30,32,78-81]. Alterations in Cx43 gap junctions and ZO-1 localization were assayed in HiPSC-CMs by immunofluorescence confocal microscopy and STORM super-resolution localization 24 hpi. In single Z-position data capture, there is a reduced Cx43 co-localization with ZO-1 at cell-cell borders by confocal microscopy (Figure 3.8D). In order to quantify Cx43/ZO-1 complexing *in situ*, we turned to super resolution localization measurements. To assess effects on Cx43/ZO-1 interaction, cross-pair correlation functions were generated from STORM data. The probability of localizing two distinct target molecules together at a given distance with a function value of 1 is interpreted as no correlation, while increased function values greater than 1 confirm complexing between molecules. By cross-pair correlation analysis we find reduced probability of Cx43/ZO-1 interaction in Ad5-infected HiPSC-CMs compared to AdlacZ controls at 24 hpi (Figure 3.8E, quantified in 3.8F). Cx43/ZO-1 STORM data in HiPSC-CMs parallels CoIP data in HaCaT cells where loss of Cx43/ZO-1 complexing was found (Figure 3.7E, 3.7F).

DISCUSSION

Viral subversion of *intra*cellular processes is a topic of intense study covering mechanisms by which viruses hijack cellular machinery to replicate and assemble progeny. There is now growing interest in manipulation of *inter*cellular junctions by viruses and how events within infected cells precipitate alterations in cell-cell coupling. Such disruptions in intercellular junctions likely contribute to mild symptoms in the respiratory system for example, but in organs relying on intercellular communication for function, such as the heart, resulting disturbances in electrical coupling would be arrhythmogenic and potentially fatal. Targeting of gap junctions has been previously reported for several viruses but our understanding of underlying mechanisms for gap junction targeting is limited [82-87]. Prior research demonstrates, in the context of adenoviral vector-mediated transduction, that the adenovirus E4 gene products regulate Cx40 and Cx43 inversely through PKA and PI3K signaling [48]. Here, we report changes in Cx43 expression occurs more rapidly during wild type Ad5 infection. Furthermore, our data demonstrate that during a wild type Ad5 infection, Cx43 and Cx40 are both negatively regulated at the mRNA level, revealing differences that may only be apparent in the context of active replication where all viral genes are working cooperatively, as would be the case in an infected heart. [48]. At the protein level, we find Cx43 but not Cx40 or Cx45 to be significantly downregulated during adenoviral infection and therefore focus on Cx43 modulation for the majority of this study. Despite no detectable loss of Cx45 at the protein level in HaCaT cells, we reveal reductions in CAR during adenoviral infection which, in the context of cardiac infection, could potentially have an indirect effect on Cx45 localization

and function in atrioventricular conduction as previously identified [33,88]. E1 genes are deleted in adenoviral vectors to prevent transactivation of adenoviral genes, including E4, which may contribute to observed temporal differences, and highlights that while the Zhang *et al* study is relevant to use of adenoviral vectors in gene transduction, it is not necessarily informative regarding wild type adenoviral pathogenesis [89-91].

The adenoviral life cycle length is dependent on cell type, and in the laboratory replication and assembly of viral progeny temporally accelerated in transformed or tumorigenic cell lines. Cytopathic effect was only apparent from 60 hpi in the immortalized HaCaT cells and terminally differentiated HiPSC-CMs used in this study. Our findings of altered gap junction function and suppression of Cx43 transcription occur within 12-24 hpi when cells would still be metabolically active and virally induced host-cell global repression is incomplete. We include later time points in Figures 3.1, 3.3, and 3.8 to provide greater temporal context over the whole viral replication and cell lysis cycle.

Cx43 transcriptional regulation is a complex process orchestrated through cell type-dependent and -independent transcription factors. For example, Nkx2.5 activation of *GJA1* expression can be repressed by Irx3, which concomitantly acts as an activator for *GJA5* (Cx40), highlighting the fine-tuned transcriptional control of gap junction genes [17]. We find repression of Cx43 and Cx40 transcription during Ad5 infection while Cx45 mRNA levels are maintained.

Indeed, work by several groups has focused on transcription factors involved in Cx43 and Cx40 with less known about Cx45 transcriptional regulation, partly due to the ambiguity of the Cx45 promoter by functional analysis [19,92]. Van der Heyden *et al*. demonstrated Cx43 is likely a Wnt1 signaling target while there were no changes to Cx45 expression providing an example of connexin isotype-specific transcriptional regulation [71]. Furthermore, host-cell chromatin remodeling during adenoviral infection is an established mechanism of silencing cellular host genes and it is possible that Cx43 and/or Cx40 but not Cx45 transcription is suppressed through chromatin remodeling involving adenoviral E1A or adenoviral E4-orf3 related mechanisms [93-95].

Of *GJA1* known and predicted transcription factors, β-catenin is particularly relevant given its multifaceted roles in complexing with Cx43 as a scaffolding protein and classical definition as an activating transcription factor for *GJA1* [18,66,67,71]. Exquisite subversion of host cell transcriptional machinery by adenoviral proteins encompasses a breadth of strategies from chromatin remodeling to render target genes inaccessible to direct manipulation of transcription factor function [63,89,96-98]. One example of direct manipulation of a transcription factor is phosphorylation of β-catenin by AKT, a well described target of adenoviral E4orf1 [53,71]. We find increased β-catenin nuclear translocation by immunofluorescence and confirm *GJA1* transcriptional repression is dependent on β-catenin transcriptional activity using LF3, a small molecule inhibitor of β-catenin/TCF/Lef complex transcriptional activity [69,70]. Furthermore, adenoviral E4orf1 expression

alone induces a comparable phosphorylation of β-catenin as achieved during Ad5 infection demonstrating sufficiency to directly affect the function of β-catenin. Nuclear factor κB (NF-κB) is reported in positive regulation *of Gja1* in murine arteries and transcriptionally active β-catenin is known to lead to inhibition of NF-κB function [99,100]. One mechanism for indirect targeting of Cx43 expression by adenovirus could therefore involve this NF-κB/β-catenin axis. Direct suppression of *GJA1* through β-catenin has not yet been described although repressive transcription cofactors have been identified including Reptin52 (complexing as β-catenin/Reptin52/TATA box binding protein), ICAT (inhibitor of β-catenin and TCF-4), and chibby, which may provide a means for direct transcriptional suppression during adenoviral infection [66,101-103]. Our findings demonstrating a previously undefined role for β-catenin in repression of *GJA1* transcription, as opposed to the previously reported positive regulatory role [18], highlight the potential for studying Cx43 biology in the context of viral infection as a powerful tool in elucidation of critical cellular mechanisms of gap junction regulation.

As gap junctions facilitate the exchange of antiviral molecules including MHC class I peptides and cGAMP [6,7,104], GJIC is an attractive target for viruses, including Ad5, as a means to limit antiviral responses by reducing recruitment of immune cells and limiting the interferon response [9,105,106]. Gap junction function can be modulated directly and independent of protein levels by post-translational modifications with extensive studies focusing on phosphorylation. Several signal transduction cascades associated with growth factor signaling and known to act

on the Cx43 C-terminus are activated during Ad5 infection to mimic growth factor signaling. Specifically the E4orf1 and E4orf4 proteins ensure robust activation of the PI3K/AKT/mTOR pathway which is well described in modulation of gap junction localization and function [27,107]. AKT phosphorylation at Ser373 is involved in Cx43 hemichannel recruitment into the gap junction proper but also represents initiation of a cascade leading to channel internalization and degradation [27,28]. PKC phosphorylation at Ser368 is associated with reduced channel open probability and is subject to *cis*-gatekeeper events involving Ser373 phosphorylation but Ser365 dephosphorylation [54,108,109]. Subsequent phosphorylation of Cx43 by MAPK at residues including Ser255/262/279/282 is associated with internalization and eventual degradation [27,72,110,111]. We established HaCaT cells overexpressing *GJA1* in order to circumvent transcriptional suppression during adenoviral infection to assay post-translational modifications to identify increased phosphorylation at Cx43 Ser373 but no induction of phosphorylation at MAPK-associated residues. The fact that Cx43 levels actually increase in these cells during Ad5 infection suggest that while transcriptional suppression of Cx43 occurs, direct targeting of the Cx43 protein through phosphorylation by adenovirus is restricted to limiting channel function and not induction of gap junction internalization and degradation. In agreement with our Cx43 Ser373 and Ser262 phosphorylation data is the finding that Cx43 is primarily junctional during adenoviral infection with reduced ER localization, supporting a model where *de novo* Cx43 synthesis is reduced and Cx43 is maintained in *de facto* gap junctions.

While the aforementioned phosphorylation events have direct effects on channel function and therefore electrical coupling, phosphorylation status also dynamically alters Cx43 complexing with other scaffolding and membrane proteins. Specifically, Cx43 interacting proteins c-Src, ZO-1, ZO-2, Occludin, Claudin-5, β-catenin, p120, N-Cadherin, Plakophilin-2, Ankyrin-G, $Na_V1.5$, and mAChR, regulate gap junction function whereby complexing is reportedly regulated through phosphorylation of the Cx43 C-terminus [18,79,112-120]. We report increased phosphorylation of Cx43 at Ser373 during Ad5 infection, an event that can alter Cx43/ZO-1 complexing and therefore tightly associated with incorporation into, and removal from, the gap junction plaque [28,29,31,32,74,81]. We confirm this dissociation by co-immunoprecipitation and our STORM data in infected cardiomyocytes also reveal reduced Cx43/ZO-1 complexing, signifying pathological remodeling that could contribute to arrhythmogenesis. Beyond the gap junction, cross-talk between junctional proteins and ion channels at the cardiomyocyte intercellular junction occurs on many levels. Indeed, it has been demonstrated that loss of Cx43 C-terminus results in disturbed $Na_V1.5$ trafficking and sodium current, further providing evidence for the changes we describe during acute adenoviral infection and Cx43 phosphorylation contributing to the arrhythmogenic substrate [119]. HiPSC-CMs now provide a model cell system in which to interrogate the impact of human adenoviral infection on excitable cells and tissues, where disruption of highly ordered intercellular structures has

substantially more severe and life-threatening effects on organ function than in epithelia, for example.

Current understanding relating to viral infection of the heart predominantly focuses on chronic infection, or end-stage disease often related to immune-related global cardiac remodeling, dilated cardiomyopathy, and even sometimes post viral clearance [36,121]. Here, we identify a rapid shut down in intercellular communication through direct and indirect targeting of Cx43 gap junctions during adenoviral infection that, in cardiomyocytes, would contribute to an arrhythmogenic substrate. Our findings therefore provide mechanistic insight into arrhythmogenesis in the context of acute infection, where sudden cardiac death in young adults is increasing attributed to adenovirus [34,35]. In addition to animal models utilizing human Coxsackievirus B3, a murine model of viral myocarditis induced by mouse adenovirus has been developed. Mouse adenovirus serotype 1 (MAV-1) infection demonstrates interferon gamma and immunoproteasome activity induce cardiac damage in a chronic infection model *in vivo* [46,47]. Furthermore, increases in mortality in neonatal mice by MAV-1 is independent of viral load, inflammatory cytokine expression, or invading leukocytes, validating the need to understand acute viral pathogenesis prior to adaptive immune system cytotoxicity [45]. While development of an animal model is necessary to truly isolate viral- *vs* immune-mediated effects, HiPSC-CMs provide a powerful system in which to examine effects of human viral infection on human heart muscle cells. Disruption of viral manipulation of cellular pathways identified here

may inform design of therapeutics to protect against sudden cardiac death during infection. More broadly, as we further understand adenoviral manipulation of Cx43 and gap junctions, critical cellular pathways regulating this important cellular function will be elucidated with implications in all organ systems and disease states beyond cardiomyopathies.

ACKNOWLEDGEMENTS

The authors thank Dr. David Ornelles (Wake Forest School of Medicine, Microbiology and Immunology) for providing adenovirus reagents and helpful discussion. Dr. Allison N. Tegge (Fralin Biomedical Research Institute, Department of Statistics, Virginia Tech) for consultation on statistical methods used and Dr. Samy Lamouille for critical review of this manuscript (Fralin Biomedical Research Institute, Department of Biological Sciences, Virginia Tech). This work was supported by a NIH NHLBI R01 grant (HL132236 to J.W.S.), an American Heart Association Predoctoral Fellowship (18PRE33960573 to P.J.C.), a NHLBI F31 grant (HL140909 to C.C.J.), and a NHLBI F31 grant (HL152649 to R.L.P.).

AUTHOR CONTRIBUTIONS

J.W.S. and P.J.C. conceived the study. P.J.C. designed and conducted the experiments. J.W.S. and P.J.C. carried out data analysis and interpretation. J.D.T. performed immunoprecipitation experiments. A.V.P. performed preliminary experiments in A549 cells. C.C.J. performed 24 h time course western blot and Triton solubility assay. R.L.P. performed experiment determining LF3 impact on adenoviral replication. M.J.Z. performed experiment determining LF3 impact on infection-independent *GJA1* levels. P.J.C. wrote the manuscript with input from C.C.J. and J.W.S.

DECLARATION OF INTERESTS

The authors declare no competing interests.

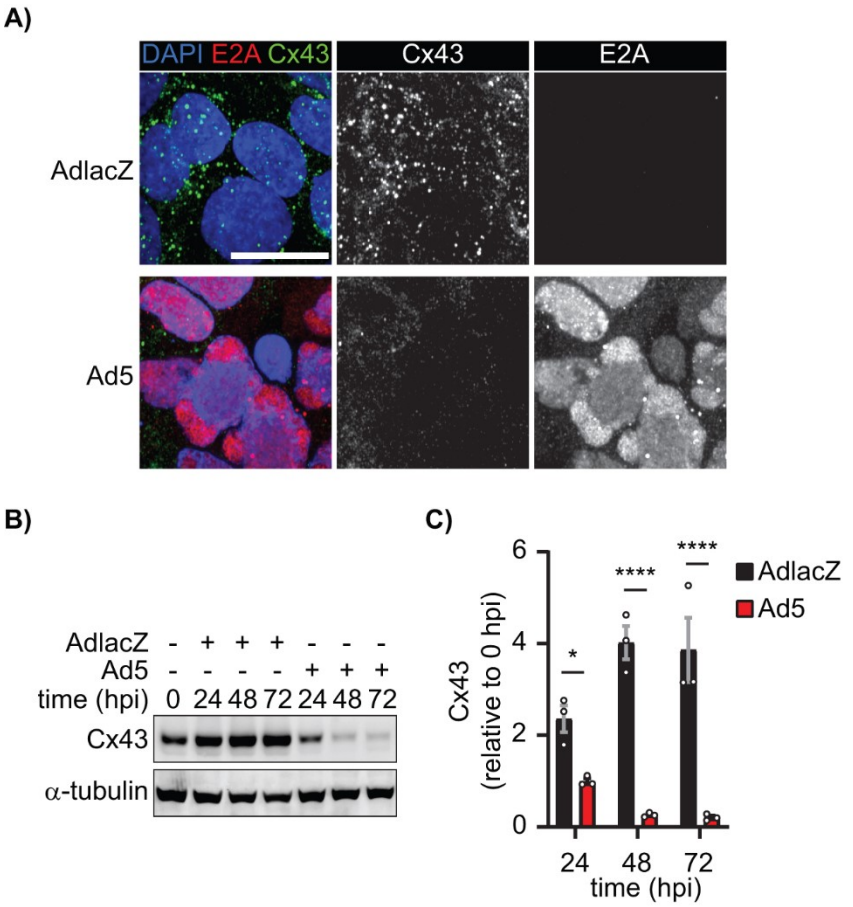

Figure 3.1) Connexin43 protein levels are reduced during adenovirus type 5 infection. HaCaT cells were infected with Ad5 or replication-incompetent AdlacZ at a multiplicity of infection (MOI) of 10 iu/cell and fixed at 48 hpi or protein harvested every 24 hpi for 72 h. **A)** Immunofluorescence confocal microscopy of HaCaT cells at 48 hpi probed for Cx43 (green) and adenovirus E2A (red) with nuclei identified using DAPI (blue). Original magnification: X100. Scale bar: 20μm. **B)** Western blot probed for Cx43 expression in HaCaT cells. Detection of α-tubulin serves as loading control. **C)** Densitometry analysis of B. Statistical analysis was performed with two-way analysis of variance (ANOVA) with Sidak's multiple comparisons test. (n=3). *p≤0.05, **p≤0.01, ***p≤0.001, ****p<0.0001. Data are represented as mean ±SEM. See also Figure 3S1.

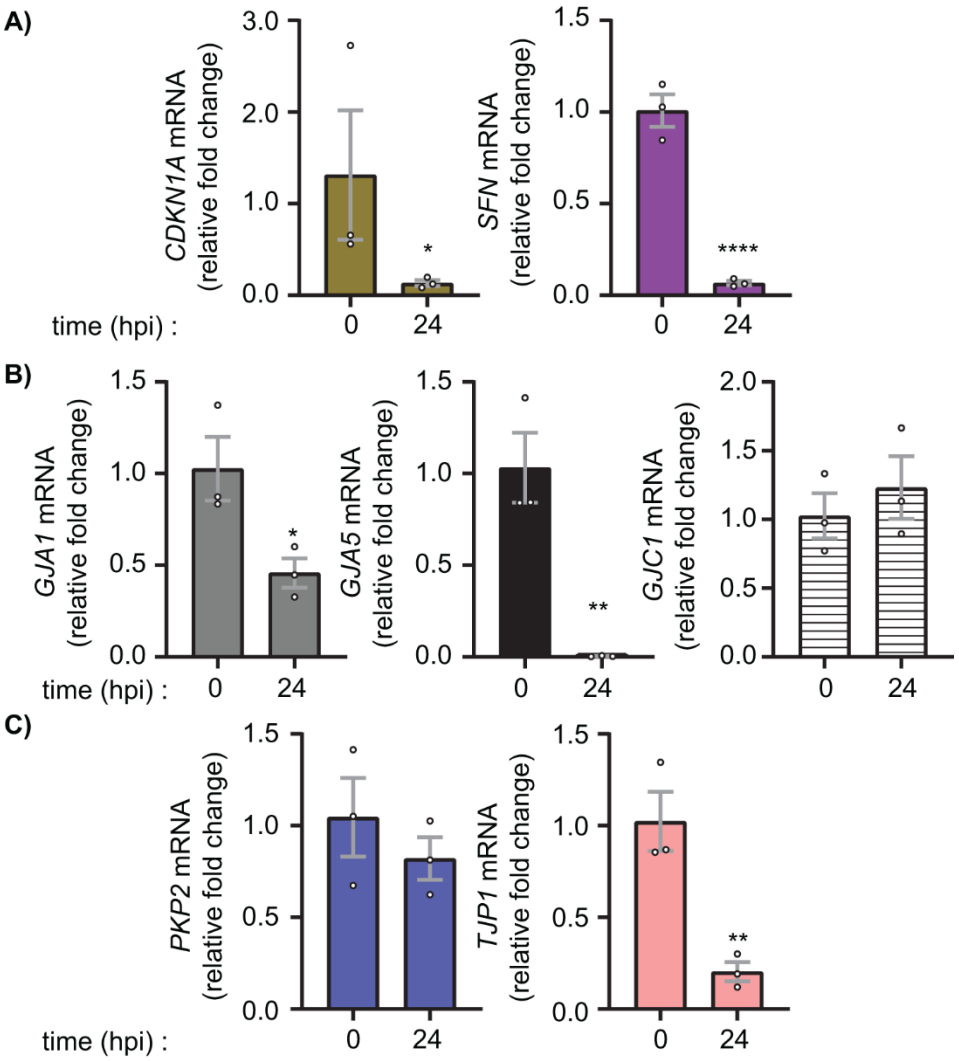

Figure 3.2) Specific targeting of gap junction gene transcription during adenovirus type 5 infection. HaCaT cells were infected with Ad5 at a MOI of 10 iu/cell and RNA was harvested at 24 hpi. **A)** RT-qPCR analysis of *CDKN1A* (p21) and *SFN* (14-3-3σ) to confirm active viral infection and known altered gene transcription. **B)** RT-qPCR analysis of gap junction family genes *GJA1* (Cx43), *GJA5* (Cx40), and *GJC1* (Cx45). **C)** RT-qPCR analysis of junctional protein genes *PKP2* (Plakophilin-2) and *TJP1* (ZO-1). Statistical analysis performed by one-way ANOVA with Dunnett's multiple comparisons test. (*n*=3). **p*≤0.05 ***p*≤0.01 ****p*≤0.001 *****p*<0.0001. Data are represented as mean ±SEM. See also Figure 3S1.

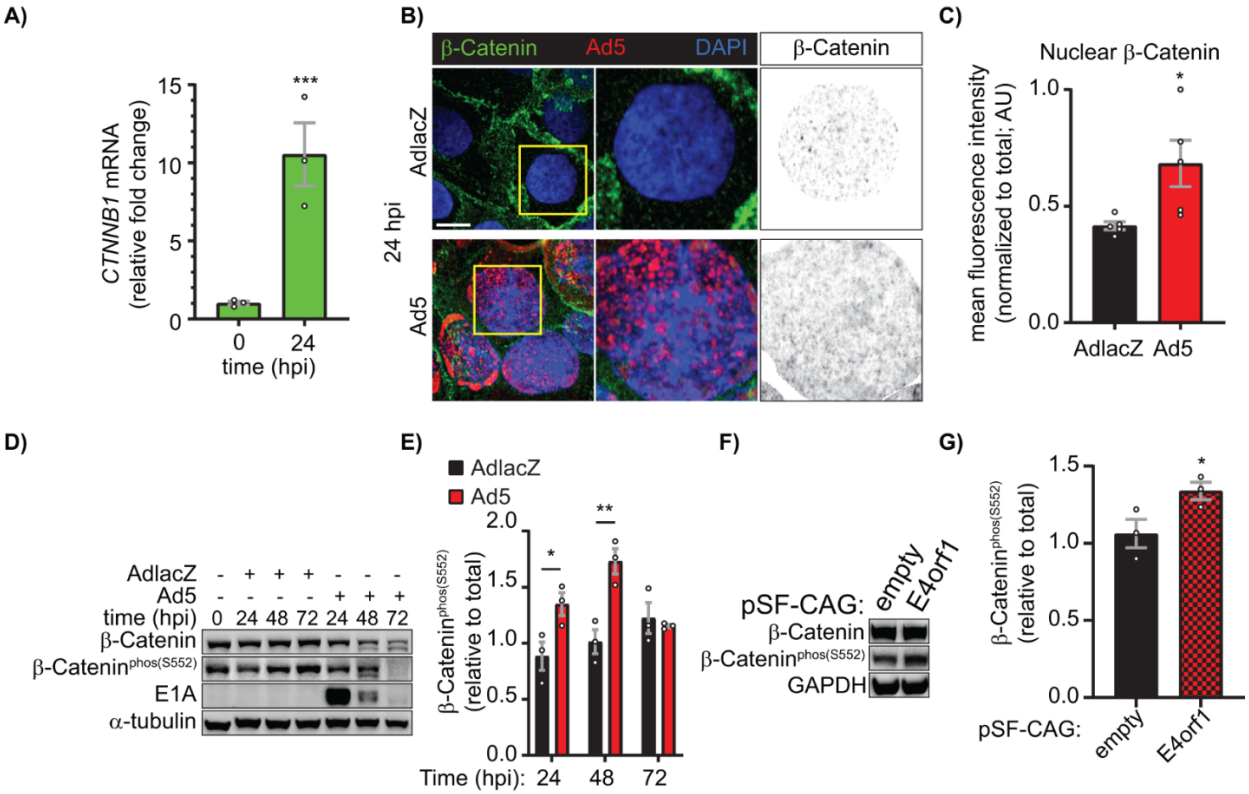

Figure 3.3) Early adenoviral factors induce β-catenin transcriptional activity through growth factor signaling. HaCaT cells were infected with Ad5 or replication-incompetent AdlacZ at a MOI of 10 iu/cell and RNA and protein were harvested or cells were fixed for immunofluorescence over a 72 h time course. **A)** RT-qPCR analysis of *CTNNB1* (β-catenin) relative fold change from 0 hpi. (*n*=3). **B)** Immunofluorescence confocal microscopy for β-catenin (green) and Ad5 (red) with nuclei identified with DAPI (blue). Greyscale images in right panels identify nuclear β-catenin levels through DAPI binary mask multiplication from a single Z-slice. Original magnification: X100. Scale bar: 10μm. **C)** Quantification of nuclear β-catenin represented in B. (*n*=5). **D)** Western blot of total β-catenin and β-catenin phospho-Ser552 (transcriptionally active) also probed for Ad5-E1A to confirm infection and α-tubulin for loading control. **E)** Quantification of D by densitometry. (*n*=3). HaCaT cells were transfected with pSF-CAG-empty vector or -E4orf1 and protein harvested 24 hours post transfection. **F)** Western blot of total β-catenin and β-catenin phospho-Ser552 (transcriptionally active) also probed for GAPDH for loading control. **G)** Quantification of F by densitometry. (*n*=3). Statistical analyses performed using the unpaired Student's t-test (A, C, G) or two-way ANOVA with Sidak's multiple comparisons test (E). *$p \leq 0.05$ **$p \leq 0.01$ ***$p \leq 0.001$ ****$p < 0.0001$. Data are represented as mean ±SEM. See also Figure 3S2, 3S3.

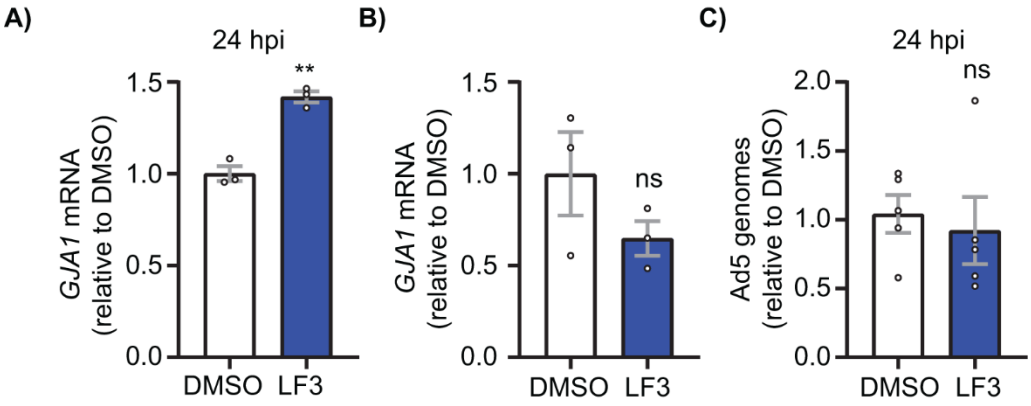

Figure 3.4) β-catenin transcriptional activity is necessary to reduce *GJA1* mRNA during adenoviral infection. HaCaT cells were treated with the β-catenin transcriptional inhibitor LF3 1 hpi or LF3 alone and harvested for RNA and DNA at indicated time points. **A)** RT-qPCR analysis of *GJA1* mRNA at 24 hpi in cells treated with LF3 or vehicle and infected at a MOI of 10 iu/cell. (*n*=3). **B)** RT-qPCR analysis of uninfected HaCaT cells treated with vehicle or LF3 for 24 h. (*n*=3). **C)** qPCR analysis of viral genomes in HaCaT cells infected with Ad5 and treated with LF3 or vehicle and harvested 24 hpi. (*n*=5). *ns:* not significant. Statistical analyses performed using the unpaired Student's t-test. $p \leq 0.05$ is considered statistically significant. ** $p \leq 0.01$. Data are represented as mean ±SEM.

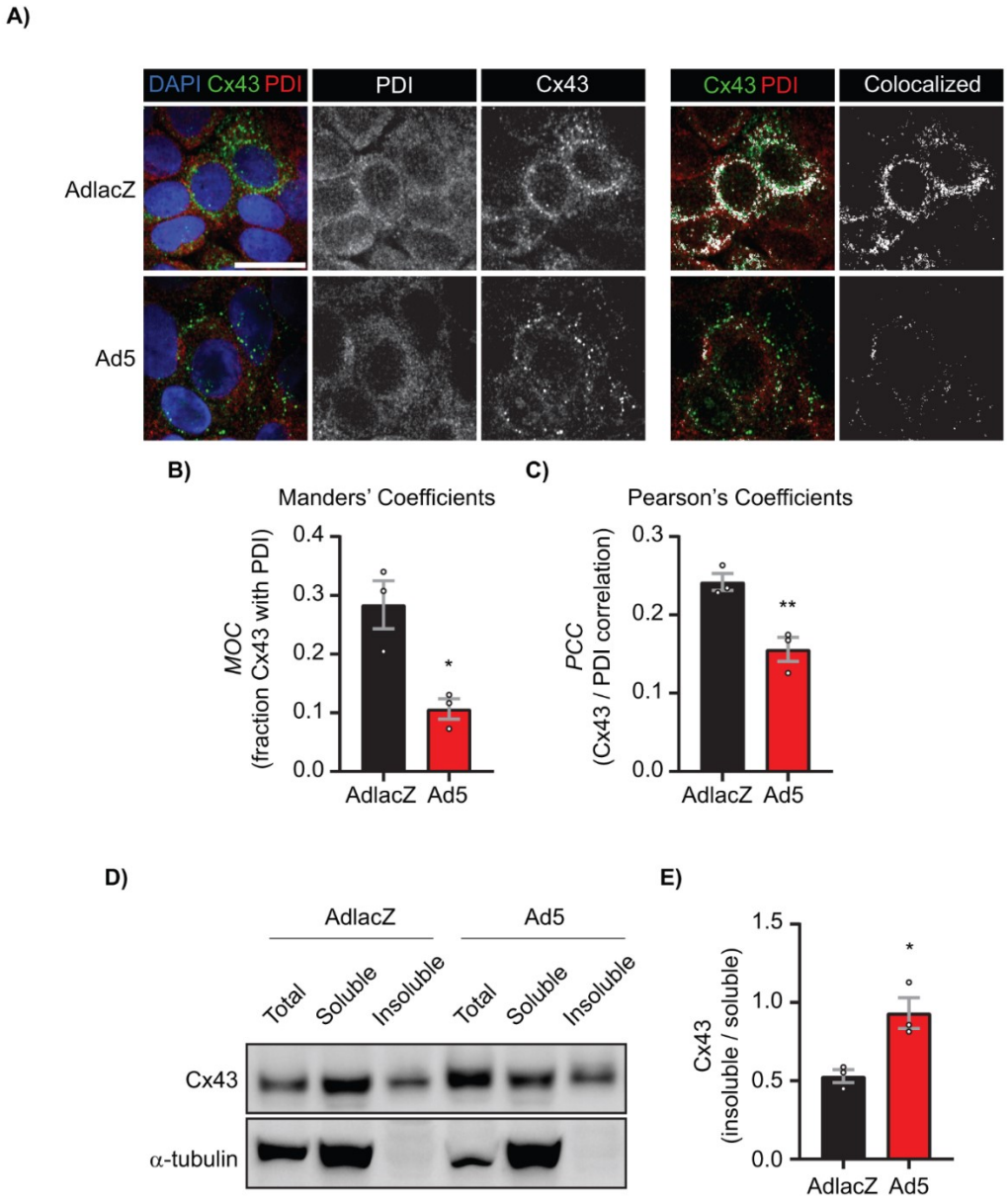

Figure 3.5) Cx43 protein occurs in reduced levels at the endoplasmic reticulum and is primarily junctional during adenovirus infection. HaCaT cells were infected with AdlacZ or Ad5 at a MOI of 10 iu/cell prior to fixation or protein harvesting at 24 hpi. **A)** AdlacZ- or Ad5-infected HaCaT cells were immunolabeled against PDI (red) to localize ER and against Cx43 (green). Cells were stained using DAPI to identify nuclei (blue). Colocalized Cx43 / PDI signal was determined with ImageJ (white). Original magnification: X100. Scale bar: 20 μm. **B)** Manders' Coefficients calculations determined using fraction Cx43 with PDI. Data points represent averages of 8 images from 3 separate experiments. **C)** Pearson's Coefficients calculations determined for Cx43 and PDI correlation. Data points represent averages of 8 images from 3 separate experiments. **D)** AdlacZ- or Ad5-infected HaCaT cells were lysed in 1% Triton X-100 solubility assay buffer prior to fractionation and western blotting. Membrane probed against Cx43 (top panel) and α-tubulin (bottom panel) for loading control. **E)** Quantification of D. Statistical analysis was performed with Student's t-test. (n=3). *p≤0.05, **p≤ 0.01. Data are represented as mean ±SEM.

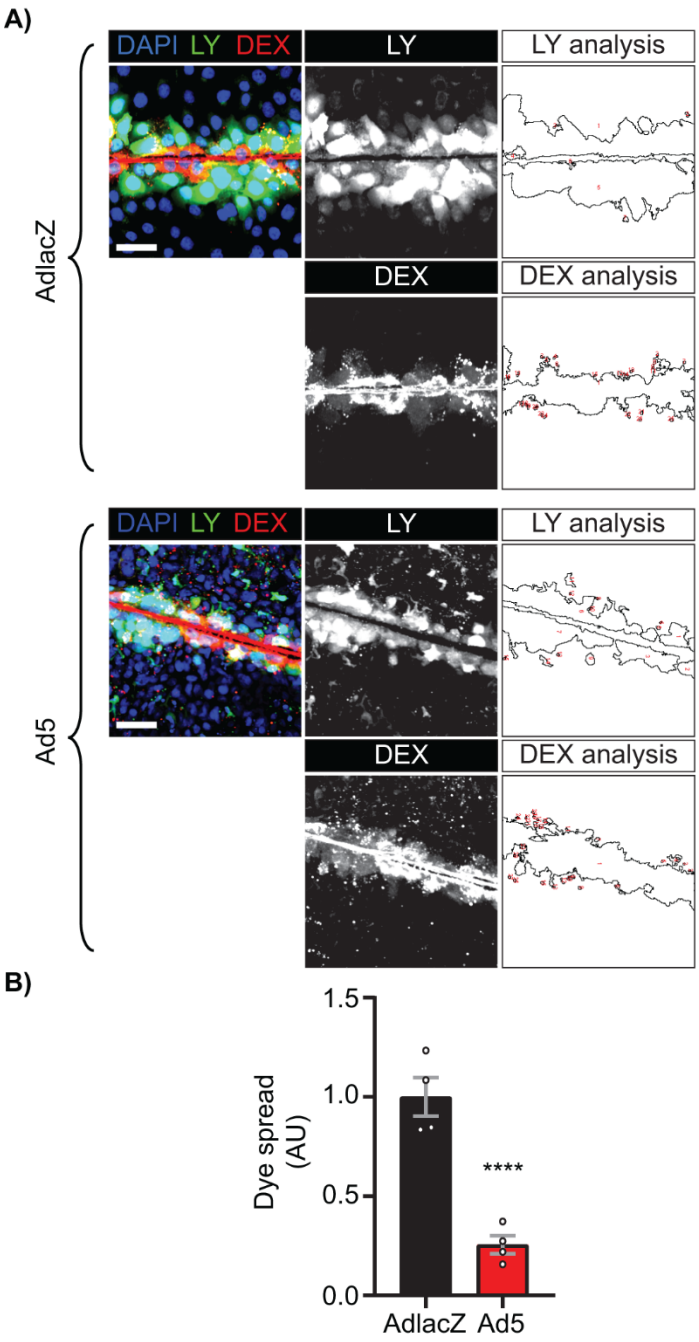

Figure 3.6) Adenovirus inhibits gap junction intercellular communication prior to reduction of Cx43 total protein levels during infection. HaCaT cells were plated to confluence on glass bottomed dishes and infected with Ad5 or replication-incompetent AdlacZ at a MOI of 10 iu/cell. The Lucifer yellow (LY) scrape-load dye-transfer assay was performed at 12 hpi with 10,000 MW Dextran-AlexaFluor647 (Dex-647) as a gap junction non-permeable control. **A)** Representative confocal microscopy images of LY (green) and Dex-647 (red) transfer with nuclei identified with DAPI (blue). Middle greyscale panels show LY and Dex-647 alone and right panels illustrate quantification of each dye spread. Original magnification: X20. Scale bar: 50μm. **B)** Quantification of dye spread in A. Statistical analysis was performed with the unpaired Student's t-test. (n=4). ****p<0.0001. Data are represented as mean ±SEM. See also Figure 3S4.

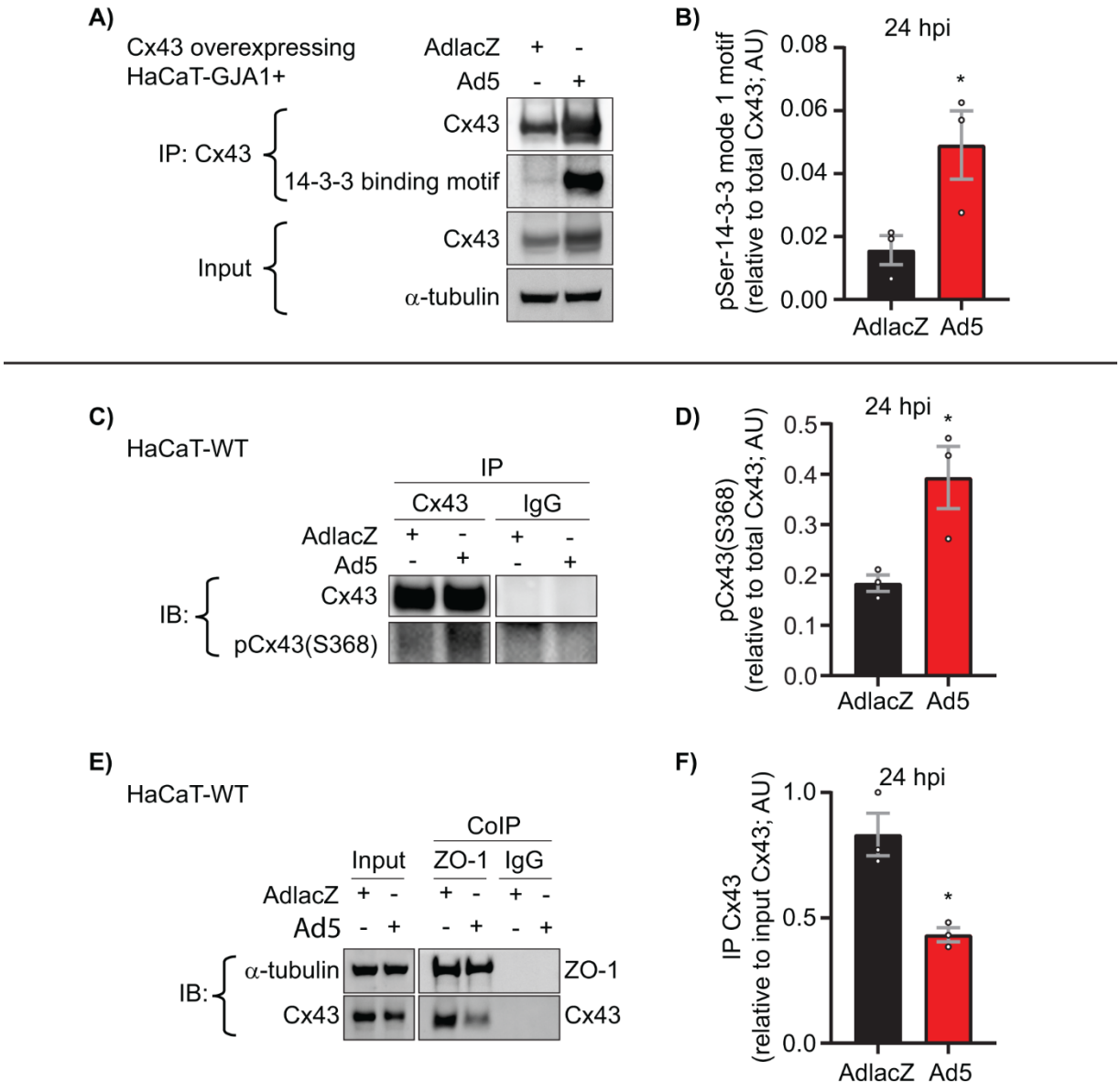

Figure 3.7) Direct targeting of Cx43 gap junctions through phosphorylation during adenovirus type 5 infection. HaCaT-GJA1+ cells or wild-type HaCaT cells were infected with Ad5 or replication-incompetent AdlacZ at a MOI of 10 iu/cell and protein was harvested at 24 hpi. **A)** Immunoprecipitation (IP) of Cx43 followed by western blot probed for phosphoSerine-14-3-3 mode-1 binding motif to detect phosphorylation of Cx43-Ser373 at 24 hpi. α-tubulin serves as loading control. **B)** Densitometry analysis of A. **C)** IP of Cx43 followed by western blot for Cx43 phosphorylation at Ser368. Cx43 IP and IgG IP are from same membrane. **D)** Densitometry analysis of C. **E)** HaCaT cells were infected with Ad5 or AdlacZ at a MOI of 10 iu/cell and protein harvested 24 hpi. Co-immunoprecipitation (CoIP) was performed for ZO-1 and Cx43 followed by western blotting. α-tubulin serves as loading control. **F)** Densitometry analysis of E. Statistical analysis performed with the unpaired Student's t-test. (n=3). *$p\leq$ 0.05 **$p\leq$0.01 ***$p\leq$0.001 ****$p<$0.0001. Data are represented as mean ±SEM. See also Figure 3S5.

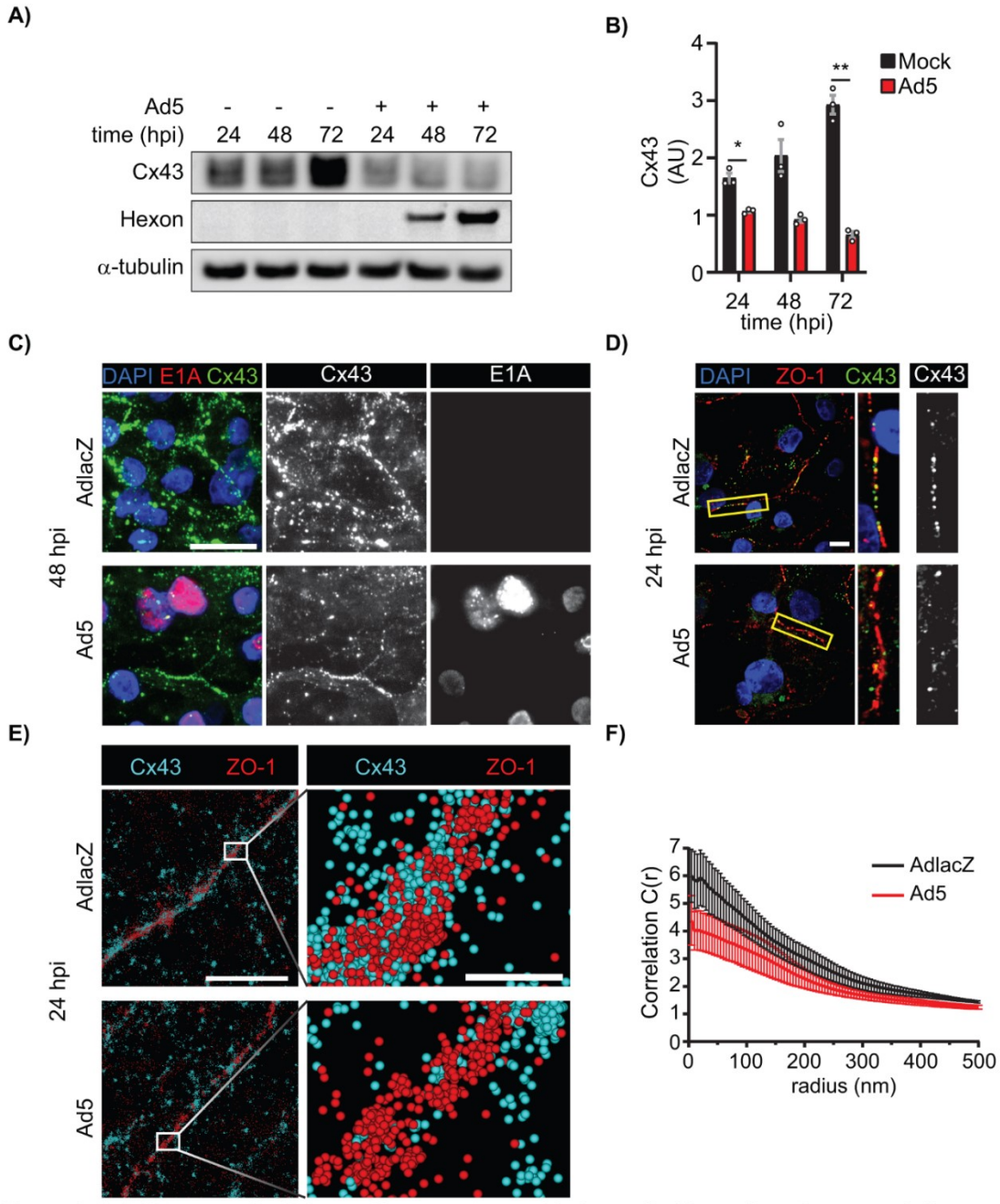

Figure 3.8) Ad5 targets Cx43 in cardiomyocytes and induces Cx43-gap junction remodeling. HiPSC-CMs were infected with Ad5 or replication-incompetent AdlacZ at a MOI of 10 iu/cell and protein harvested or fixed for immunolabeling over a 72 h time course. **A)** Western blot probed for Cx43 expression in HiPSC-CMs. Detection of Ad5-Hexon protein expression serves to confirm infection and α-tubulin serves as loading control. **B)** Densitometry analysis of A. **C)** Immunofluorescence confocal microscopy of HiPSC-CMs at 48 hpi probed for Cx43 (green) and adenovirus E1A (red) with nuclei identified using DAPI (blue). Original magnification: X100. Scale bar: 20μm. **D)** Immunofluorescence confocal microscopy of HiPSC-CMs 24 hpi probed for Cx43 (green) and ZO-1 (red) with nuclei identified using DAPI (blue). Original magnification: X100. Scale bar: 10μm. Images representative of 3 separate experiments. **E)** Super resolution stochastic optical reconstruction microscopy (STORM) derived point-cloud localizations of Cx43 (cyan) and ZO-1 (red) in Ad5- and AdlacZ-infected HiPSC-CMs 24 hpi. Zoomed out panels (left) scale bar: 2μm. Zoomed in panels (right) scale bar: 200nm. Sphere size: 30nm. **F)** Cross-Pair correlation functions for Cx43/ZO-1 complexing in E. (*n*=10). Statistical analysis was performed with two-way analysis of variance (ANOVA) with Sidak's multiple comparisons test (B) (*n*=3). *p≤0.05, **p≤0.01, ***p≤0.001, ****p<0.0001. Data are represented as mean ±SEM.

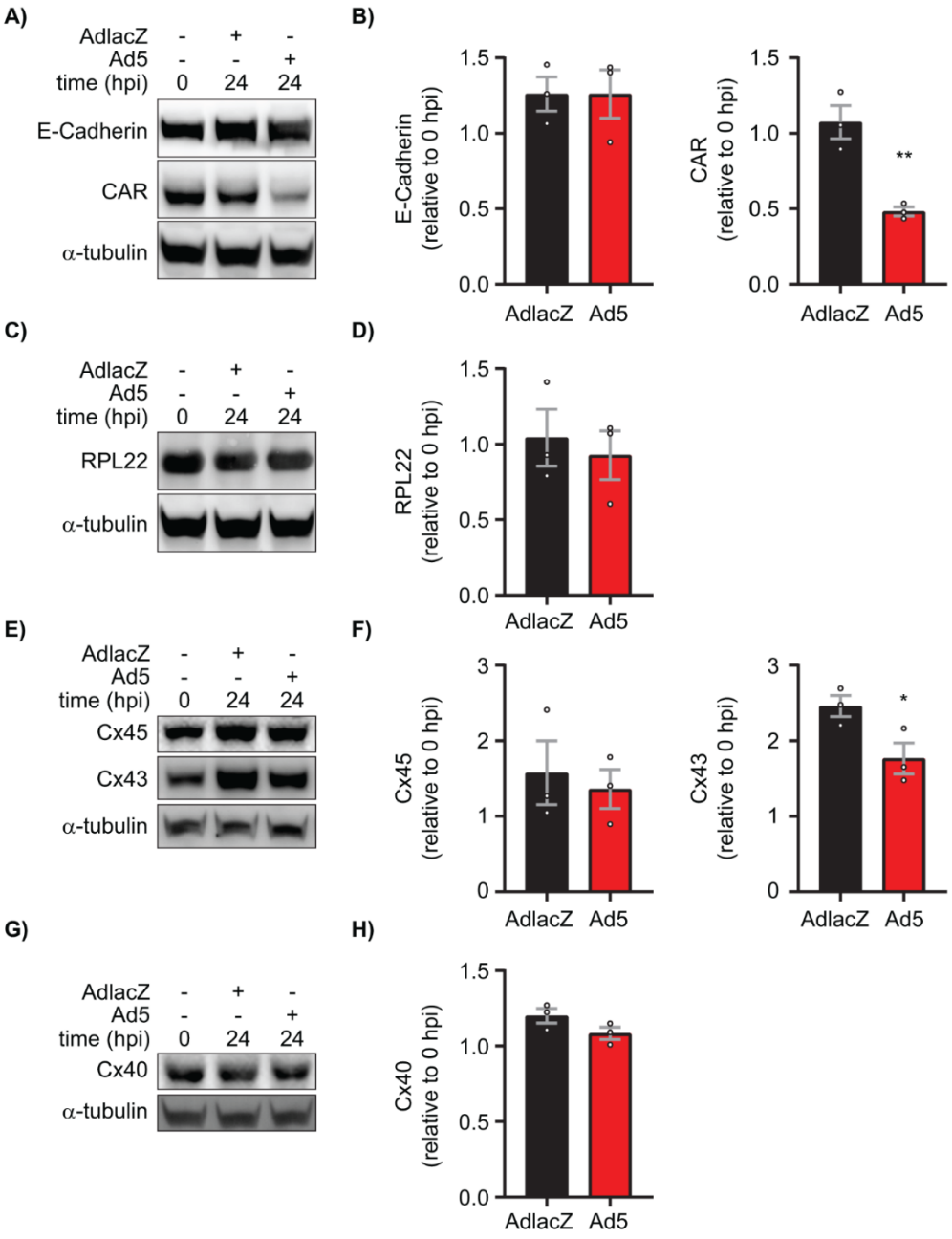

Figure 3S1) Specific host-cell proteins are targeting during adenoviral infection. Related to Figure 3.1 and 3.2. HaCaT cells were infected with Ad5 or AdlacZ at a MOI of 10 iu/cell and protein lysates harvested at 0 hpi and 24 hpi followed by western blotting. **A)** Western blot probed against E-Cadherin (top panel) and CAR (center panel) with α-tubulin probed for a loading control (bottom panel). **B)** Quantification of A. **C)** Western blot probed against RPL22 (top panel) with α-tubulin probed for a loading control (bottom panel). **D)** Quantification of C. **E)** Western blot probed against Cx45 (top panel) and Cx43 (center panel) with α-tubulin probed for a loading control (bottom panel). **F)** Quantification of E. **G)** Western blot probed against Cx40 (top panel) with α-tubulin probed for a loading control (bottom panel). **H)** Quantification of G. Statistical analysis was performed with Student's t-test. (n=3). *$p \leq 0.05$, **$p \leq 0.01$. Data are represented as mean ±SEM.

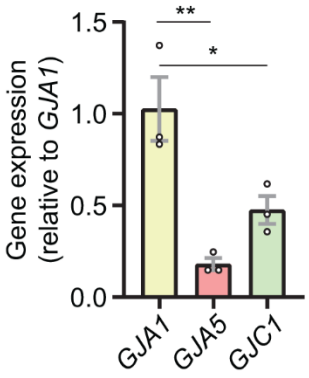

Figure 3S2) *GJA1* expression is higher than *GJA5* and *GJC1* in untreated HaCaT cells. Related to Figure 3.2. RT-qPCR was performed on HaCaT cells to determine baseline expression of *GJA1*, *GJA5*, and *GJC1*. Statistical analysis was performed with one-way analysis of variance (ANOVA) with Tukey's multiple comparisons test. (n=3). *p≤0.05, **p≤0.01. Data are represented as mean ±SEM.

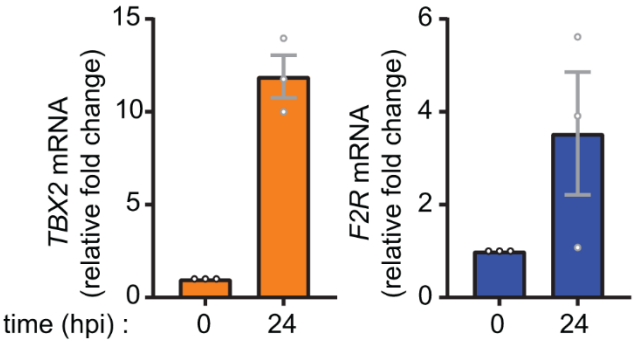

Figure 3S3) *GJA1*-candidate transcription factors are elevated during Ad5 infection. Related to Figure 3.3. HaCaT cells were infected with Ad5 at a MOI of 10 iu/cell and RNA harvested at 24 hpi. RT-qPCR analysis of Ad5-infected HaCaT cells for transcription factor genes *TBX2* and *F2R* which are previously shown to regulate *GJA1* transcription relative to 0 hpi. Data are represented as mean ±SEM.

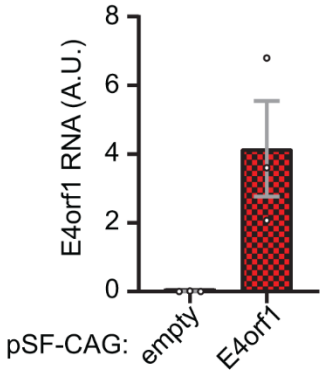

Figure 3S4) Detection of E4orf1 mRNA in transfected HaCaT cells. Related to Figure 3.3. HaCaT cells were transfected with pSF-CAG-empty or -E4orf1 and RNA harvested 24 hours post transfection. E4orf1 is detected by RT-qPCR in transfected HaCaT cells. n=3. Data are represented as mean ±SEM.

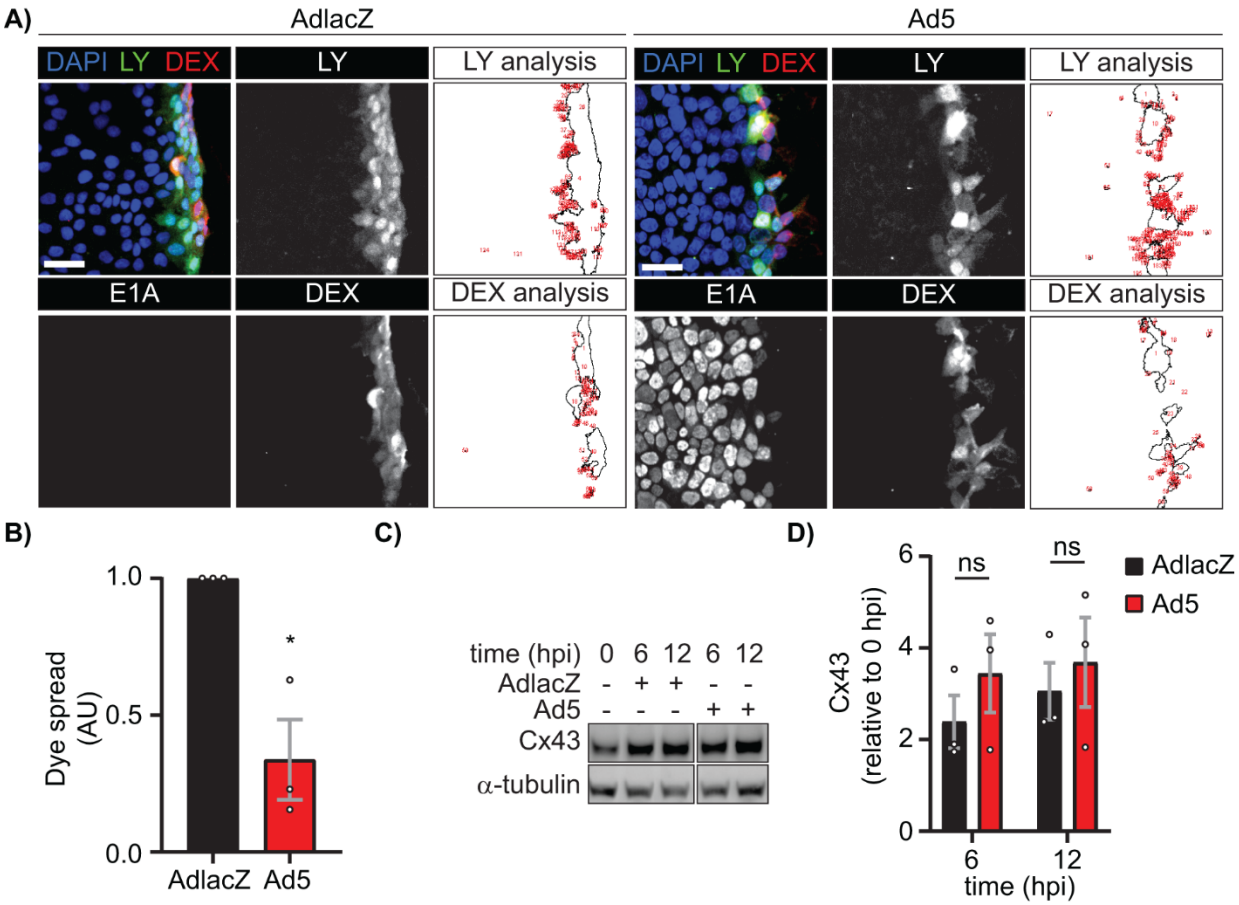

Figure 3S5) Adenovirus infection reduces gap junction function. Related to Figure 3.6. HaCaT cells were infected with Ad5 or replication-incompetent AdLacZ at a MOI of 10 iu/cell and protein was harvested at 6 and 12 hpi in addition to LY scrape-load dye-transfer assay at 24 hpi. **A)** Representative confocal microscopy images of LY (green) and Dex-647 (red) transfer with nuclei identified with DAPI (blue). Middle greyscale panels show LY or Dex-647 alone and right panels illustrate quantification of each dye spread. Original magnification: X20. Scale bar: 50μm. **B)** Quantification of A (*n*=3). **C)** Western blot probed for Cx43 expression with α-tubulin serving as loading control. **D)** Densitometric analysis of C (*n*=3). Statistical analysis performed by unpaired Student's t-test (B) or two-way ANOVA with Sidak's multiple comparisons test (D). **p*≤0.05, *ns*: not significant. Data are represented as mean ±SEM.

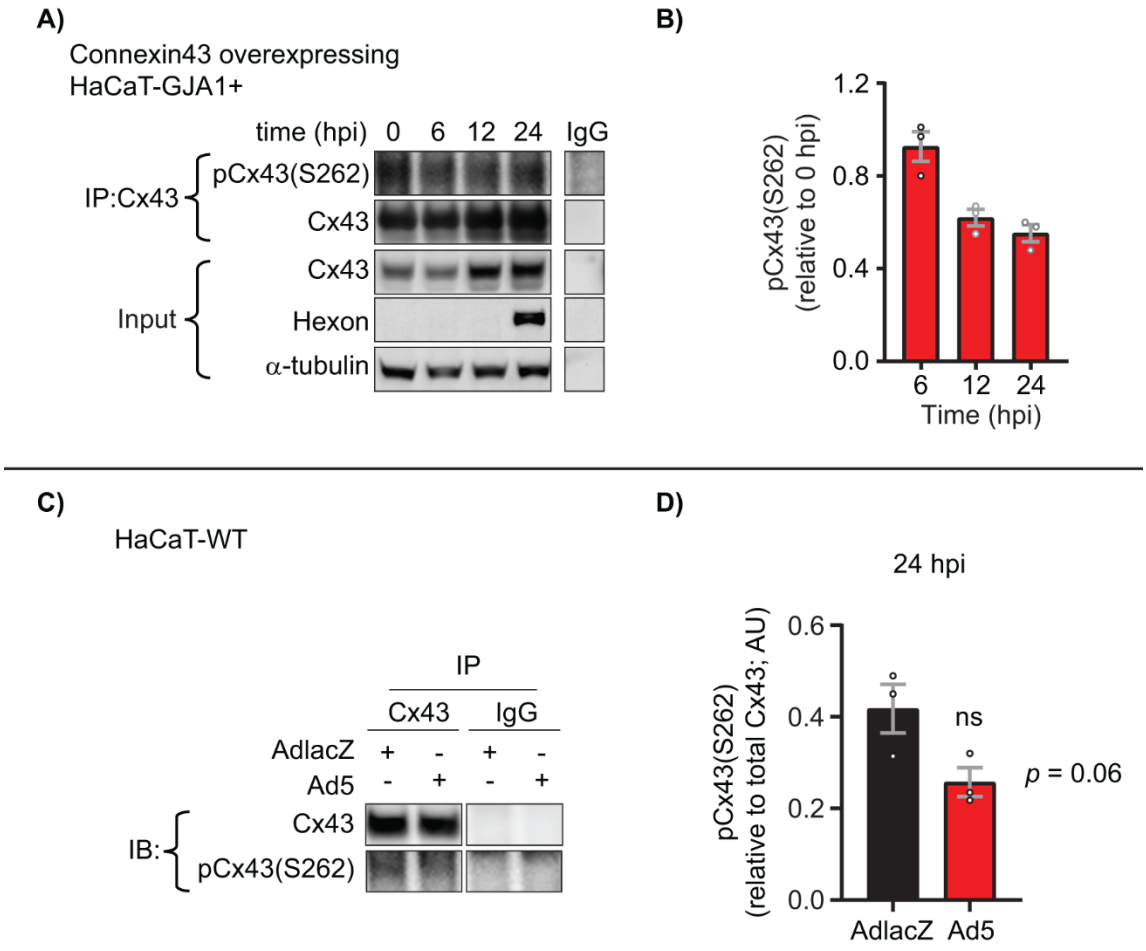

Figure 3S6) Adenovirus does not induce Cx43 phosphorylation at Ser262. Related to Figure 3.7. **A)** HaCaT-GJA1+ cells were infected with Ad5 at a MOI of 10 iu/cell and protein harvested 6, 12, and 24 hpi. Immunoprecipitation of Cx43 was performed following by western blot and probed for Cx43 phosphorylation at Ser262 (pCx43(S262)) and total Cx43. Immunoprecipitated Cx43 and IgG are from same membrane and exposure. Detection of Hexon confirms infection and α-tubulin serves as loading control. **B)** Densitometry of A. **C)** Wild-type HaCaT cells were infected with Ad5 or replication-incompetent AdlacZ at a MOI of 10 iu/cell and protein harvested 24 hpi. Immunoprecipitation of Cx43 was performed followed by western blot and probed for pCx43(S262) and total Cx43. Immunoprecipitated Cx43 and IgG are from same membrane and exposure. **D)** Densitometry of C. Statistical analyses performed using unpaired Student's t-test. (n=3). $p \leq 0.05$ is considered statistically significant. *ns*: not significant. Data are represented as mean ±SEM.

REFERENCES

1 Unwin, P. N. & Zampighi, G. Structure of the junction between communicating cells. *Nature* **283**, 545-549, doi:10.1038/283545a0 (1980).

2 Vozzi, C., Dupont, E., Coppen, S. R., Yeh, H. I. & Severs, N. J. Chamber-related differences in connexin expression in the human heart. *J Mol Cell Cardiol* **31**, 991-1003, doi:10.1006/jmcc.1999.0937 (1999).

3 Gutstein, D. E. *et al.* Conduction slowing and sudden arrhythmic death in mice with cardiac-restricted inactivation of connexin43. *Circulation research* **88**, 333-339, doi:10.1161/01.res.88.3.333 (2001).

4 Kanagaratnam, P., Rothery, S., Patel, P., Severs, N. J. & Peters, N. S. Relative expression of immunolocalized connexins 40 and 43 correlates with human atrial conduction properties. *Journal of the American College of Cardiology* **39**, 116-123, doi:https://doi.org/10.1016/S0735-1097(01)01710-7 (2002).

5 Poelzing, S. & Rosenbaum, D. S. Altered connexin43 expression produces arrhythmia substrate in heart failure. *Am J Physiol Heart Circ Physiol* **287**, H1762-1770, doi:10.1152/ajpheart.00346.2004 (2004).

6 Ablasser, A. *et al.* Cell intrinsic immunity spreads to bystander cells via the intercellular transfer of cGAMP. *Nature* **503**, 530-534, doi:10.1038/nature12640 (2013).

7 Neijssen, J. *et al.* Cross-presentation by intercellular peptide transfer through gap junctions. *Nature* **434**, 83-88, doi:10.1038/nature03290 (2005).

8 Patel, S. J., King, K. R., Casali, M. & Yarmush, M. L. DNA-triggered innate immune responses are propagated by gap junction communication. *Proceedings of the National Academy of Sciences* **106**, 12867, doi:10.1073/pnas.0809292106 (2009).

9 Schoggins, J. W. *et al.* A diverse range of gene products are effectors of the type I interferon antiviral response. *Nature* **472**, 481, doi:10.1038/nature09907 https://www.nature.com/articles/nature09907#supplementary-information (2011).

10 Sharma, S. *et al.* Triggering the Interferon Antiviral Response Through an IKK-Related Pathway. *Science* **300**, 1148, doi:10.1126/science.1081315 (2003).

11 Townsend, A. R. *et al.* The epitopes of influenza nucleoprotein recognized by cytotoxic T lymphocytes can be defined with short synthetic peptides. *Cell* **44**, 959-968, doi:10.1016/0092-8674(86)90019-x (1986).

12 Braciale, T. J. *et al.* Antigen presentation pathways to class I and class II MHC-restricted T lymphocytes. *Immunological reviews* **98**, 95-114 (1987).

13 Zinkernagel, R. M. & Doherty, P. C. Restriction of in vitro T cell-mediated cytotoxicity in lymphocytic choriomeningitis within a syngeneic or semiallogeneic system. *Nature* **248**, 701-702, doi:10.1038/248701a0 (1974).

14 Beardslee, M. A., Laing, J. G., Beyer, E. C. & Saffitz, J. E. Rapid turnover of connexin43 in the adult rat heart. *Circ Res* **83**, 629-635, doi:10.1161/01.res.83.6.629 (1998).
15 Laird, D. W., Castillo, M. & Kasprzak, L. Gap junction turnover, intracellular trafficking, and phosphorylation of connexin43 in brefeldin A-treated rat mammary tumor cells. *J Cell Biol* **131**, 1193-1203, doi:10.1083/jcb.131.5.1193 (1995).
16 Fallon, R. F. & Goodenough, D. A. Five-hour half-life of mouse liver gap-junction protein. *J Cell Biol* **90**, 521-526, doi:10.1083/jcb.90.2.521 (1981).
17 Zhang, S. S. *et al.* Iroquois homeobox gene 3 establishes fast conduction in the cardiac His-Purkinje network. *Proc Natl Acad Sci U S A* **108**, 13576-13581, doi:10.1073/pnas.1106911108 (2011).
18 Ai, Z., Fischer, A., Spray, D. C., Brown, A. M. & Fishman, G. I. Wnt-1 regulation of connexin43 in cardiac myocytes. *J Clin Invest* **105**, 161-171, doi:10.1172/jci7798 (2000).
19 Oyamada, M., Takebe, K. & Oyamada, Y. Regulation of connexin expression by transcription factors and epigenetic mechanisms. *Biochim Biophys Acta* **1828**, 118-133, doi:10.1016/j.bbamem.2011.12.031 (2013).
20 James, C. C., Zeitz, M. J., Calhoun, P. J., Lamouille, S. & Smyth, J. W. Altered translation initiation of Gja1 limits gap junction formation during epithelial-mesenchymal transition. *Molecular biology of the cell*, doi:10.1091/mbc.E17-06-0406 (2018).
21 Smyth, J. W. & Shaw, R. M. Autoregulation of connexin43 gap junction formation by internally translated isoforms. *Cell Rep* **5**, 611-618, doi:10.1016/j.celrep.2013.10.009 (2013).
22 Zeitz, M. J. *et al.* Dynamic UTR Usage Regulates Alternative Translation to Modulate Gap Junction Formation during Stress and Aging. *Cell reports* **27**, 2737-2747 e2735, doi:10.1016/j.celrep.2019.04.114 (2019).
23 Laird, D. W. Connexin phosphorylation as a regulatory event linked to gap junction internalization and degradation. *Biochimica et Biophysica Acta (BBA) - Biomembranes* **1711**, 172-182, doi:https://doi.org/10.1016/j.bbamem.2004.09.009 (2005).
24 Moreno, A. P. & Lau, A. F. Gap junction channel gating modulated through protein phosphorylation. *Progress in Biophysics and Molecular Biology* **94**, 107-119, doi:https://doi.org/10.1016/j.pbiomolbio.2007.03.004 (2007).
25 Solan, J. L. & Lampe, P. D. Key connexin 43 phosphorylation events regulate the gap junction life cycle. *J Membr Biol* **217**, 35-41, doi:10.1007/s00232-007-9035-y (2007).
26 Park, D. J. *et al.* Akt phosphorylates Connexin43 on Ser373, a "mode-1" binding site for 14-3-3. *Cell communication & adhesion* **14**, 211-226, doi:10.1080/15419060701755958 (2007).
27 Smyth, J. W. *et al.* A 14-3-3 mode-1 binding motif initiates gap junction internalization during acute cardiac ischemia. *Traffic* **15**, 684-699, doi:10.1111/tra.12169 (2014).

28 Dunn, C. A. & Lampe, P. D. Injury-triggered Akt phosphorylation of Cx43: a ZO-1-driven molecular switch that regulates gap junction size. *J Cell Sci* **127**, 455-464, doi:10.1242/jcs.142497 (2014).
29 Segretain, D. *et al.* A proposed role for ZO-1 in targeting connexin 43 gap junctions to the endocytic pathway. *Biochimie* **86**, 241-244, doi:https://doi.org/10.1016/j.biochi.2004.05.003 (2004).
30 Barker, R. J., Price, R. L. & Gourdie, R. G. Increased association of ZO-1 with connexin43 during remodeling of cardiac gap junctions. *Circ Res* **90**, 317-324, doi:10.1161/hh0302.104471 (2002).
31 Rhett, J. M., Jourdan, J. & Gourdie, R. G. Connexin 43 connexon to gap junction transition is regulated by zonula occludens-1. *Molecular biology of the cell* **22**, 1516-1528, doi:10.1091/mbc.e10-06-0548 (2011).
32 Toyofuku, T. *et al.* Direct association of the gap junction protein connexin-43 with ZO-1 in cardiac myocytes. *J Biol Chem* **273**, 12725-12731, doi:10.1074/jbc.273.21.12725 (1998).
33 Lisewski, U. *et al.* The tight junction protein CAR regulates cardiac conduction and cell-cell communication. *J Exp Med* **205**, 2369-2379, doi:10.1084/jem.20080897 (2008).
34 Savon, C. *et al.* A myocarditis outbreak with fatal cases associated with adenovirus subgenera C among children from Havana City in 2005. *Journal of clinical virology : the official publication of the Pan American Society for Clinical Virology* **43**, 152-157, doi:10.1016/j.jcv.2008.05.012 (2008).
35 Bowles, N. E. *et al.* Detection of viruses in myocardial tissues by polymerase chain reaction. evidence of adenovirus as a common cause of myocarditis in children and adults. *J Am Coll Cardiol* **42**, 466-472, doi:10.1016/s0735-1097(03)00648-x (2003).
36 Dennert, R., Crijns, H. J. & Heymans, S. Acute viral myocarditis. *Eur Heart J* **29**, 2073-2082, doi:10.1093/eurheartj/ehn296 (2008).
37 Zhang, Y. & Bergelson, J. M. Adenovirus receptors. *J Virol* **79**, 12125-12131, doi:10.1128/JVI.79.19.12125-12131.2005 (2005).
38 Cooper, L. T. Myocarditis. *New England Journal of Medicine* **360**, 1526-1538, doi:10.1056/NEJMra0800028 (2009).
39 Martino, T. A., Liu, P. & Sole, M. J. Viral infection and the pathogenesis of dilated cardiomyopathy. *Circulation Research* **74**, 182-188, doi:10.1161/01.RES.74.2.182 (1994).
40 Pankuweit, S. & Klingel, K. Viral myocarditis: from experimental models to molecular diagnosis in patients. *Heart Fail Rev* **18**, 683-702, doi:10.1007/s10741-012-9357-4 (2013).
41 Gauntt, C. J. *et al.* Coxsackievirus-induced chronic myocarditis in murine models. *Eur Heart J* **16 Suppl O**, 56-58, doi:10.1093/eurheartj/16.suppl_o.56 (1995).
42 Kearney, M. T., Cotton, J. M., Richardson, P. J. & Shah, A. M. Viral myocarditis and dilated cardiomyopathy: mechanisms, manifestations, and management. *Postgraduate Medical Journal* **77**, 4, doi:10.1136/pmj.77.903.4 (2001).

43 Jogler, C. *et al.* Replication properties of human adenovirus in vivo and in cultures of primary cells from different animal species. *Journal of virology* **80**, 3549-3558, doi:10.1128/JVI.80.7.3549-3558.2006 (2006).
44 Blair, G. E., Dixon, S. C., Griffiths, S. A. & Zajdel, M. E. Restricted replication of human adenovirus type 5 in mouse cell lines. *Virus Res* **14**, 339-346 (1989).
45 Chandrasekaran, A. *et al.* Age-Dependent Effects of Immunoproteasome Deficiency on Mouse Adenovirus Type 1 Pathogenesis. *Journal of Virology* **93**, e00569-00519, doi:10.1128/JVI.00569-19 (2019).
46 McCarthy, M. K. *et al.* Interferon-dependent immunoproteasome activity during mouse adenovirus type 1 infection. *Virology* **498**, 57-68, doi:10.1016/j.virol.2016.08.009 (2016).
47 McCarthy, M. K. *et al.* Proinflammatory Effects of Interferon Gamma in Mouse Adenovirus 1 Myocarditis. *Journal of Virology* **89**, 468-479, doi:10.1128/jvi.02077-14 (2015).
48 Zhang, F. *et al.* Adenovirus vector E4 gene regulates connexin 40 and 43 expression in endothelial cells via PKA and PI3K signal pathways. *Circ Res* **96**, 950-957, doi:10.1161/01.RES.0000165867.95291.7b (2005).
49 Fang, D. *et al.* Phosphorylation of beta-catenin by AKT promotes beta-catenin transcriptional activity. *The Journal of biological chemistry* **282**, 11221-11229, doi:10.1074/jbc.M611871200 (2007).
50 Sharma, A. *et al.* Human Induced Pluripotent Stem Cell–Derived Cardiomyocytes as an In Vitro Model for Coxsackievirus B3–Induced Myocarditis and Antiviral Drug Screening Platform. *Circulation Research* **115**, 556-566, doi:10.1161/CIRCRESAHA.115.303810 (2014).
51 Suomalainen, M., Nakano, M. Y., Boucke, K., Keller, S. & Greber, U. F. Adenovirus-activated PKA and p38/MAPK pathways boost microtubule-mediated nuclear targeting of virus. *The EMBO journal* **20**, 1310-1319, doi:10.1093/emboj/20.6.1310 (2001).
52 Yousuf, M. A. *et al.* Protein Kinase C Signaling in Adenoviral Infection. *Biochemistry* **55**, 5938-5946, doi:10.1021/acs.biochem.6b00858 (2016).
53 Frese, K. K. *et al.* Selective PDZ protein-dependent stimulation of phosphatidylinositol 3-kinase by the adenovirus E4-ORF1 oncoprotein. *Oncogene* **22**, 710-721, doi:10.1038/sj.onc.1206151 (2003).
54 Lampe, P. D. *et al.* Phosphorylation of connexin43 on serine368 by protein kinase C regulates gap junctional communication. *J Cell Biol* **149**, 1503-1512, doi:10.1083/jcb.149.7.1503 (2000).
55 Green, M. & Loewenstein, P. M. Human Adenoviruses: Propagation, Purification, Quantification, and Storage. *Current Protocols in Microbiology* **00**, 14C.11.11-14C.11.19, doi:10.1002/9780471729259.mc14c01s00 (2006).
56 Bolte, S. & Cordelieres, F. P. A guided tour into subcellular colocalization analysis in light microscopy. *Journal of microscopy* **224**, 213-232, doi:10.1111/j.1365-2818.2006.01706.x (2006).

57 Babica, P., Sovadinová, I. & Upham, B. L. in *Gap Junction Protocols* (eds Mathieu Vinken & Scott R. Johnstone) 133-144 (Springer New York, 2016).
58 Sarnow, P., Ho, Y. S., Williams, J. & Levine, A. J. Adenovirus E1b-58kd tumor antigen and SV40 large tumor antigen are physically associated with the same 54 kd cellular protein in transformed cells. *Cell* **28**, 387-394, doi:https://doi.org/10.1016/0092-8674(82)90356-7 (1982).
59 Yew, P. R. & Berk, A. J. Inhibition of p53 transactivation required for transformation by adenovirus early 1B protein. *Nature* **357**, 82-85, doi:10.1038/357082a0 (1992).
60 Teodoro, J. G. & Branton, P. E. Regulation of p53-dependent apoptosis, transcriptional repression, and cell transformation by phosphorylation of the 55-kilodalton E1B protein of human adenovirus type 5. *Journal of Virology* **71**, 3620 (1997).
61 Querido, E. *et al.* Degradation of p53 by adenovirus E4orf6 and E1B55K proteins occurs via a novel mechanism involving a Cullin-containing complex. *Genes & development* **15**, 3104-3117, doi:10.1101/gad.926401 (2001).
62 Yew, P. R., Liu, X. & Berk, A. J. Adenovirus E1B oncoprotein tethers a transcriptional repression domain to p53. *Genes & Development* **8**, 190-202, doi:10.1101/gad.8.2.190 (1994).
63 Dobner, T., Horikoshi, N., Rubenwolf, S. & Shenk, T. Blockage by Adenovirus E4orf6 of Transcriptional Activation by the p53 Tumor Suppressor. *Science* **272**, 1470, doi:10.1126/science.272.5267.1470 (1996).
64 El-Deiry, W. S. *et al.* WAF1, a potential mediator of p53 tumor suppression. *Cell* **75**, 817-825, doi:https://doi.org/10.1016/0092-8674(93)90500-P (1993).
65 Hermeking, H. *et al.* 14-3-3sigma is a p53-regulated inhibitor of G2/M progression. *Mol Cell* **1**, 3-11 (1997).
66 Valenta, T., Hausmann, G. & Basler, K. The many faces and functions of β-catenin. *The EMBO journal* **31**, 2714-2736, doi:10.1038/emboj.2012.150 (2012).
67 Spagnol, G. *et al.* Connexin43 Carboxyl-Terminal Domain Directly Interacts with beta-Catenin. *Int J Mol Sci* **19**, doi:10.3390/ijms19061562 (2018).
68 Taurin, S., Sandbo, N., Qin, Y., Browning, D. & Dulin, N. O. Phosphorylation of beta-catenin by cyclic AMP-dependent protein kinase. *J Biol Chem* **281**, 9971-9976, doi:10.1074/jbc.M508778200 (2006).
69 Fang, L. *et al.* A Small-Molecule Antagonist of the beta-Catenin/TCF4 Interaction Blocks the Self-Renewal of Cancer Stem Cells and Suppresses Tumorigenesis. *Cancer Res* **76**, 891-901, doi:10.1158/0008-5472.can-15-1519 (2016).
70 Zhao, L., Sun, L., Lu, Y., Li, F. & Xu, H. A small-molecule LF3 abrogates β-catenin/TCF4-mediated suppression of NaV1.5 expression in HL-1

cardiomyocytes. *Journal of Molecular and Cellular Cardiology*, doi:https://doi.org/10.1016/j.yjmcc.2019.08.007 (2019).
71 van der Heyden, M. A. *et al.* Identification of connexin43 as a functional target for Wnt signalling. *J Cell Sci* **111 (Pt 12)**, 1741-1749 (1998).
72 Nimlamool, W., Andrews, R. M. & Falk, M. M. Connexin43 phosphorylation by PKC and MAPK signals VEGF-mediated gap junction internalization. *Molecular biology of the cell* **26**, 2755-2768, doi:10.1091/mbc.E14-06-1105 (2015).
73 Sirnes, S., Kjenseth, A., Leithe, E. & Rivedal, E. Interplay between PKC and the MAP kinase pathway in Connexin43 phosphorylation and inhibition of gap junction intercellular communication. *Biochem Biophys Res Commun* **382**, 41-45, doi:10.1016/j.bbrc.2009.02.141 (2009).
74 Solan, J. L. & Lampe, P. D. Specific Cx43 phosphorylation events regulate gap junction turnover in vivo. *FEBS Lett* **588**, 1423-1429, doi:10.1016/j.febslet.2014.01.049 (2014).
75 Solan, J. L. *et al.* Phosphorylation at S365 is a gatekeeper event that changes the structure of Cx43 and prevents down-regulation by PKC. *The Journal of cell biology* **179**, 1301-1309, doi:10.1083/jcb.200707060 (2007).
76 Johansen, D., Cruciani, V., Sundset, R., Ytrehus, K. & Mikalsen, S. O. Ischemia induces closure of gap junctional channels and opening of hemichannels in heart-derived cells and tissue. *Cellular physiology and biochemistry : international journal of experimental cellular physiology, biochemistry, and pharmacology* **28**, 103-114, doi:10.1159/000331719 (2011).
77 Liao, C. K., Cheng, H. H., Wang, S. D., Yeih, D. F. & Wang, S. M. PKCvarepsilon mediates serine phosphorylation of connexin43 induced by lysophosphatidylcholine in neonatal rat cardiomyocytes. *Toxicology* **314**, 11-21, doi:10.1016/j.tox.2013.08.001 (2013).
78 Kostin, S. Zonula occludens-1 and connexin 43 expression in the failing human heart. *Journal of cellular and molecular medicine* **11**, 892-895, doi:10.1111/j.1582-4934.2007.00063.x (2007).
79 Zemljic-Harpf, A. E. *et al.* Vinculin directly binds zonula occludens-1 and is essential for stabilizing connexin-43-containing gap junctions in cardiac myocytes. *J Cell Sci* **127**, 1104-1116, doi:10.1242/jcs.143743 (2014).
80 Bruce, A. F., Rothery, S., Dupont, E. & Severs, N. J. Gap junction remodelling in human heart failure is associated with increased interaction of connexin43 with ZO-1. *Cardiovasc Res* **77**, 757-765, doi:10.1093/cvr/cvm083 (2008).
81 Hunter, A. W., Barker, R. J., Zhu, C. & Gourdie, R. G. Zonula occludens-1 alters connexin43 gap junction size and organization by influencing channel accretion. *Molecular biology of the cell* **16**, 5686-5698, doi:10.1091/mbc.e05-08-0737 (2005).
82 Basu, R., Banerjee, K., Bose, A. & Das Sarma, J. Mouse Hepatitis Virus Infection Remodels Connexin43-Mediated Gap Junction Intercellular Communication In Vitro and <em>In

Vivo</em&gt. *Journal of Virology* **90**, 2586, doi:10.1128/JVI.02420-15 (2016).
83 Koster-Patzlaff, C., Hosseini, S. M. & Reuss, B. Persistent Borna Disease Virus infection changes expression and function of astroglial gap junctions in vivo and in vitro. *Brain research* **1184**, 316-332, doi:10.1016/j.brainres.2007.09.062 (2007).
84 Castellano, P. & Eugenin, E. A. Regulation of gap junction channels by infectious agents and inflammation in the CNS. *Front Cell Neurosci* **8**, 122-122, doi:10.3389/fncel.2014.00122 (2014).
85 Hsiao, H. J., Liu, P. A., Yeh, H. I. & Wang, C. Y. Classical swine fever virus down-regulates endothelial connexin 43 gap junctions. *Arch Virol* **155**, 1107-1116, doi:10.1007/s00705-010-0693-1 (2010).
86 Fischer, N. O., Mbuy, G. N. & Woodruff, R. I. HSV-2 disrupts gap junctional intercellular communication between mammalian cells in vitro. *J Virol Methods* **91**, 157-166 (2001).
87 Oelze, I., Kartenbeck, J., Crusius, K. & Alonso, A. Human papillomavirus type 16 E5 protein affects cell-cell communication in an epithelial cell line. *Journal of Virology* **69**, 4489 (1995).
88 Lim, B. K. *et al.* Coxsackievirus and adenovirus receptor (CAR) mediates atrioventricular-node function and connexin 45 localization in the murine heart. *J Clin Invest* **118**, 2758-2770, doi:10.1172/jci34777 (2008).
89 Bondesson, M., Svensson, C., Linder, S. & Akusjarvi, G. The carboxy-terminal exon of the adenovirus E1A protein is required for E4F-dependent transcription activation. *The EMBO journal* **11**, 3347-3354 (1992).
90 Raychaudhuri, P., Rooney, R. & Nevins, J. R. Identification of an E1A-inducible cellular factor that interacts with regulatory sequences within the adenovirus E4 promoter. *The EMBO journal* **6**, 4073-4081 (1987).
91 Goldsmith, K. T., Dion, L. D., Curiel, D. T. & Garver, R. I., Jr. trans E1 component requirements for maximal replication of E1-defective recombinant adenovirus. *Virology* **248**, 406-419, doi:10.1006/viro.1998.9293 (1998).
92 Teunissen, B. E. & Bierhuizen, M. F. Transcriptional control of myocardial connexins. *Cardiovasc Res* **62**, 246-255, doi:10.1016/j.cardiores.2003.12.011 (2004).
93 Arany, Z., Sellers, W. R., Livingston, D. M. & Eckner, R. E1A-associated p300 and CREB-associated CBP belong to a conserved family of coactivators. *Cell* **77**, 799-800, doi:10.1016/0092-8674(94)90127-9 (1994).
94 Ferrari, R. *et al.* Adenovirus small E1A employs the lysine acetylases p300/CBP and tumor suppressor Rb to repress select host genes and promote productive virus infection. *Cell host & microbe* **16**, 663-676, doi:10.1016/j.chom.2014.10.004 (2014).
95 Soria, C., Estermann, F. E., Espantman, K. C. & O'Shea, C. C. Heterochromatin silencing of p53 target genes by a small viral protein. *Nature* **466**, 1076-1081, doi:10.1038/nature09307 (2010).

96 Hale, T. K. & Braithwaite, A. W. The adenovirus oncoprotein E1a stimulates binding of transcription factor ETF to transcriptionally activate the p53 gene. *J Biol Chem* **274**, 23777-23786, doi:10.1074/jbc.274.34.23777 (1999).
97 Bridges, R. G., Sohn, S.-Y., Wright, J., Leppard, K. N. & Hearing, P. The Adenovirus E4-ORF3 Protein Stimulates SUMOylation of General Transcription Factor TFII-I to Direct Proteasomal Degradation. *mBio* **7**, e02184-02115, doi:10.1128/mBio.02184-15 (2016).
98 Zheng, Y., Stamminger, T. & Hearing, P. E2F/Rb Family Proteins Mediate Interferon Induced Repression of Adenovirus Immediate Early Transcription to Promote Persistent Viral Infection. *PLoS Pathog* **12**, e1005415, doi:10.1371/journal.ppat.1005415 (2016).
99 Ma, B., Fey, M. & Hottiger, M. O. WNT/β-catenin signaling inhibits CBP-mediated RelA acetylation and expression of proinflammatory NF-κB target genes. *Journal of Cell Science* **128**, 2430, doi:10.1242/jcs.168542 (2015).
100 Alonso, F. *et al.* An angiotensin II- and NF-kappaB-dependent mechanism increases connexin 43 in murine arteries targeted by renin-dependent hypertension. *Cardiovasc Res* **87**, 166-176, doi:10.1093/cvr/cvq031 (2010).
101 Bauer, A. *et al.* Pontin52 and reptin52 function as antagonistic regulators of beta-catenin signalling activity. *The EMBO journal* **19**, 6121-6130, doi:10.1093/emboj/19.22.6121 (2000).
102 Tago, K. *et al.* Inhibition of Wnt signaling by ICAT, a novel beta-catenin-interacting protein. *Genes Dev* **14**, 1741-1749 (2000).
103 Takemaru, K. *et al.* Chibby, a nuclear beta-catenin-associated antagonist of the Wnt/Wingless pathway. *Nature* **422**, 905-909, doi:10.1038/nature01570 (2003).
104 Chen, Q. *et al.* Carcinoma-astrocyte gap junctions promote brain metastasis by cGAMP transfer. *Nature* **533**, 493-498, doi:10.1038/nature18268 (2016).
105 Schoggins, J. W. & Rice, C. M. Interferon-stimulated genes and their antiviral effector functions. *Current opinion in virology* **1**, 519-525, doi:10.1016/j.coviro.2011.10.008 (2011).
106 Wu, J. *et al.* Cyclic GMP-AMP is an endogenous second messenger in innate immune signaling by cytosolic DNA. *Science* **339**, 826-830, doi:10.1126/science.1229963 (2013).
107 O'Shea, C. C., Choi, S., McCormick, F. & Stokoe, D. Adenovirus overrides cellular checkpoints for protein translation. *Cell cycle (Georgetown, Tex.)* **4**, 883-888, doi:10.4161/cc.4.7.1791 (2005).
108 Richards, T. S. *et al.* Protein kinase C spatially and temporally regulates gap junctional communication during human wound repair via phosphorylation of connexin43 on serine368. *The Journal of cell biology* **167**, 555-562, doi:10.1083/jcb.200404142 (2004).

109 Solan, J. L. *et al.* Phosphorylation at S365 is a gatekeeper event that changes the structure of Cx43 and prevents down-regulation by PKC. *The Journal of cell biology* **179**, 1301-1309, doi:10.1083/jcb.200707060 (2007).
110 Warn-Cramer, B. J., Cottrell, G. T., Burt, J. M. & Lau, A. F. Regulation of connexin-43 gap junctional intercellular communication by mitogen-activated protein kinase. *J Biol Chem* **273**, 9188-9196, doi:10.1074/jbc.273.15.9188 (1998).
111 Warn-Cramer, B. J. *et al.* Characterization of the mitogen-activated protein kinase phosphorylation sites on the connexin-43 gap junction protein. *J Biol Chem* **271**, 3779-3786, doi:10.1074/jbc.271.7.3779 (1996).
112 Hervé, J.-C., Derangeon, M., Sarrouilhe, D., Giepmans, B. N. G. & Bourmeyster, N. Gap junctional channels are parts of multiprotein complexes. *Biochimica et Biophysica Acta (BBA) - Biomembranes* **1818**, 1844-1865, doi:https://doi.org/10.1016/j.bbamem.2011.12.009 (2012).
113 Giepmans, B. N. G., Hengeveld, T., Postma, F. R. & Moolenaar, W. H. Interaction of c-Src with Gap Junction Protein Connexin-43: ROLE IN THE REGULATION OF CELL-CELL COMMUNICATION. *Journal of Biological Chemistry* **276**, 8544-8549, doi:10.1074/jbc.M005847200 (2001).
114 Singh, D., Solan, J. L., Taffet, S. M., Javier, R. & Lampe, P. D. Connexin 43 interacts with zona occludens-1 and -2 proteins in a cell cycle stage-specific manner. *J Biol Chem* **280**, 30416-30421, doi:10.1074/jbc.M506799200 (2005).
115 Li, M. W. M., Mruk, D. D., Lee, W. M. & Cheng, C. Y. Connexin 43 and plakophilin-2 as a protein complex that regulates blood–testis barrier dynamics. *Proceedings of the National Academy of Sciences* **106**, 10213-10218, doi:10.1073/pnas.0901700106 (2009).
116 Nagasawa, K. *et al.* Possible involvement of gap junctions in the barrier function of tight junctions of brain and lung endothelial cells. *Journal of Cellular Physiology* **208**, 123-132, doi:10.1002/jcp.20647 (2006).
117 Wei, C.-J., Francis, R., Xu, X. & Lo, C. W. Connexin43 Associated with an N-cadherin-containing Multiprotein Complex Is Required for Gap Junction Formation in NIH3T3 Cells. *Journal of Biological Chemistry* **280**, 19925-19936, doi:10.1074/jbc.M412921200 (2005).
118 Sato Priscila, Y. *et al.* Interactions Between Ankyrin-G, Plakophilin-2, and Connexin43 at the Cardiac Intercalated Disc. *Circulation Research* **109**, 193-201, doi:10.1161/CIRCRESAHA.111.247023 (2011).
119 Agullo-Pascual, E. *et al.* Super-resolution imaging reveals that loss of the C-terminus of connexin43 limits microtubule plus-end capture and NaV1.5 localization at the intercalated disc. *Cardiovascular research* **104**, 371-381, doi:10.1093/cvr/cvu195 (2014).
120 Yue, P. *et al.* Ischemia Impairs the Association Between Connexin 43 and M3 Subtype of Acetylcholine Muscarinic Receptor (M3-mAChR) in Ventricular Myocytes. *Cellular Physiology and Biochemistry* **17**, 129-136, doi:10.1159/000092074 (2006).

121 Fung, G., Luo, H., Qiu, Y., Yang, D. & McManus, B. Myocarditis. *Circulation research* **118**, 496-514, doi:10.1161/CIRCRESAHA.115.306573 (2016).

Figure Legends

Figure 3.1) Connexin43 protein levels are reduced during adenovirus type 5 infection. HaCaT cells were infected with Ad5 or replication-incompetent AdlacZ at a multiplicity of infection (MOI) of 10 iu/cell and fixed at 48 hpi or protein harvested every 24 hpi for 72 h. **A)** Immunofluorescence confocal microscopy of HaCaT cells at 48 hpi probed for Cx43 (green) and adenovirus E2A (red) with nuclei identified using DAPI (blue). Original magnification: X100. Scale bar: 20μm. **B)** Western blot probed for Cx43 expression in HaCaT cells. Detection of α-tubulin serves as loading control. **C)** Densitometry analysis of B. Statistical analysis was performed with two-way analysis of variance (ANOVA) with Sidak's multiple comparisons test. (n=3). *p≤0.05, **p≤0.01, ***p≤0.001, ****p<0.0001. Data are represented as mean ±SEM. See also Figure S1.

Figure 3.2) Specific targeting of gap junction gene transcription during adenovirus type 5 infection. HaCaT cells were infected with Ad5 at a MOI of 10 iu/cell and RNA was harvested at 24 hpi. **A)** RT-qPCR analysis of *CDKN1A* (p21) and *SFN* (14-3-3σ) to confirm active viral infection and known altered gene transcription. **B)** RT-qPCR analysis of gap junction family genes *GJA1* (Cx43), *GJA5* (Cx40), and *GJC1* (Cx45). **C)** RT-qPCR analysis of junctional protein genes *PKP2* (Plakophilin-2) and *TJP1* (ZO-1). Statistical analysis performed by one-way ANOVA with Dunnett's multiple comparisons test. (n=3). *p≤0.05

**p≤0.01 ***p≤0.001 ****p<0.0001. Data are represented as mean ±SEM. See also Figure S1.

Figure 3.3) Early adenoviral factors induce β-catenin transcriptional activity through growth factor signaling. HaCaT cells were infected with Ad5 or replication-incompetent AdlacZ at a MOI of 10 iu/cell and RNA and protein were harvested or cells were fixed for immunofluorescence over a 72 h time course. **A)** RT-qPCR analysis of *CTNNB1* (β-catenin) relative fold change from 0 hpi. (n=3). **B)** Immunofluorescence confocal microscopy for β-catenin (green) and Ad5 (red) with nuclei identified with DAPI (blue). Greyscale images in right panels identify nuclear β-catenin levels through DAPI binary mask multiplication from a single Z-slice. Original magnification: X100. Scale bar: 10μm. **C)** Quantification of nuclear β-catenin represented in B. (n=5). **D)** Western blot of total β-catenin and β-catenin phospho-Ser552 (transcriptionally active) also probed for Ad5-E1A to confirm infection and α-tubulin for loading control. **E)** Quantification of D by densitometry. (n=3). HaCaT cells were transfected with pSF-CAG-empty vector or -E4orf1 and protein harvested 24 hours post transfection. **F)** Western blot of total β-catenin and β-catenin phospho-Ser552 (transcriptionally active) also probed for GAPDH for loading control. **G)** Quantification of F by densitometry. (n=3). Statistical analyses performed using the unpaired Student's t-test (A, C, G) or two-way ANOVA with Sidak's multiple comparisons test (E). *p≤0.05 **p≤0.01 ***p≤0.001 ****p<0.0001. Data are represented as mean ±SEM. See also Figure S2, S3.

Figure 3.4) β-catenin transcriptional activity is necessary to reduce GJA1 mRNA during adenoviral infection. HaCaT cells were treated with the β-catenin transcriptional inhibitor LF3 1 hpi or LF3 alone and harvested for RNA and DNA at indicated time points. **A)** RT-qPCR analysis of *GJA1* mRNA at 24 hpi in cells treated with LF3 or vehicle and infected at a MOI of 10 iu/cell. (*n*=3). B) RT-qPCR analysis of uninfected HaCaT cells treated with vehicle or LF3 for 24 h. (*n*=3). **C)** qPCR analysis of viral genomes in HaCaT cells infected with Ad5 and treated with LF3 or vehicle and harvested 24 hpi. (*n*=5). *ns*: not significant. Statistical analyses performed using the unpaired Student's t test. $p \leq 0.05$ is considered statistically significant. ** $p \leq 0.01$. Data are represented as mean ±SEM.

Figure 3.5) Cx43 protein occurs in reduced levels at the endoplasmic reticulum and is primarily junctional during adenovirus infection. HaCaT cells were infected with AdlacZ or Ad5 at a MOI of 10 iu/cell prior to fixation or protein harvesting at 24 hpi. **A)** AdlacZ- or Ad5-infected HaCaT cells were immunolabeled against PDI (red) to localize ER and against Cx43 (green). Cells were stained using DAPI to identify nuclei (blue). Colocalized Cx43 / PDI signal was determined with ImageJ (white). Original magnification: X100. Scale bar: 20 μm. **B)** Manders' Coefficients calculations determined using fraction Cx43 with PDI. Data points represent averages of 8 images from 3 separate experiments. **C)** Pearson's Coefficients calculations determined for Cx43 and PDI correlation.

Data points represent averages of 8 images from 3 separate experiments. **D)** AdlacZ- or Ad5-infected HaCaT cells were lysed in 1% Triton X-100 solubility assay buffer prior to fractionation and western blotting. Membrane probed against Cx43 (top panel) and α-tubulin (bottom panel) for loading control. **E)** Quantification of D. Statistical analysis was performed with Student's t-test. (*n*=3). *$p \leq 0.05$, **$p \leq 0.01$. Data are represented as mean ±SEM.

Figure 3.6) Adenovirus inhibits gap junction intercellular communication prior to reduction of Cx43 total protein levels during infection. HaCaT cells were plated to confluence on glass bottomed dishes and infected with Ad5 or replication-incompetent AdlacZ at a MOI of 10 iu/cell. The Lucifer yellow (LY) scrape-load dye-transfer assay was performed at 12 hpi with 10,000 MW Dextran-AlexaFluor647 (Dex-647) as a gap junction non-permeable control. **A)** Representative confocal microscopy images of LY (green) and Dex-647 (red) transfer with nuclei identified with DAPI (blue). Middle greyscale panels show LY and Dex-647 alone and right panels illustrate quantification of each dye spread. Original magnification: X20. Scale bar: 50μm. **B)** Quantification of dye spread in A. Statistical analysis was performed with the unpaired Student's t-test. (*n*=4). ****$p < 0.0001$. Data are represented as mean ±SEM. See also Figure S4.

Figure 3.7) Direct targeting of Cx43 gap junctions through phosphorylation during adenovirus type 5 infection. HaCaT-GJA1+ cells or wild-type HaCaT cells were infected with Ad5 or replication-incompetent AdlacZ at a MOI of 10

iu/cell and protein was harvested at 24 hpi. **A)** Immunoprecipitation (IP) of Cx43 followed by western blot probed for phosphoSerine-14-3-3 mode-1 binding motif to detect phosphorylation of Cx43-Ser373 at 24 hpi. α-tubulin serves as loading control. **B)** Densitometry analysis of A. **C)** IP of Cx43 followed by western blot for Cx43 phosphorylation at Ser368. Cx43 IP and IgG IP are from same membrane. **D)** Densitometry analysis of C. **E)** HaCaT cells were infected with Ad5 or AdlacZ at a MOI of 10 iu/cell and protein harvested 24 hpi. Co-immunoprecipitation (CoIP) was performed for ZO-1 and Cx43 followed by western blotting. α-tubulin serves as loading control. **F)** Densitometry analysis of E. Statistical analysis performed with the unpaired Student's t-test. (n=3). *p≤0.05 **p≤0.01 ***p≤0.001 ****p<0.0001. Data are represented as mean ±SEM. See also Figure S5.

Figure 3.8) Ad5 targets Cx43 in cardiomyocytes and induces Cx43-gap junction remodeling. HiPSC-CMs were infected with Ad5 or replication-incompetent AdlacZ at a MOI of 10 iu/cell and protein harvested or fixed for immunolabeling over a 72 h time course. **A)** Western blot probed for Cx43 expression in HiPSC-CMs. Detection of Ad5-Hexon protein expression serves to confirm infection and α-tubulin serves as loading control. **B)** Densitometry analysis of A. **C)** Immunofluorescence confocal microscopy of HiPSC-CMs at 48 hpi probed for Cx43 (green) and adenovirus E1A (red) with nuclei identified using DAPI (blue). Original magnification: X100. Scale bar: 20μm. **D)** Immunofluorescence confocal microscopy of HiPSC-CMs 24 hpi probed for Cx43 (green) and ZO-1 (red) with nuclei identified using DAPI (blue). Original

magnification: X100. Scale bar: 10μm. Images representative of 3 separate experiments. **E)** Super resolution stochastic optical reconstruction microscopy (STORM) derived point-cloud localizations of Cx43 (cyan) and ZO-1 (red) in Ad5- and AdlacZ-infected HiPSC-CMs 24 hpi. Zoomed out panels (left) scale bar: 2μm. Zoomed in panels (right) scale bar: 200nm. Sphere size: 30nm. **F)** Cross-Pair correlation functions for Cx43/ZO-1 complexing in E. (n=10). Statistical analysis was performed with two-way analysis of variance (ANOVA) with Sidak's multiple comparisons test (B) (n=3). *p≤0.05, **p≤0.01, ***p≤0.001, ****p<0.0001. Data are represented as mean ±SEM.

Figure 3S1) Specific host-cell proteins are targeting during adenoviral infection. Related to Figure 1 and 2. HaCaT cells were infected with Ad5 or AdlacZ at a MOI of 10 iu/cell and protein lysates harvested at 0 hpi and 24 hpi followed by western blotting. **A)** Western blot probed against E-Cadherin (top panel) and CAR (center panel) with α-tubulin probed for a loading control (bottom panel). **B)** Quantification of A. **C)** Western blot probed against RPL22 (top panel) with α-tubulin probed for a loading control (bottom panel). **D)** Quantification of C. **E)** Western blot probed against Cx45 (top panel) and Cx43 (center panel) with α-tubulin probed for a loading control (bottom panel). **F)** Quantification of E. **G)** Western blot probed against Cx40 (top panel) with α-tubulin probed for a loading control (bottom panel). **H)** Quantification of G. Statistical analysis was performed with Student's t-test. (n=3). *p≤0.05, **p≤0.01. Data are represented as mean ±SEM.

Figure 3S2) *GJA1* expression is higher than *GJA5* and *GJC1* in untreated HaCaT cells. Related to Figure 2. RT-qPCR was performed on HaCaT cells to determine baseline expression of *GJA1*, *GJA5*, and *GJC1*. Statistical analysis was performed with one-way analysis of variance (ANOVA) with Tukey's multiple comparisons test. (n=3). *p≤0.05, **p≤0.01. Data are represented as mean ±SEM.

Figure 3S3) GJA1-candidate transcription factors are elevated during Ad5 infection. Related to Figure 3. HaCaT cells were infected with Ad5 at a MOI of 10 iu/cell and RNA harvested at 24 hpi. RT-qPCR analysis of Ad5-infected HaCaT cells for transcription factor genes *TBX2* and *F2R* which are previously shown to regulate *GJA1* transcription relative to 0 hpi. Data are represented as mean ±SEM.

Figure 3S4) Detection of E4orf1 mRNA in transfected HaCaT cells. Related to Figure 3. HaCaT cells were transfected with pSF-CAG-empty or -E4orf1 and RNA harvested 24 hours post transfection. E4orf1 is detected by RT-qPCR in transfected HaCaT cells. n=3. Data are represented as mean ±SEM.

Figure 3S5) Adenovirus infection reduces gap junction function. Related to Figure 6. HaCaT cells were infected with Ad5 or replication-incompetent AdLacZ at a MOI of 10 iu/cell and protein was harvested at 6 and 12 hpi in addition to LY

scrape-load dye-transfer assay at 24 hpi. **A)** Representative confocal microscopy images of LY (green) and Dex-647 (red) transfer with nuclei identified with DAPI (blue). Middle greyscale panels show LY or Dex-647 alone and right panels illustrate quantification of each dye spread. Original magnification: X20. Scale bar: 50μm. **B)** Quantification of A (*n*=3). **C)** Western blot probed for Cx43 expression with α-tubulin serving as loading control. **D)** Densitometric analysis of C (*n*=3). Statistical analysis performed by unpaired Student's t-test (B) or two-way ANOVA with Sidak's multiple comparisons test (D). *$p \leq 0.05$, *ns*: not significant. Data are represented as mean ±SEM.

Figure 3S6) Adenovirus does not induce Cx43 phosphorylation at Ser262. Related to Figure 7. **A)** HaCaT-GJA1+ cells were infected with Ad5 at a MOI of 10 iu/cell and protein harvested 6, 12, and 24 hpi. Immunoprecipitation of Cx43 was performed following by western blot and probed for Cx43 phosphorylation at Ser262 (pCx43(S262)) and total Cx43. Immunoprecipitated Cx43 and IgG are from same membrane and exposure. Detection of Hexon confirms infection and α-tubulin serves as loading control. **B)** Densitometry of A. **C)** Wild-type HaCaT cells were infected with Ad5 or replication-incompetent AdlacZ at a MOI of 10 iu/cell and protein harvested 24 hpi. Immunoprecipitation of Cx43 was performed followed by western blot and probed for pCx43(S262) and total Cx43. Immunoprecipitated Cx43 and IgG are from same membrane and exposure. **D)** Densitometry of C. Statistical analyses performed using unpaired Student's t-test.

(*n*=3). $p \leq 0.05$ is considered statistically significant. *ns*: not significant. Data are represented as mean ±SEM.

Chapter 4

Manuscript 2

In Preparation

TITLE

Adenoviral infection stabilizes intercellular junctions to enhance viral spread.

Patrick J. Calhoun[1,2], Carissa C. James[1,3], James W. Smyth*[1,2,4]

[1]Fralin Biomedical Research institute, Roanoke, VA 24016, USA

[2]Department of Biological Sciences, Virginia Tech, Blacksburg, VA 24060, USA

[3]Graduate Program in Translational Biology, Medicine, and Health, Virginia Tech, Blacksburg, VA 24060, USA

[4]Virginia Tech Carilion School of Medicine, Roanoke, VA, 24016, USA

*correspondence

smythj@vtc.vt.edu

Abstract

Adenoviruses are causative agents for many pathologies including acute respiratory disease and viral myocarditis. Gap junctions comprise connexin proteins and metabolically, electrically, and immunologically couple cells. Furthermore, distinct intercellular junction structures can regulate the expression and localization of one another. Previously, we reported reduced connexin43 (Cx43) phosphorylation at a known internalization motif, leading us to hypothesize that gap junctions are maintained during adenoviral infection in order to stabilize intercellular junctions and adenoviral receptors therein. Utilizing immunofluorescence confocal microscopy, we demonstrate that Cx43 reductions are primarily cytosolic with Cx43 preserved at the plasma membrane. Click-IT chemistry, a non-radioactive pulse-chase technique, reveals that Cx43 ½ life is extended during adenoviral infection. In order to test if remainingCx43 exists in *de facto* gap junctions (i.e. not undocked or cytosolic connexons) we utilized 1 % Triton X-100 solubility assay and find Cx43 is primarily junctional during adenoviral infection. Having demonstrated increases in junctional Cx43, we next asked how tightly coupled cells were during adenoviral infection and by ECIS measurements of electrical resistance we demonstrate a transient increase in mechanical coupling during infection. Taken together, our future aims are to uncover changes in Coxsackievirus and adenovirus receptor (CAR) protein localization to determine if adenoviral-induced changes to subcellular architecture predisposes neighboring cells to infection and enhances viral

spread. These findings will add to the existing model of adenoviral infection and more broadly, contribute to the therapeutic design of adenoviral vectors for cancer and gene therapy.

Introduction

Gap junctions occur in arrays of structures at intercellular interfaces where they facilitate the transfer of ions, metabolites, second messengers, and other small molecules less than approximately 1 kDa in size (reviewed in [1]). Connexin proteins comprise gap junctions and of the 21 human connexins, connexin43 (Cx43; gene name *GJA1*) is the most ubiquitously expressed and plays critical developmental and homeostatic roles throughout various tissues. It is more recently appreciated that the immunological second messenger 2'3'-cyclic guanosine monophosphate-adenosine monophosphate (cGAMP), produced by detection of cytosolic DNA by cGAMP synthetase (cGAS), is transferred via gap junctions from infected cells to uninfected cells and thus capable of propagating the antiviral immune response.[2,3] While it is established that many viruses directly antagonize various protein components of the cGAS pathway, functional redundancy for inhibition of antiviral responses may occur by targeting of gap junctions.[4]

Adenoviruses are dsDNA tumor viruses responsible for a spectrum of pathogenesis including acute respiratory diseases, viral myocarditis, and meningoencephalitis.[5-12] A critical step in adenoviral infection is viral attachment and uptake which is facilitated by, at least in part for species C adenoviruses (serotypes 1, 2, 5, 6), the Coxsackievirus and adenovirus receptor (CAR) as well as integrin α_V proteins (both β_3 and β_5).[13,14] CAR localizes to intercellular

junctions and in epithelial cells primarily to tight junctions where cell-cell adhesion is achieved by homophilic and heterophilic interactions.[15] Integrin proteins act as adhesion molecules and sensors for cellular attachment to the extracellular matrix. CAR expression has been demonstrated to be dispensable, yet enhancing, for adenoviral infection or transduction *in vitro*.[14,16] Additionally, cells lacking integrin αV proteins are bound by adenovirus yet entry is blocked.[13,17] Taken together, these two interactions work in concert so that species C adenoviruses bind CAR with high affinity, stabilizing extracellular virus, and increasing with integrin αV proteins and subsequent viral endocytosis.

cGAS is a pattern recognition receptor for detecting cytosolic nucleic acids, including RNA but primarily DNA, and is important for detecting pathogens and initiating innate immune defenses in many cell types.[18-22] cGAS activation leads to the production of cGAMP which activates STING resulting in STING homodimerization and translocation to perinuclear regions.[23,24] STING homodimers recruit TANK binding kinase 1 (TBK-1) and interferon regulatory factor 3 (IRF-3) resulting in STING and IRF-3 phosphorylation by TBK-1.[25] Phosphorylated IRF-3 translocate to the nucleus where it binds transcriptional coactivators and interferon stimulatory response elements (ISRE) of interferon stimulated genes (ISG) to activate transcription.[26-28] Importantly, cGAMP is a critical molecule in this signaling cascade and as mentioned above, can transfer via gap junctions and initiate this cascade in uninfected neighboring cells.[2,3]

CAR is classically described to localize to tight junctions in polarized epithelial cells yet significant cross-talk and colocalization between distinct intercellular junctional components exists. An example of this calcium-dependent alterations observed in gap junction intercellular communication by E-cadherin, a component of adherens junctions.[29] Furthermore, it has been shown that blocking N-cadherin with antibodies blocks gap junction intercellular communication, highlighting the importance of cross-talk and interdependency between apparently distinct junctional components.[30] Specifically in regard to CAR, a cardiac specific inducible CAR knock out mouse model demonstrates a >40% reduction in Cx43.[31] Additionally, knockdown of Cx43 causes a significant decrease of surface localized CAR as detected by surface biotinylation, further supporting the model that these proteins affect the expression and localization of one another.[32]

We previously demonstrated the targeting of Cx43 gap junctions by human adenovirus serotype 5 (Ad5) at the level of transcription.[33] Gap junction intercellular communication was reduced concomitant with a Cx43 phosphorylation events leading to altered gap junction channel conductance during adenoviral infection. Interestingly however, those data also support the possibility that gap junctions are not targeted for internalization during infection despite negative gene regulation of *de novo* gap junctions. Here we investigate the maintenance of existing gap junctions during adenoviral infection as a potential mechanism to maintaining junctional adhesion molecules, including

CAR, between infected and uninfected cells as a means to direct viral spread more efficiently than diffusion alone. Adenocarinomic human alveolar basal epithelial (A549) cells and spontaneously immortalized keratinocyte (HaCaT) cells were infected with Ad5 in order to assay changes in intercellular junctions. We demonstrate that although cytoplasmic Cx43 is depleted during infection, Cx43 at the cell membrane is retained. Furthermore, we find Cx43 is primarily junctional and exhibits increased half-life highlighting structural gap junction maintenance during infection. We established an Ad5-induced interferon response dependent upon gap junctions in a more physiologically relevant low multiplicity of infection (MOI) through cGAMP transfer. We then utilized a fluorescence reporter mutant Ad5 in a low MOI model to perform localization and colocalization experiments to ask if uninfected neighboring cells preferentially localize to junctional complexes at the uninfected-infected cell-cell interface. Finally, in order to confirm these structural alterations result in increased viral spread, we performed real-time live imaging microscopy in Cx43 overexpressing and Cx43 knockout cells.

Materials and Methods

Cell culture

HEK293FT, HEK293A (Thermo Fisher), A549 (ATCC), and HaCaT (AddexBio) cells were maintained and passaged in DMEM, high glucose, with L-Glutamine (Genesee Scientific) supplemented with 10 % fetal bovine serum (FBS), non-

essential amino acids (Life Technologies), and MycoZap Plus-CL (Lonza) unless otherwise specified. Cells were maintained in a humidified atmosphere of 5 % CO_2 at 37 °C.

Viruses and infection

Ad5 was obtained from ATCC and propagated in A549 cells. AdlacZ was generated according to manufacturer's instructions from pAd/CMV/V5-GW/lacZ (Thermo Fisher). Ad-late/RFP was a kind gift from Dr. Robin Parks (Ottawa Hospital Research Institute, Department of Medicine) and was propagated in A549 cells. Viruses were purified by CsCl ultracentrifugation as previously described and titer determined by immunofluorescence confocal microscopy in HEK293A cells.[34] All infections were performed in serum-free DMEM and supplemented with equal volume of supplemented DMEM (10 % FBS) 1-hour post infection (hpi).

RT-qPCR

Cells were lysed in TRIzol (Thermo Fisher) and clarified by phenol-chloroform phase separation before RNA isolation using PureLink RNA mini kit (Thermo Fisher) and PureLink on-column DNase digestion (Thermo Fisher) according to manufacturer's instructions. cDNA was generated with iScript Reverse Transcription Supermix for RT-qPCR (BioRad) according to manufacturer's instructions. Real-time PCR was performed with SYBR Select Master Mix for CFX (Thermo Fisher) on a QuantStudio 6 Flex system (Thermo Fisher).

18SrRNA (forward primer-GGCCCTGTAATTGGAATGAGTC; reverse primer-CCAAGATCCAACTACGAGCTT) and *GAPDH* (forward primer-ACATCGCTCAGACACCATG; reverse primer-TGTAGTTGAGGTCAATGAAGGG) were utilized as internal references. Gene expression data was collected for *IRF-7* (forward primer-TACCATCTACCTGGGCTTCG; reverse primer-TGCTGCTATCCAGGGAAGAC), *MX1* (forward primer-GCCACCACAGAGGCTCTCAG; reverse primer-CTCAGCTGGTCCTGGATCTCCT), and *TRIM29* (forward primer-CACCGGACACCATGAAGAGA; reverse primer-ACGAGGGCTGGTATGATGTC).

Western blotting

Cells were lysed in RIPA buffer (50 mM Tris pH 7.4, 150 mM NaCl, 1 mM EDTA, 1 % Triton X-100 (Sigma Aldrich), 1 % sodium deoxycholate, 2 mM NaF, 200 µM Na_3VO_4, 0.1 % sodium dodecyl sulfate, 5 mM n-ethylmaleimide) supplemented with HALT Protease and Phosphatase Inhibitor Cocktail (Thermo Fisher). Protein was clarified by sonication and centrifugation and concentration determined by DC protein assay (BioRad). 4X LDS Sample Buffer (Thermo Fisher) was added to samples prior to being heated to 70 °C for 10 min and subjected to SDS-PAGE using NuPAGE Bis-Tris 4-20 % gradient gels and MES (Thermo Fisher) running buffer according to manufacturer's instructions. Proteins were transferred to PVDF (BioRad) membrane and fixed in methanol followed by air drying. PVDF

membranes were reactivated in methanol followed by blocking in 5 % nonfat milk (Carnation) or 5 % bovine serum albumin (Fisher) in TNT buffer (0.1 % Tween 20, 150 mM NaCl, 50 mM Tris pH 8.0) for 1 h at room temperature. Primary antibody labeling was performed overnight at 4 °C using primary antibodies rabbit anti-Cx43 (1:5000; Sigma-Aldrich), and mouse anti-α-tubulin (1:5000; Sigma Aldrich). Membranes were washed 6 times before secondary antibody labeling for 1 h at room temperature with goat secondary antibodies conjugated to AlexaFluor555 or AlexaFluor647 (Thermo Fisher). Fluorescently labeled membranes were soaked in methanol and air dried prior to imaging. Membranes were imaged on a Chemidoc MP imaging system (BioRad).

Immunofluorescence confocal microscopy

Cells were fixed for 20 min with 4 % PFA in PBS at room temperature or for 5 min with -20 °C methanol on ice. Cells were permeabilized and blocked with 5 % normal goat serum (Invitrogen) and 0.1 or 0.5 % Triton X-100 (Sigma Aldrich) in PBS for 1 h at room temperature. Primary antibody labeling was performed for 1 h at room temperature using rabbit anti-Cx43 (1:2000; Sigma Aldrich) and mouse anti-E2A [B6-8] (1:250; generously provided by Dr. David Ornelles). Cells were washed 6 times prior to secondary antibody labeling for 1 h at room temperature with goat secondary antibodies conjugated to AlexaFluor488 or AlexaFluor555 (Thermo Fisher). During secondary antibody labeling cells were counterstained with DAPI and wheat germ agglutinin (WGA) conjugated AlexaFluor647. Slides were mounted using Prolong Gold Antifade (Life Technologies).

Triton X-100 solubility assay

Cells were harvested in 1% Triton X-100 buffer (50mM Tris, pH 7.4, 1 % Triton X-100, 2 mM EDTA, 2 mM ethylene glycols-bis(β-aminoethyl ether)-*N,N,N,N*-tetraacetic acid [EGTA], 250 mM NaCl, 1 mM NaF, 0.1 mM Na_3VO_4) supplemented with HALT Protease and Phosphatase Inhibitor (Thermo Fisher). Samples were rotated at 4 °C for 1 h. A small volume was removed to serve as the total protein fraction. Remaining lysate was centrifuged for 30 min at 15,000 x *g* at 4 °C and supernatant reserved as soluble fraction. Pellets containing insoluble proteins were resuspended in 4X Bolt LDS sample buffer (Thermo Fisher). All samples were sonicated and centrifuged for 20 min. at 10,000 x *g* at 4°C followed by addition of 4X Bolt LDS sample buffer supplemented with 400 mM DTT prior to western blotting.

Click-iT half-life

HaCaT cells were grown to confluency followed by removal of media and 3 washes with PBS. Serum/methionine/cysteine-free DMEM (Thermo Fisher) with AdlacZ or Ad5 at a MOI of 10 iu/cell was added to cells and incubated for 1 h at 37 °C followed by a 1 h pulse with Click-iT L-Azidohomoalanine (50 μM final concentration; Thermo Fisher) added directly to virus containing-starvation media. Samples were harvested over a 12 h time course every 2 hpi into lysis buffer (50 mM Tris-HCl, 1 % SDS) supplemented with HALT Protease and Phosphatase Inhibitor (Thermo Fisher). Lysates were incubated on ice for 15 min

followed by sonication and centrifugation at 10,000 x *g* for 20 min at 4 °C. Protein concentration was determined using DC protein assay (BioRad) and lysates protein normalized to 4 µg/µL. 400 µg protein was utilized for the click reaction using Click-iT Protein Reaction Buffer Kit and tetramethylrhodamine (TAMRA) alkyne (40 µM final concentration; Thermo Fisher) according to manufacturer's instructions. Immunoprecipitation was performed as previously described described.[35] Briefly, Cx43 was immunoprecipitated from precleared lysates with 1 µg rabbit anti-Cx43 (Sigma-Aldrich) and protein G Dynabeads (Thermo Fisher). Western blotting was performed as described above and pulsed Cx43 detected using antibody labeling of TAMRA (1:1000; Thermo Fisher).

Electrical cell-substrate impedance sensing (ECIS)

HaCaT cells were plated to confluency on an 8W10E+ 8 well array (Applied BioPhysics) prior to infecting with AdlacZ or Ad5 at a MOI of 10 iu/cell. Impedance was assayed on a Z-Theta station (Applied BioPhysics) with Applied BioPhysics – ECIS software (Applied BioPhysics) utilizing multiple frequencies measurements over an 80 h timecourse. A frequency of 4000 Hz results in electrical current passing through the space between intercellular junctions and resistance at 4000 Hz was normalized within treatments.

Super-resolution STORM localization and analysis

Cells were fixed with -20 °C methanol on ice for 5 min followed by 3 washes with PBS. Cells were blocked with 5 % normal donkey serum and 0.1 % or 0.5 %

Triton X-100 in PBS for 1 h at room temperature. Primary antibody labeling was performed for 1 h at room temperature with rabbit anti-Cx43 (1:2000; Sigma-Aldrich) and mouse anti-ZO-1 (1:500; BD Biosciences). Cells were washed 6 times prior to secondary antibody labeling for 1 h at room temperature with donkey antibodies conjugated to Alexa Fluor 647 (Thermo Fisher) or CF568 (Biotium). Cells were washed 6 times and stochastic optical reconstruction microscopy (STORM) conducted with a Vutara 350 microscope (Bruker). Cells were imaged in 50 mM Tris-HCl, 10 mM NaCl, 10 % (wt/vol) glucose buffer containing 20 mM mercaptoethylamine, 1% (vol/vol) 2-mercaptoethanol, 168 active units/ml glucose oxidase, and 1404 active units/ml catalase. 5000 frames were acquired for each probe and 3D images were reconstructed in Vutara SRX software. Coordinates of localized molecules were used to calculate pair correlation functions in the Vutara SRX software.

Statistics

All quantification was performed on experiments repeated at least three times. Data are presented as mean ± SEM. Statistical analysis was conducted with GraphPad Prism 8.2.0 (GraphPad Software, Inc. La Jolla, CA). Data were analyzed for significance using Student's t test, one-way ANOVA, two-way ANOVA, with Sidak's (when comparing Ad5-infected to control within time points across multiple time points) or Dunnet's (when comparing infected time points to 0 hpi) multiple comparison tests. A value of $p < 0.05$ was considered statistically significant.

Results

Cx43 is maintained at the plasma membrane during adenoviral infection

We previously demonstrated Cx43 is targeted during adenoviral infection at the level of transcription.[33] Utilizing A549 cells expressing higher levels of endogenous Cx43, we discovered maintenance of Cx43 localized at cell-cell contacts by immunofluorescence confocal microscopy (Figure 4.1A). Given that A549 cells are cancer-derived, we turned to the more biologically relevant non-transformed HaCaT epithelial cell line for additional experiments that we previously utilized to determine transcriptional and post-translational targeting of Cx43 by Ad5. We next asked if maintenance of Cx43 at cell-cell contacts extended the half-life of Cx43. In Ad5-infected HaCaT cells we discover an increased half-life of 56% by utilizing a nonradioactive pulse-chase assay (Figure 4.1B, quantified in 4.1C).

Cells become more mechanically coupled early during Ad5 infection

We previously demonstrated reduced GJIC and phosphorylation consistent with altered channel conductance in Ad5-infected HaCaT cells. Given our findings here involving maintenance of gap junctions during infection, we next sought to determine how mechanically coupled Ad5-infected cells were over time. Electrical Cell-substrate Impedance Sensing (ECIS) allows for measurements of electrical resistance across a monolayer of cells to determine changes in

mechanical coupling. Utilizing ECIS to acquire electrical resistance measurements across a monolayer of infected HaCaT cells during an 80 h timecourse, we find a 14% increase in mechanical coupling at 28 hpi that is maintained until the onset of CPE (> 48 hpi) (Figure 4.2).

Future Direction / In Progress – Interrogate interferon responses in uninfected neighbor cells via cGAMP

Given that gap junctions propagate the antiviral immune response through transfer of cGAMP, we hypothesized that the previously demonstrated decrease in GJIC would result in a reduced innate immune response from a mixed population of infected and uninfected cells. HaCaT cells infected with Ad5 at a MOI of 10 iu/cell demonstrate an increased IFN response as assayed by ISG expression as early as 6 hpi (Figure 4.3). Given AdlacZ fails to express adenoviral genes that antagonize the immune response, Ad5-infected HaCaT cell ISG expression is relative to uninfected HaCaT cells. Ad5 is well described to suppress both innate and adaptive immune responses in cells and a 100% infected monolayer may therefore fail to capture the biological function of gap junctions for innate immune signaling.[36] In order to address this, we next will utilize a low MOI infection of 0.05 iu/cell in order to assay the biological importance of gap junctions in initiating the IFN response in a population of infected and uninfected cells. Furthermore, in order to determine if cGAMP is the *de facto* driving molecule of IFN expression in uninfected cells, we will utilize immunofluorescence confocal microscopy analysis of STING localization.[37]

Future Direction / In Progress – Determine Ad5 infection changes in receptor availability on uninfected neighboring cells

CAR proteins are involved in intercellular mechanical coupling at gap junctions, and facilitate the attachment and rapid internalization of Ad5 cooperatively with integrin α_V. Having demonstrated that cells are more mechanically coupled during Ad5 infection, we hypothesized that cell-surface CAR is increased during adenoviral infection on uninfected cells. In order to undertake colocalization experiments and localize infected cells in a low MOI infection model, we used Ad-late/RFP, an Ad5 mutant deleted of E3 expressing RFP under control of the endogenous major late promoter validated to be functionally wild-type *in vitro*.[38] We first will examine Cx43 expression in Ad-late/RFP to determine differences between wild type Ad5 and Ad-late/RFP in both high (10) and low (0.05) MOI infection models by immunofluorescence confocal microscopy, western blotting, and RT-qPCR. In order to determine changes in uninfected cell CAR localization we will employ immunofluorescence confocal microscopy colocalization with Cx43 or WGA-labeled cell membranes. Additionally, we will assay changes in basolateral localization of CAR in confocal imaging. Given the importance of integrin α_V proteins for infectability of cells, we will carry out colocalization analysis by IF of CAR and integrin α_V. Super resolution STORM microscopy localization will be carried out to quantify the spatial relationship of CAR *in situ*. Cross-pair correlation functions are generated from STORM data with the probability of localizing two distinct target molecules at a given distance with a

function value of 1 is interpreted as no correlation with increasing function values confirming complexing by two molecules. We will interrogate changes in Cx43, CAR and integrin α_V localization in uninfected neighbor cells by STORM through colocalization and cluster analyses.

Discussion

Viral infection and subsequent spread or progeny have classically been considered two disparate parts of the infectious cycle. Infection itself consists of viral uptake, a varying degree of cellular reprogramming, and ultimately viral replication and egress. While viral spread is driven by diffusion of infectious particles, it is becoming increasingly appreciated that viruses have evolved methods to direct egress and thus direct viral spread. The utilization of cell-cell junctional proteins by several viruses as receptors for attachment and internalization further highlights this focused route of transmission. We previously demonstrated transcriptional and post-translational targeting of gap junctions by human adenovirus.[33] During Ad5 infection, we observed intracellular depletions of Cx43 while membrane localized Cx43 is preserved. Here we demonstrate that existing gap junction structures are maintained during infection, resulting in proximal recruitment of additional cell-cell junctional proteins and influencing viral spread.

Cx43 gap junction synthesis, forward trafficking, channel-gating, and internalization, is under exquisite cellular control with a relatively rapid turnover compared to other cell-cell junctional components. This is accomplished by transcriptional and translational regulation, as well as at the level of post-translational modifications occurring primarily at the Cx43 c-terminus. Many cell type-dependent transcription factors have been identified as regulating *GJA1* expression including TBX2, PAR1, AP, SP1, NKX2.5, STAT3, and IRX3 during development and for homeostasis.[39-44] β-catenin has recently been demonstrated to transcriptionally repress *GJA1* in addition to the classical definition as an activator in the context of adenoviral infection.[33,45] Cx43 translational regulation is altered during TGF-β treatment and hypoxia resulting in changes to internal translation initiation and gap junction formation due to altered 5' UTR length.[46,47] Independent of total protein, gap junction function can be modified through post-translational modifications with extensive studies focusing on phosphorylation (reviewed in [48-50]). Specifically, it has been demonstrated that MAPK phosphorylation of Cx43 at Ser255/262/279/282 is associated with internalization.[35,51-53] We previously identified reduced phosphorylation of Cx43 at Ser262 suggesting gap junction internalization is not induced during adenoviral infection.[33] Here, we find increased Cx43 half-life in agreement with the model that although *de novo* Cx43 is reduced during adenoviral infection, Cx43 internalization is reduced. MAPK phosphorylation at Ser262 has been shown to precede ubiquitination, internalization, and degradation through clathrin-dependent, proteasome-dependent, and lysosomal pathways.[54-56] Additional

work elucidating adenoviral manipulation to these internalization processes will further clarify mechanistically how gap junctions are being maintained during adenoviral infection.

Extensive cross-talk and interdependency among classically defined disparate junctional families has been demonstrated between gap junctions and adherens junctions, tight junctions, and desmosomes. An example of multijunction cross-talk at the cardiac intercalated disc is the tethering of gap junctions, adherens junctions, and cardiac desmosomes through interactions between Cx43, plakophilin-2, and ankyrin-G.[57] We hypothesized that Cx43 maintenance results in gap junction stabilization as a viral mechanism to recruit CAR on uninfected neighboring cells to proximal cell membranes. CAR, localized to tight junctions in epithelial cells, is a primary receptor for Ad5 and is critical in cardiac development as loss of CAR is embryonic-lethal in mice.[58] Ablation of CAR expression induces a reduction in Cx43 expression; however, altered expression or localization of Cx43 effects on CAR have yet to be described.[31] Given the interdependency of localization and expression between junctional complexes, we next sought to determine the junctional status of Cx43 (i.e. gap junction maintenance or connexin43/connexon maintenance) during adenoviral infection where we demonstrate Cx43 is primarily junctional by Triton X-100 solubility fractionation. Interestingly, human papilloma virus type 16 (HPV16), another virus described to target Cx43 through the HPV16 E6 protein, results in increases of intracellular Cx43 translocating from the membrane revealing unique viral

approaches in the manipulation of Cx43 localization and macromolecular structures.[59]

Overexpression of Cx43 increases transepithelial resistance implicating gap junctions in mechanical coupling in addition to intercellular communication.[60,61] Having demonstrated increased junctional Cx43 during adenoviral infection, we next sought to determine changes in mechanical coupling during infection. By ECIS we demonstrate a transient increase in electrical resistance across a monolayer of infected cells indicative of enhanced mechanical coupling. Cx43, in addition to many other membrane proteins, contains a PDZ binding motif enabling binding to PDZ domain-containing proteins, including the scaffolding protein zonula occludens-1 (ZO-1), affecting intracellular signaling events from the plasma membrane (reviewed in [62]). Blocking Cx43/ZO-1 complexing utilizing a Cx43 c-terminal mimetic peptide reduces transepithelial barrier resistance revealing a role for Cx43/ZO-1 complexing in mechanical coupling.[63] Additionally, overexpression of CAR is demonstrated to increase transepithelial resistance but resistance is attenuated in a PDZ binding motif-deleted CAR mutant, indicating intracellular interactions of CAR through PDZ domain binding further support mechanical coupling.[64] We previously demonstrated gap junction remodeling through reduced Cx43/ZO-1 complexing in both epithelial cells and cardiomyocytes.[33] The transient induction of electrical resistance during adenoviral infection is therefore independent of Cx43/ZO-1 complexing and we

attribute this increase in mechanical coupling to junction protein abundance and/or stabilization.

Our future directions and work in progress focuses on elucidating if this transient increase in mechanical coupling coincides with increases in CAR and/or integrin α_V on apposed cells at the infected-uninfected interface and if changes are detected, does this contribute to directional and more efficient adenoviral spread.

Acknowledgements

The authors thank Dr. David Ornelles (Wake Forest School of Medicine, Microbiology and Immunology) for providing adenovirus reagents and helpful discussion. Dr. Michael Zeitz and Rachel Padget, M.S. (Fralin Biomedical Research Institute) for critical review of this manuscript. Dr. Allison N. Tegge (Fralin Biomedical Research Institute, Department of Statistics, Virginia Tech) for consultation on statistical methods used. This work was supported by a NIH NHLBI R01 grant (HL132236 to J.W.S.), an American Heart Association Predoctoral Fellowship (18PRE33960573 to P.J.C.), and a NHLBI F31 grant (HL140909 to C.C.J.).

Author contributions

J.W.S. and P.J.C. conceived the study. P.J.C. designed and conducted the experiments. J.W.S. and P.J.C. carried out data analysis and interpretation.

C.C.J. performed Click-iT half-life experiments. P.J.C. wrote the manuscript with input from J.W.S.

Declaration of interests

The authors declare no competing interests.

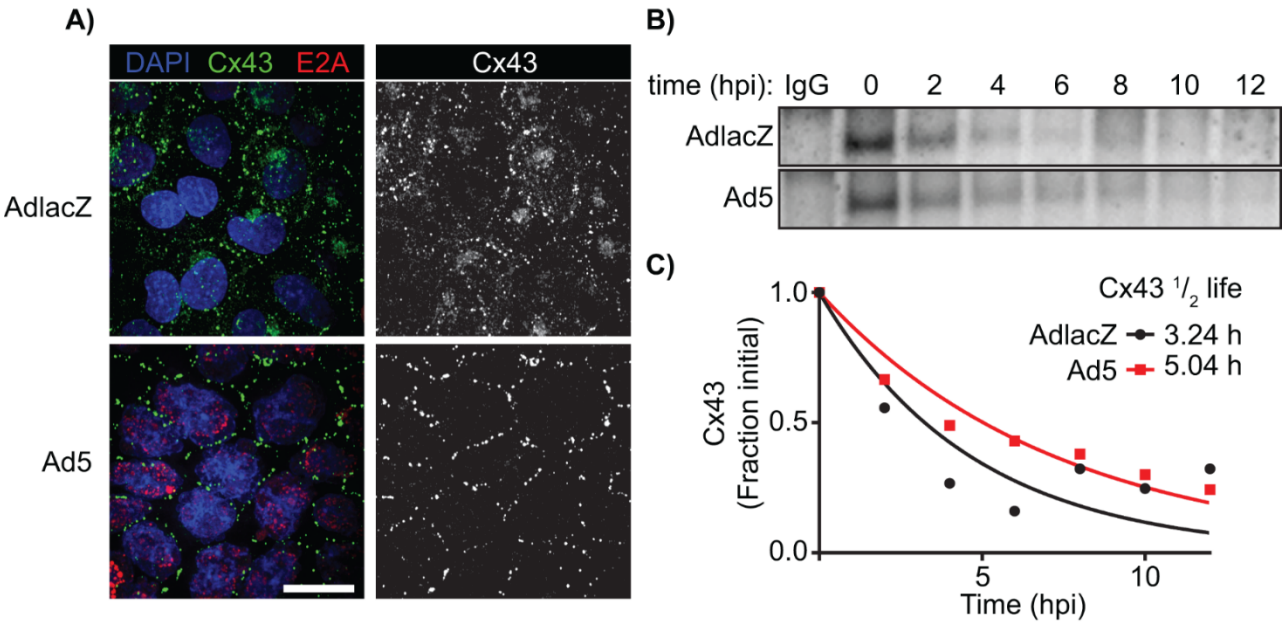

Figure 4.1) Cx43 is maintained at the plasma membrane during adenoviral infection. A549 (A) or HaCaT (B-E) cells were infected with AdlacZ or Ad5 at a MOI of 10 iu/cell. **A)** Immunofluorescence confocal microscopy of AdlacZ- or Ad5-infected A549 cells at 24 hpi. Cx43 is shown in green in merged image or white in single channel. Ad5 E2A is shown in red. DAPI is shown in blue. Original magnification: X60. Scale bar: 20 μm. Images are representative of 3 separate experiments. **B)** Infected HaCaT cells were pulsed using Click-IT chemistry then harvested every 2 hpi for 12 h prior to immunoprecipitation for Cx43. Immunoprecipitated lysates were subjected to western blotting and probed with TAMRA to detect labeled Cx43 protein. **C)** Quantification of B and calculated half-life. *n*=1.

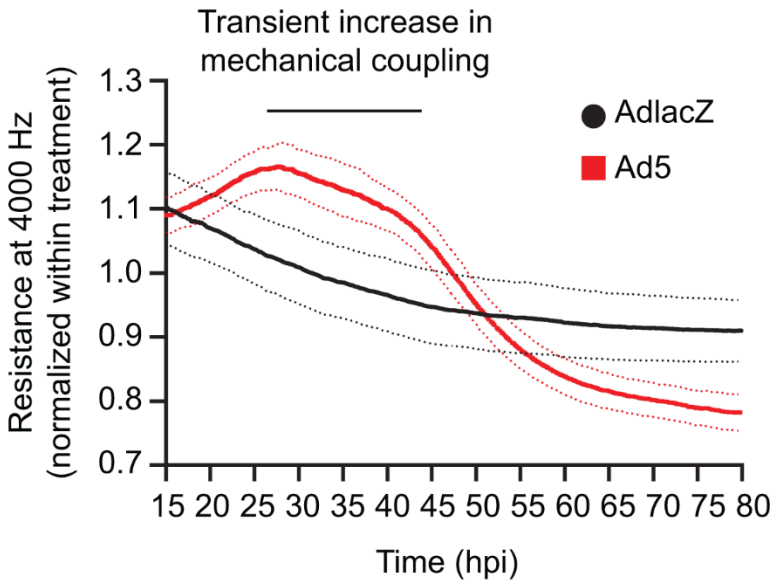

Figure 4.2) Cells become more mechanically coupled early during Ad5 infection. HaCaT cells were infected with AdlacZ or Ad5 at a MOI of 10 iu/cell then assayed by ECIS over time. Resistance data is shown at 4000 Hz normalized within treatments.

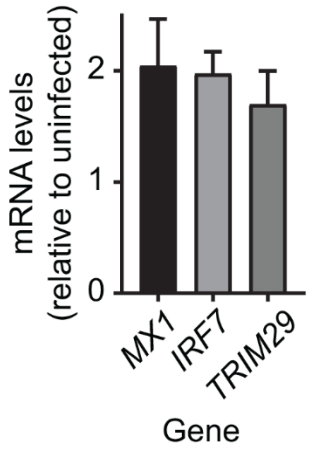

Figure 4.3) Interferon stimulated genes are upregulated during adenoviral infection. HaCaT cells were infected with Ad5 at a MOI of 10 iu/cell and RNA harvested 6 hpi. The ISGs MX1, IRF7, and TRIM29 were assayed by RT-qPCR when normalized to 18SrRNA and GAPDH as internal references. Data is Ad5 infected relative to uninfected. *n*=3. Data are presented as mean ±SEM.

References

1 Nielsen, M. S. *et al.* Gap junctions. *Compr Physiol* **2**, 1981-2035, doi:10.1002/cphy.c110051 (2012).

2 Ablasser, A. *et al.* Cell intrinsic immunity spreads to bystander cells via the intercellular transfer of cGAMP. *Nature* **503**, 530-534, doi:10.1038/nature12640 (2013).

3 Chen, Q. *et al.* Carcinoma-astrocyte gap junctions promote brain metastasis by cGAMP transfer. *Nature* **533**, 493-498, doi:10.1038/nature18268 (2016).

4 Lau, L., Gray, E. E., Brunette, R. L. & Stetson, D. B. DNA tumor virus oncogenes antagonize the cGAS-STING DNA-sensing pathway. *Science* **350**, 568-571, doi:10.1126/science.aab3291 (2015).

5 Reyes-Andrade, J. *et al.* Meningoencephalitis due to adenovirus in a healthy infant mimicking severe bacterial sepsis. *Pediatr Infect Dis J* **33**, 416-419, doi:10.1097/inf.0000000000000128 (2014).

6 Tamiya, M., Komatsu, H., Hirabayashi, M., Imura, M. & Hoshino, H. Neonatal meningoencephalitis caused by human adenovirus species F infection. *Pediatrics international : official journal of the Japan Pediatric Society* **61**, 99-101, doi:10.1111/ped.13722 (2019).

7 Bowles, N. E. *et al.* Detection of viruses in myocardial tissues by polymerase chain reaction: evidence of adenovirus as a common cause of myocarditis in children and adults. *Journal of the American College of Cardiology* **42**, 466-472, doi:https://doi.org/10.1016/S0735-1097(03)00648-X (2003).

8 Treacy, A. *et al.* First report of sudden death due to myocarditis caused by adenovirus serotype 3. *J Clin Microbiol* **48**, 642-645, doi:10.1128/JCM.00815-09 (2010).

9 Andreoletti, L., Leveque, N., Boulagnon, C., Brasselet, C. & Fornes, P. Viral causes of human myocarditis. *Arch Cardiovasc Dis* **102**, 559-568, doi:10.1016/j.acvd.2009.04.010 (2009).

10 Tabain, I. *et al.* Adenovirus respiratory infections in hospitalized children: clinical findings in relation to species and serotypes. *Pediatr Infect Dis J* **31**, 680-684, doi:10.1097/INF.0b013e318256605e (2012).

11 Ghasemi, Y. *et al.* Serotype determination of adenoviruses in children with respiratory infection. *Indian J Pediatr* **81**, 639-643, doi:10.1007/s12098-013-1286-2 (2014).

12 Ma, G. *et al.* Species C is Predominant in Chinese Children with Acute Respiratory Adenovirus Infection. *Pediatr Infect Dis J* **34**, 1042, doi:10.1097/INF.0000000000000791 (2015).

13 Wickham, T. J., Mathias, P., Cheresh, D. A. & Nemerow, G. R. Integrins αvβ3 and αvβ5 promote adenovirus internalization but not virus attachment. *Cell* **73**, 309-319, doi:https://doi.org/10.1016/0092-8674(93)90231-E (1993).

14 Bergelson, J. M. *et al.* Isolation of a Common Receptor for Coxsackie B Viruses and Adenoviruses 2 and 5. *Science* **275**, 1320-1323, doi:10.1126/science.275.5304.1320 (1997).
15 Cohen, C. J. *et al.* The coxsackievirus and adenovirus receptor is a transmembrane component of the tight junction. *Proceedings of the National Academy of Sciences* **98**, 15191-15196, doi:10.1073/pnas.261452898 (2001).
16 Lyle, C. & McCormick, F. Integrin αvβ5 is a primary receptor for adenovirus in CAR-negative cells. *Virology Journal* **7**, 148, doi:10.1186/1743-422X-7-148 (2010).
17 Bai, M., Campisi, L. & Freimuth, P. Vitronectin receptor antibodies inhibit infection of HeLa and A549 cells by adenovirus type 12 but not by adenovirus type 2. *J Virol* **68**, 5925-5932 (1994).
18 Gao, D. *et al.* Cyclic GMP-AMP synthase is an innate immune sensor of HIV and other retroviruses. *Science (New York, N.Y.)* **341**, 903-906, doi:10.1126/science.1240933 (2013).
19 Schoggins, J. W. *et al.* Pan-viral specificity of IFN-induced genes reveals new roles for cGAS in innate immunity. *Nature* **505**, 691-695, doi:10.1038/nature12862 (2014).
20 Sun, L., Wu, J., Du, F., Chen, X. & Chen, Z. J. Cyclic GMP-AMP synthase is a cytosolic DNA sensor that activates the type I interferon pathway. *Science (New York, N.Y.)* **339**, 786-791, doi:10.1126/science.1232458 (2013).
21 Watson, R. O. *et al.* The Cytosolic Sensor cGAS Detects Mycobacterium tuberculosis DNA to Induce Type I Interferons and Activate Autophagy. *Cell host & microbe* **17**, 811-819, doi:10.1016/j.chom.2015.05.004 (2015).
22 Wu, J. *et al.* Cyclic GMP-AMP is an endogenous second messenger in innate immune signaling by cytosolic DNA. *Science* **339**, 826-830, doi:10.1126/science.1229963 (2013).
23 Saitoh, T. *et al.* Atg9a controls dsDNA-driven dynamic translocation of STING and the innate immune response. *Proceedings of the National Academy of Sciences of the United States of America* **106**, 20842-20846, doi:10.1073/pnas.0911267106 (2009).
24 Sun, W. *et al.* ERIS, an endoplasmic reticulum IFN stimulator, activates innate immune signaling through dimerization. *Proceedings of the National Academy of Sciences of the United States of America* **106**, 8653-8658, doi:10.1073/pnas.0900850106 (2009).
25 Liu, S. *et al.* Phosphorylation of innate immune adaptor proteins MAVS, STING, and TRIF induces IRF3 activation. *Science* **347**, aaa2630, doi:10.1126/science.aaa2630 (2015).
26 Yoneyama, M. *et al.* Direct triggering of the type I interferon system by virus infection: activation of a transcription factor complex containing IRF-3 and CBP/p300. *The EMBO journal* **17**, 1087-1095, doi:10.1093/emboj/17.4.1087 (1998).
27 Weaver, B. K., Kumar, K. P. & Reich, N. C. Interferon regulatory factor 3 and CREB-binding protein/p300 are subunits of double-stranded RNA-

activated transcription factor DRAF1. *Molecular and cellular biology* **18**, 1359-1368, doi:10.1128/mcb.18.3.1359 (1998).
28 Lin, R., Heylbroeck, C., Pitha, P. M. & Hiscott, J. Virus-dependent phosphorylation of the IRF-3 transcription factor regulates nuclear translocation, transactivation potential, and proteasome-mediated degradation. *Molecular and cellular biology* **18**, 2986-2996, doi:10.1128/mcb.18.5.2986 (1998).
29 Jongen, W. M. *et al.* Regulation of connexin 43-mediated gap junctional intercellular communication by Ca2+ in mouse epidermal cells is controlled by E-cadherin. *Journal of Cell Biology* **114**, 545-555, doi:10.1083/jcb.114.3.545 (1991).
30 Meyer, R. A., Laird, D. W., Revel, J. P. & Johnson, R. G. Inhibition of gap junction and adherens junction assembly by connexin and A-CAM antibodies. *Journal of Cell Biology* **119**, 179-189, doi:10.1083/jcb.119.1.179 (1992).
31 Lisewski, U. *et al.* The tight junction protein CAR regulates cardiac conduction and cell-cell communication. *J Exp Med* **205**, 2369-2379, doi:10.1084/jem.20080897 (2008).
32 Li, M. W. M., Mruk, D. D., Lee, W. M. & Cheng, C. Y. Connexin 43 and plakophilin-2 as a protein complex that regulates blood–testis barrier dynamics. *Proceedings of the National Academy of Sciences* **106**, 10213-10218, doi:10.1073/pnas.0901700106 (2009).
33 Calhoun, P. J. & Smyth, J. W. *Investigating viral subversion of intercellular communication* Ph.D. thesis, Virginia Tech, (2020).
34 Green, M. & Loewenstein, P. M. Human Adenoviruses: Propagation, Purification, Quantification, and Storage. *Current Protocols in Microbiology* **00**, 14C.11.11-14C.11.19, doi:10.1002/9780471729259.mc14c01s00 (2006).
35 Smyth, J. W. *et al.* A 14-3-3 mode-1 binding motif initiates gap junction internalization during acute cardiac ischemia. *Traffic* **15**, 684-699, doi:10.1111/tra.12169 (2014).
36 Hendrickx, R. *et al.* Innate immunity to adenovirus. *Human gene therapy* **25**, 265-284, doi:10.1089/hum.2014.001 (2014).
37 Dobbs, N. *et al.* STING Activation by Translocation from the ER Is Associated with Infection and Autoinflammatory Disease. *Cell host & microbe* **18**, 157-168, doi:10.1016/j.chom.2015.07.001 (2015).
38 Saha, B. & Parks, R. J. Histone Deacetylase Inhibitor Suberoylanilide Hydroxamic Acid Suppresses Human Adenovirus Gene Expression and Replication. *Journal of Virology* **93**, e00088-00019, doi:10.1128/JVI.00088-19 (2019).
39 Zhang, S. S. *et al.* Iroquois homeobox gene 3 establishes fast conduction in the cardiac His-Purkinje network. *Proc Natl Acad Sci U S A* **108**, 13576-13581, doi:10.1073/pnas.1106911108 (2011).
40 Dupays, L. *et al.* Dysregulation of connexins and inactivation of NFATc1 in the cardiovascular system of Nkx2-5 null mutants. *J Mol Cell Cardiol* **38**, 787-798, doi:10.1016/j.yjmcc.2005.02.021 (2005).

41 Vine, A. L., Leung, Y. M. & Bertram, J. S. Transcriptional regulation of connexin 43 expression by retinoids and carotenoids: similarities and differences. *Molecular carcinogenesis* **43**, 75-85, doi:10.1002/mc.20080 (2005).
42 Ghouili, F. & Martin, L. J. Cooperative regulation of Gja1 expression by members of the AP-1 family cJun and cFos in TM3 Leydig and TM4 Sertoli cells. *Gene* **635**, 24-32, doi:10.1016/j.gene.2017.09.017 (2017).
43 Villares, G. J. *et al.* Overexpression of protease-activated receptor-1 contributes to melanoma metastasis via regulation of connexin 43. *Cancer Res* **69**, 6730-6737, doi:10.1158/0008-5472.can-09-0300 (2009).
44 Ribeiro, I. *et al.* Tbx2 and Tbx3 regulate the dynamics of cell proliferation during heart remodeling. *PloS one* **2**, e398-e398, doi:10.1371/journal.pone.0000398 (2007).
45 Ai, Z., Fischer, A., Spray, D. C., Brown, A. M. & Fishman, G. I. Wnt-1 regulation of connexin43 in cardiac myocytes. *J Clin Invest* **105**, 161-171, doi:10.1172/jci7798 (2000).
46 James, C. C., Zeitz, M. J., Calhoun, P. J., Lamouille, S. & Smyth, J. W. Altered translation initiation of Gja1 limits gap junction formation during epithelial-mesenchymal transition. *Molecular biology of the cell*, doi:10.1091/mbc.E17-06-0406 (2018).
47 Zeitz, M. J. *et al.* Dynamic UTR Usage Regulates Alternative Translation to Modulate Gap Junction Formation during Stress and Aging. *Cell Reports* **27**, 2737-2747.e2735, doi:10.1016/j.celrep.2019.04.114 (2019).
48 Laird, D. W. Connexin phosphorylation as a regulatory event linked to gap junction internalization and degradation. *Biochimica et Biophysica Acta (BBA) - Biomembranes* **1711**, 172-182, doi:https://doi.org/10.1016/j.bbamem.2004.09.009 (2005).
49 Solan, J. L. & Lampe, P. D. Kinase programs spatiotemporally regulate gap junction assembly and disassembly: Effects on wound repair. *Semin Cell Dev Biol* **50**, 40-48, doi:10.1016/j.semcdb.2015.12.010 (2016).
50 Solan, J. L. & Lampe, P. D. Specific Cx43 phosphorylation events regulate gap junction turnover in vivo. *FEBS Lett* **588**, 1423-1429, doi:10.1016/j.febslet.2014.01.049 (2014).
51 Nimlamool, W., Andrews, R. M. & Falk, M. M. Connexin43 phosphorylation by PKC and MAPK signals VEGF-mediated gap junction internalization. *Molecular biology of the cell* **26**, 2755-2768, doi:10.1091/mbc.E14-06-1105 (2015).
52 Warn-Cramer, B. J., Cottrell, G. T., Burt, J. M. & Lau, A. F. Regulation of connexin-43 gap junctional intercellular communication by mitogen-activated protein kinase. *J Biol Chem* **273**, 9188-9196, doi:10.1074/jbc.273.15.9188 (1998).
53 Warn-Cramer, B. J. *et al.* Characterization of the mitogen-activated protein kinase phosphorylation sites on the connexin-43 gap junction protein. *J Biol Chem* **271**, 3779-3786, doi:10.1074/jbc.271.7.3779 (1996).

54 Leithe, E., Brech, A. & Rivedal, E. Endocytic processing of connexin43 gap junctions: a morphological study. *The Biochemical journal* **393**, 59-67, doi:10.1042/BJ20050674 (2006).
55 Leithe, E. & Rivedal, E. Epidermal growth factor regulates ubiquitination, internalization and proteasome-dependent degradation of connexin43. *J Cell Sci* **117**, 1211-1220, doi:10.1242/jcs.00951 (2004).
56 Leithe, E. & Rivedal, E. Ubiquitination and down-regulation of gap junction protein connexin-43 in response to 12-O-tetradecanoylphorbol 13-acetate treatment. *J Biol Chem* **279**, 50089-50096, doi:10.1074/jbc.M402006200 (2004).
57 Sato Priscila, Y. *et al.* Interactions Between Ankyrin-G, Plakophilin-2, and Connexin43 at the Cardiac Intercalated Disc. *Circulation Research* **109**, 193-201, doi:10.1161/CIRCRESAHA.111.247023 (2011).
58 Dorner, A. A. *et al.* Coxsackievirus-adenovirus receptor (CAR) is essential for early embryonic cardiac development. *Journal of Cell Science* **118**, 3509-3521, doi:10.1242/jcs.02476 (2005).
59 Sun, P. *et al.* HPV16 E6 Controls the Gap Junction Protein Cx43 in Cervical Tumour Cells. *Viruses* **7**, 5243-5256, doi:10.3390/v7102871 (2015).
60 Churko, J. M., Langlois, S., Pan, X., Shao, Q. & Laird, D. W. The potency of the fs260 connexin43 mutant to impair keratinocyte differentiation is distinct from other disease-linked connexin43 mutants. *The Biochemical journal* **429**, 473-483, doi:10.1042/BJ20100155 (2010).
61 Nagasawa, K. *et al.* Possible involvement of gap junctions in the barrier function of tight junctions of brain and lung endothelial cells. *Journal of Cellular Physiology* **208**, 123-132, doi:10.1002/jcp.20647 (2006).
62 Lee, H. J. & Zheng, J. J. PDZ domains and their binding partners: structure, specificity, and modification. *Cell communication and signaling : CCS* **8**, 8, doi:10.1186/1478-811x-8-8 (2010).
63 Obert, E. *et al.* Targeting the tight junction protein, zonula occludens-1, with the connexin43 mimetic peptide, αCT1, reduces VEGF-dependent RPE pathophysiology. *J Mol Med (Berl)* **95**, 535-552, doi:10.1007/s00109-017-1506-8 (2017).
64 Excoffon, K. J. D. A., Hruska-Hageman, A., Klotz, M., Traver, G. L. & Zabner, J. A role for the PDZ-binding domain of the coxsackie B virus and adenovirus receptor (CAR) in cell adhesion and growth. *Journal of Cell Science* **117**, 4401-4409, doi:10.1242/jcs.01300 (2004).

Chapter 5
Conclusions

Gap junctions play important roles in homeostasis, development, and organ function by coupling cells metabolically, electrically, and immunologically. Given gap junction-mediated roles in antiviral defenses, it is logical that viruses would target these cellular structures, yet research in this area has been lacking. Here we have demonstrated that connexin43 (Cx43) is targeted at the level of transcription with reductions in both mRNA and protein levels. We further identify Cx43 phosphorylation associated with reduced channel conductance, revealing adenoviral-induced rapid phosphorylation inhibiting gap junctions prior to loss of Cx43. Utilizing a small molecule inhibitor approach, we find β-catenin transcriptional activity is necessary for reductions in *de novo* gap junction synthesis and the adenoviral protein E4orf1 is sufficient to induce phosphorylation of β-catenin to a transcriptionally active state. Interestingly, despite reductions in *de novo* gap junction synthesis, gap junctions are not directly targeted for internalization and degradation during infection, resulting in cells with increased junctional Cx43 and mechanical coupling (Figure 5.1). The question remains: how are increases in mechanical coupling and gap junction maintenance (albeit, reduced channel conductance gap junctions) evolutionarily advantageous to human adenovirus. Reductions in Cx43 and gap junction intercellular communication are likely to limit the spread of cyclic guanosine monophosphate – adenosine monophosphate (cGAMP) given the recent discoveries demonstrating a role for this molecule in propagating immune responses in a population of cells via gap junctions. Furthermore, it is possible

that there are other small molecules, miRNAs, or short linear peptides that may have a role in immune signaling that are likewise antagonized through the reduction of GJIC. We additionally demonstrated gap junction remodeling that occurs through loss of interaction with the scaffolding protein zonula occludens-1 (ZO-1) and attribute this reduced association with stalled Cx43 dynamics, both incorporation into and removal from gap junction plaques. This model is further supported by Cx43 half-life and triton solubility data.

Reasons for maintenance of gap junctions and increases in mechanical coupling are less clear. Ad5 infection results in maintenance of *de facto* gap junctions, decreases in *de novo* synthesis, and increased junctional Cx43. Specifically, in regards to forward trafficking, the loss of *de novo* synthesis and altered kinase activity during Ad5 infection may be sufficient to reduce Cx43 hemichannel pools (undocked connexons). Although a focus of this study has been on adenoviral-mediated targeting of GJIC, it is possible that this gap junction remodeling is a viral-mediated mechanism to deplete hemichannels. Cx43 hemichannels are capable of releasing ATP, a purinergic signaling molecule, well described in adaptive immune responses including recruiting macrophages. It is possible that Ad5 has evolved a two-pronged approach in restricting GJIC and reducing hemichannels which would result in a highly orchestrated targeting of both innate and adaptive immune responses through transcriptional and post-translational modifications of Cx43 gap junctions.

Given the number of viruses that utilize intercellular junction proteins, including Ad5 binding of the Coxsackievirus and adenovirus receptor (CAR) protein, we

hypothesize stabilization of intercellular junctions is a means of predisposing uninfected neighboring cells to viral invasion by proximal recruitment of intercellular adhesion molecules including CAR. Indeed, there is widespread use of intercellular proteins as primary and secondary receptors, as well as entry factors, for numerous viruses. Our previous understanding of viruses that manipulate Cx43 gap junctions is limited primarily to human papilloma virus and murine hepatitis virus; however, this may be a feature utilized by other viruses in order to direct and influence viral spread. Future work will focus on elucidating junctional architectural changes in uninfected neighboring cells and how this influences viral spread.

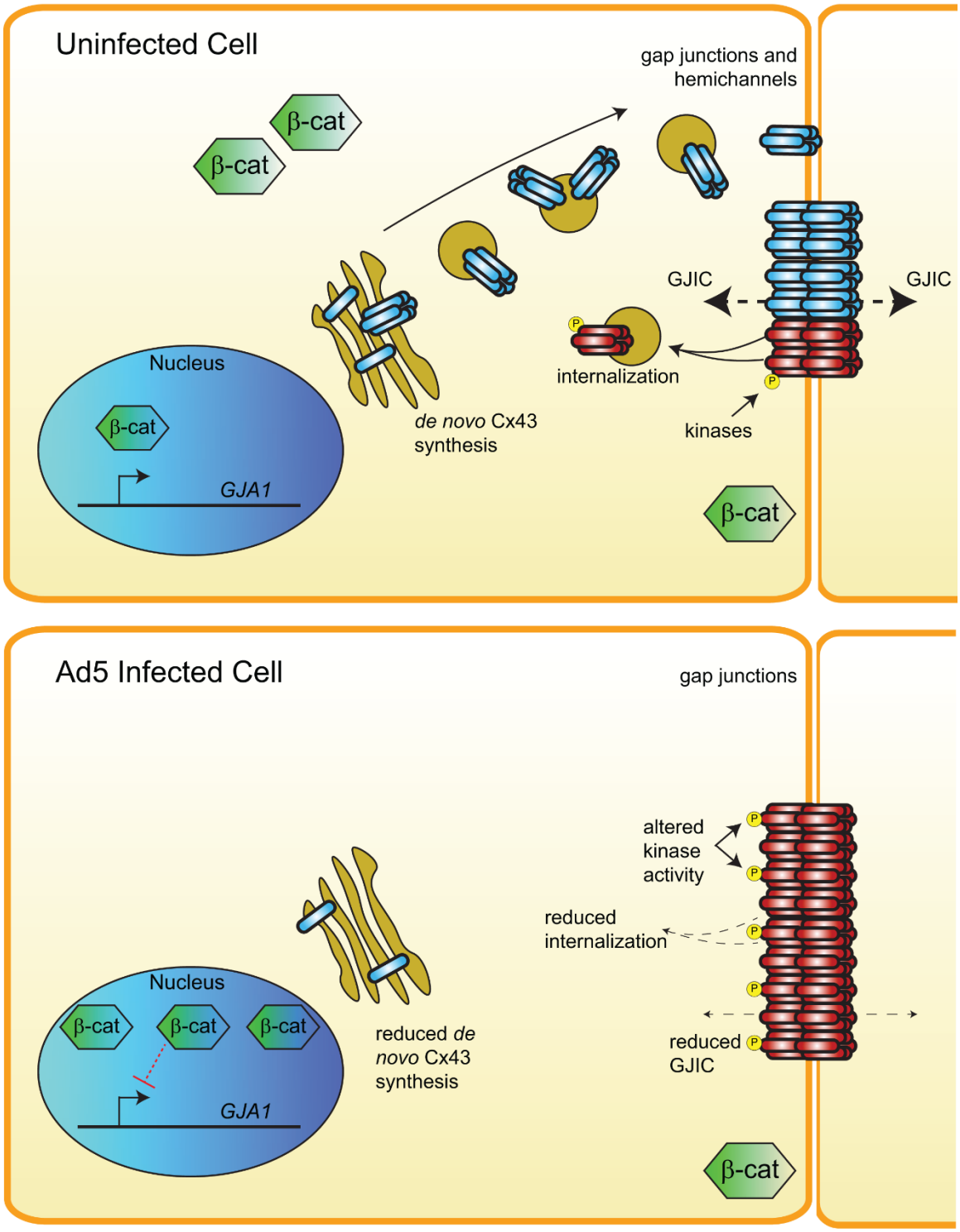

Figure 5.1) Graphical summary of key findings. In uninfected cells, *GJA1* expression is regulated by numerous transcription factors, including β-catenin.

After *de novo* mRNA synthesis, processing, and co-translational insertion into the membrane of the ER, Cx43 is trafficked through the vesicular trafficking pathway along microtubules to the plasma membrane. Cx43 connexons (hemichannels) may be deposited to the plasma membrane or retained in the cytoplasm. Cx43 associates with multiple scaffolding proteins including ZO-1 which retains it from the gap junction proper. Following initiation of a phosphorylation cascade by PKC, Cx43 hemichannels are released from ZO-1 and dock with a hemichannel on an apposed cell forming *de facto* gap junctions. Next, Cx43 is phosphorylated by AKT and undergoes reduced channel open probability and altered channel conductance followed by MAPK phosphorylation and internalization. In Ad5-infected cells, a novel role for β-catenin transcriptional suppression resulting in reductions of Cx43 mRNA and protein was identified resultant of adenoviral E4orf1-induced phosphorylation of β-catenin and subsequently less Cx43 localized in the ER. Altered kinase activity resulted in primarily junctional Cx43, indicative of loss of hemichannels and cytoplasmic pools, however in a primarily AKT-phosphorylated closed state. Phosphorylation and half-life data support a model where Cx43 gap junctions are maintained during adenoviral infection despite negative gene regulation.